UNIVERSITÉ DU QUÉBEC À MONTRÉAL

PRODUCTION DE CHALEUR, FLUX DE CHALEUR ET FLUX DE GÉO-NEUTRINOS DANS LES ENVIRONS DE SNOLAB

MÉMOIRE

PRÉSENTÉ

COMME EXIGENCE PARTIELLE

DE LA MAÎTRISE EN SCIENCE DE LA TERRE

PAR

CATHERINE PHANEUF

DÉCEMBRE 2012

REMERCIEMENTS

En premier lieu, je tiens à remercier très sincèrement mon directeur de mémoire, monsieur Jean-Claude Mareschal, d'abord pour m'avoir donné la possibilité de réaliser ce travail, ensuite pour sa confiance et son encadrement et pour son soutient surtout durant les moments d'impatience. Mes remerciements vont aussi à ma codirectrice, Claire Perry.

Merci à mes collègues de classe et de bureau, Erika, Paola et Jean-Michel pour les échanges, l'entraide et la compagnie. Merci à Jean-Claude Mareschal, Claude Jaupart, Hélène Bouquerel, Chantal Gosselin et John Armitage pour l'agréable compagnie durant les missions de terrain. Merci à Raynald Lapointe et Chantal Gosselin de m'avoir expliqué le fonctionnement de la presse et de la broyeuse et pour les conseils techniques afin de préparer les échantillons pour leur analyse en radioéléments. Merci également à Virginie pour son coup de pouce avec le broyage des échantillons.

Merci à Claude Jaupart, Hélène Bouquerel, Thierry Rivet et Angela Limare pour l'aide et les explications sur la procédure de préparation des échantillons et pour la réalisation de la mesure de conductivité thermique. Je remercie aussi toute l'équipe du laboratoire de dynamique des fluides de l'IPGP pour leur chaleureux accueil lors de mon stage.

Je tiens également à remercier le centre de recherche du GÉOTOP pour toutes les activités et événements qui ont été organisés, dont les congrès étudiants auxquels j'ai participé. Un merci particulier à Nicole Turcot, secrétaire de direction, et à Sandrine Solignac, coordonnatrice, pour l'aide qu'elles m'ont apportée sur le plan des tâches administratives.

De même, mes remerciements vont à tout le personnel du laboratoire SLOWPOKE de l'institut de génie nucléaire, pour avoir autorisé l'accès au laboratoire et aux outils, et pour les résultats de concentration en radioéléments des échantillons.

Mes reconnaissances vont au centre de recherche du GÉOTOP et à la faculté des sciences de l'UQAM, pour l'aide financière apportée ainsi qu'aux Fonds de recherche de Québec Nature et technologies pour m'avoir octroyé la bourse de stages internationaux.

Finalement, j'aimerais profiter de l'occasion pour remercier l'ensemble de mes proches

et amis, spécialement mes parents, Elise et Michel, ma soeur, Mylène, ainsi que mon beau-frère, Daniel, pour le soutien et les encouragements. Merci à vous tous de croire en moi. Merci à mon petit Olivier, qui me donne l'énergie et le courage de continuer.

AVANT-PROPOS

Ce travail de recherche présente, de façon intégrale, le mémoire de maîtrise que j'ai déposé en décembre 2012 au département des sciences de la Terre et de l'Atmosphère de l'Université du Québec à Montréal comme exigence partielle de la maîtrise.

Ce mémoire de recherche comprend une introduction générale du sujet, suivie de deux articles et d'une conclusion générale. La langue originale des articles (anglaise) a été conservée afin d'éviter toute erreur d'interprétation pouvant survenir par la traduction des textes. Par contre, l'introduction et la conclusion générale sont rédigées en français. Dans le but éventuel de soumettre les articles à des revues scientifiques, ils sont présentés de façon à satisfaire les critères relatifs aux règles internationales de publication, soit en format manuscrit, avec les résumés au début et les tableaux et figures à la fin. De plus, chacun des articles est précédé d'un résumé en français, traduit de l'original anglais.

Le premier article s'intitule *Airborne radiometric surveys and crustal heat production near SNOLAB, Canada.* Le second article porte le titre suivant : *Estimating the global crustal geo-neutrino flux, including a local study near SNOLAB, Canada.* La rédaction de ces articles résulte d'une collaboration étroite avec mon directeur de maîtrise, monsieur Jean-Claude Mareschal, professeur de Géophysique au département des sciences de la Terre et de l'Atmosphère et chercheur au centre de recherche en géochimie et géodynamique (GÉOTOP-UQAM-McGill).

TABLE DES MATIÈRES

INTRODUCTION GÉNÉRALE

Généralités

Depuis la publication de la Théorie Analytique de la Chaleur par Fourier (1822) et surtout depuis le premier modèle de refroidissement de la Terre par Kelvin (Thompson, 1862), les géologues et géophysiciens étudient le budget énergétique de la Terre afin de mieux comprendre son histoire et son évolution. Certaines des grandes questions soulevées à l'époque de Kelvin, sur le mécanisme de transport de chaleur et les sources d'énergie de la Terre, ont trouvé des réponses mais d'autres questions restent posées.

Aujourd'hui, nous savons que la Terre s'est formée par accrétion de masse dans la nébuleuse solaire il y a 4.55 Ga et que, depuis sa formation, elle se refroidit en perdant une partie de sa chaleur primordiale. Cette chaleur est évacuée par les mouvements de convection dans le manteau et le noyau et par conduction dans la lithosphère. La convection entretient les phénomènes tectoniques et magmatiques qui sont responsables d'une partie de la morphologie de la surface de notre planète.

Mais à quelle vitesse ce refroidissement se fait-il ? Comment le régime convectif et les processus géologiques évoluent-ils avec ce refroidissement ?

Le budget énergétique terrestre

Actuellement, nous connaissons la perte totale d'énergie de la Terre, qui est de 46 $\pm$ 2 terawatts (1 TW = 10^{12} Watts). Cette perte totale est déterminée par la somme des contributions continentale et océanique, qui sont respectivement de 14 et 32 TW (Jaupart et al., 2007).

La valeur de 14 TW de chaleur perdue à travers la lithosphère continentale est déterminée par l'intégration des plus de 35,000 valeurs de flux de chaleur mesurées en région continentale. Ces valeurs proviennent de la récente compilation de Derrick Hasterok mise à jour en 2011. Cette compilation est disponible à http ://www.heatflow.und.edu/.

La plus grande partie de la perte de chaleur de la Terre s'effectue à travers le plancher océanique. On compte un grand nombre de mesures de flux de chaleur (plus de 20,000) sur le plancher océanique, mais ces mesures sont perturbées par la circulation hydrothermale. Par conséquent, ces mesures sous-estiment le flux total en négligeant le transport de chaleur par les fluides hydrothermaux (Lowell et al., 1995). C'est pourquoi la contribution océanique est calculée à partir de modèles de refroidissement du plancher océanique. Ces modèles prédisent le flux de chaleur en fonction de l'âge du plancher océanique. La distribution des âges découle directement de l'hypothèse de l'expansion des fonds océaniques et est calculée à partir de cartes d'anomalies magnétiques marines (Royer et al., 1992; Müller et al., 1997; Sclater et al., 1980). En procédant de cette façon, nous obtenons une contribution océanique de 29 TW.

L'apport des points chauds doit aussi être pris en compte dans la perte de chaleur à travers la lithosphère océanique. Cet apport estimé à 3 TW est déterminé par le volume de bombements bathymétriques et la vitesse des plaques qui leur sont associées. Ces bombements résultent directement de la flottabilité du manteau réchauffé par la présence de plumes mantelliques ascendantes. Leur amplitude est proportionnelle à la différence de température entre les plumes et le manteau avoisinant. Cette valeur représente une limite inférieure puisqu'une plaque peut entrer en subduction avant même que la totalité de la chaleur supplémentaire ait eu le temps d'être évacuée à la surface.

En additionnant les 3 TW de contribution des points chauds, le flux de chaleur océanique s'élève à 32 TW. Avec les 14 TW de perte de chaleur des continents, nous obtenons un grand total de 46 TW (Jaupart et al., 2007).

Nous connaissons encore mal les contributions relatives des différentes composantes à ce budget. Ces composantes comprennent la production de chaleur de la croûte et du manteau, le flux de chaleur à la frontière noyau/manteau et le refroidissement séculaire du manteau. D'autres sources, telles que la contraction thermique, la différentiation croûte/manteau, la chaleur latente dans le manteau ainsi que la dissipation des marées contribuent aussi au budget. Mais la somme de leurs contributions, inférieure à 1 TW, est moins que l'incertitude de $\pm$ 2 TW sur la perte totale d'énergie.

Jusqu'à présent, la seule composante dont la contribution est bien établie est la production de chaleur dans la croûte continentale. Son apport de 7 TW a été fixé par les diverses campagnes d'échantillonnage réalisées à travers toute la croûte continentale ainsi que par les études de flux de chaleur. Par contre, les estimations des autres composantes restent très incertaines.

Le refroidissement séculaire du manteau peut être déterminé à partir de la pétrologie des basaltes Archéens provenant des dorsales mid-océaniques. En déterminant la température de liquidus de ces roches, Abbott et al. (1994) ont conclu que le manteau s'est refroidi de 150 degrés Kelvins (K) en 3 Ga. Si le refroidisssment séculaire présent ne diffère pas trop de sa moyenne à long terme, un taux de refroidissement de 50 K/Ga représente une contribution de 8 TW.

Différentes approches ont été développées et utilisées pour estimer le flux de chaleur à la frontière noyau/manteau. L'une d'elles utilise le flux de chaleur conduit le long de l'adiabatique. De cette façon, le flux de chaleur à la frontière noyau/manteau doit être supérieur à 5 TW (Lay et al., 2008). Cette méthode dépend des valeurs du gradient de température et de la conductivité thermique du manteau profond qui sont très mal connues. Une autre approche est basée sur l'efficacité de la géodynamo. Le flux de chaleur à la frontière noyau/manteau fournit l'énergie nécessaire pour maintenir la convection dans le noyau et entretenir la géodynamo. Ainsi l'énergie dissipée par la géodynamo permet de déterminer le flux de chaleur minimum requis. D'après cette méthode, Buffett (2002) obtient un flux de 5-14 TW. Cette fourchette est très large en raison de la grande incertitude sur l'efficacité thermodynamique de la dynamo.

Récemment découverte par Oganov and Ono (2004), la transition de phase du minéral perovskite (Pv) en un polymorphe plus dense, le post-perovskite (Ppv), permet également d'estimer le flux de chaleur à la frontière noyau/manteau. En utilisant cette nouvelle approche, ?Lay et al. (2008) estiment un flux de chaleur de 9-17 TW.

En résumé, le flux de chaleur à la frontière noyau/manteau est très mal contraint et les estimations de son apport au budget énergétique terrestre varient entre 5 et 17 TW. De la même façon, la contribution de la production de chaleur dans le manteau est mal connue.

Le manteau est inaccessible et donc impossible à échantillonner directement pour mesurer la radioactivité. Dans ces conditions, la méthode utilisée pour estimer la concentration en radio-éléments et la radioactivité du le manteau repose sur des modèles géochimiques et l'analyse des météorites. Les météories chondritiques, à partir desquels nous supposons que la Terre s'est formée, représentent des échantillons de matériel silicaté non-différencié. Ces échantillons permettent d'évaluer la composition de la Terre silicatée, que nous appelerons BSE pour Bulk Silicate Earth, qui représente la composition moyenne de l'ensemble croûte et manteau. La production de chaleur déterminée à partir de ces modèles s'élève à 20 TW pour BSE. La différentiation de la croûte, qui enlève 7 TW, laisse une contribution mantellique de 13 TW avec une incertitude de $\pm 20\%$.

Tandis que plusieurs chercheurs tentent d'améliorer les estimations du flux de chaleur à la frontière noyau/manteau, un nouveau développement très prometteur est apparu récemment. Il s'agit de l'utilisation d'observatoires de neutrinos pour détecter des géo-neutrinos, c'est-à-dire des neutrinos provenant de la désintégration des éléments radioactifs dans la Terre. Ce nouveau développement pourrait permettre, par l'observation de ces neutrinos d'origine terrestre, de déterminer la concentration en radioéléments dans le manteau et d'obtenir une meilleure estimation de la production de chaleur du manteau. Finalement, nous pourrons mieux calculer les autres composantes du budget et estimer le taux de refroidissement séculaire.

Les géo-neutrinos

Les neutrinos sont des particules élémentaires de masse quasi-nulle dont l'existence avait été supposée par Pauli (1930) qui tentait d'expliquer le spectre continu de la désintégration β. C'est beaucoup plus tard, lors d'une expérience développée par Cowan et Reines à la centrale nucléaire de Savannah River, que ces particules furent détectées directement pour la première fois (Cowan, C.L., Reines, Jr., F., Harrison, F.B., Kruse, H.W., McGuire, A.D., 1956).

Ces particules possèdent l'unique caractéristique d'intéragir seulement par les forces faibles, ce qui leur permet de passer sans intéraction à travers la matière à une vitesse proche

de celle de la lumière. De ce fait, elles peuvent transporter de l'information provenant de sources très lointaines. C'est pour cette raison qu'après leur découverte, les physiciens et astrophysiciens se sont immédiatement intéressé à ce processus, afin d'étudier les réactions de fusion nucléaire au coeur des étoiles et du soleil. En 1969, dans la mine d'or de Homestake, au Dakota du sud, on a observé les premiers neutrinos d'origine solaire. Depuis, plusieurs observatoires observent ces particules afin d'étudier les mécanismes de fusion nucléaire et de résoudre différents problèmes d'astrophysique.

Un développement très prometteur pour les géosciences a eu lieu dans quelques-uns de ces observatoires d'astro-physique. Diverses modifications apportées aux détecteurs ont permis l'observation directe d'anti-neutrinos, les neutrinos électroniques d'origine terrestre, aussi appelés géo-neutrinos. Ces anti-neutrinos électroniques sont engendrés lors de la désintégration β dans la chaîne de désintégration des isotopes radioactifs d'uranium, thorium et potassium. La désintégration des noyaux atomiques de ces isotopes est la plus importante source de chaleur à l'intérieur de la Terre.

L'utilisation de ces géo-neutrinos avait été suggérée par Eder G. (1966) et par Marx (1969). Dans les années 80s, Krauss et al. (1984) ont discuté de leur unique potentiel pour les géosciences, de mesurer la radioactivité et la concentration en radioéléments. Depuis, plusieurs chercheurs s'y sont intéressés et beaucoup d'études ont été publiées, discutant du potentiel pour déterminer la production de chaleur radiogénique et pour tester le modèle de BSE (Kobayashi and Fukao, 1991; Rothschild et al., 1998; Raghavan et al., 1998; Fiorentini et al., 2003, 2005; Mantovani et al., 2004).

Dans un détecteur de géo-neutrinos, qui est composé de liquide scintillateur, l'interaction entre un anti-neutrino électronique et un proton engendre un positron et un neutron. Lorsque le neutron est désintégré en un proton et électron avec un délai exact de 210 μs, cette désintégration émet un rayonnement gamma de 2.2 MeV, de concert avec le signal d'annihilation du positron. C'est cette exacte coïncidence qui permet de s'assurer que l'évènement est du à la désintégration d'un anti-neutrino issu de la réaction inverse de la désintégration β. Toutefois, à cause de sa très faible section efficace, cette réaction reste très difficile à observer. Même avec un très gros détecteur, le nombre d'événements est de quelques di-

zaines par année. Un autre obstacle provient du bruit des réacteurs nucléaires avoisinant qui domine les observations.

En 2005, le groupe de collaboration KamLAND a publié les premiers résultats sur les géo-neutrinos détectés à l'observatoire de géo-neutrino Kamioka (KamLAND), au Japon (Araki, T. and 89 collaborators, 2005). Ces résultats ont permis de démontrer la capacité des détecteurs de géo-neutrinos à mesurer la radioactivité et la concentration en radioéléments. Mais la grande incertitude due au fort signal des réacteurs nucléaires avoisinants et à la radioactivité crustale de la région n'a, jusqu'à maintenant, permis aucune amélioration spectaculaire de nos connaissances. D'autres résultats ont été récemment publiés (Bellini, G. and 89 collaborators, 2010; Gando, A. and 65 collaborators, 2011).

Un nouveau détecteur de géo-neutrinos sera bientôt mis en activité à l'observatoire de Neutrinos de Sudbury (SNOLAB) qui entre dans la phase SNO+. Cet observatoire a l'avantage d'être moins exposé que KamLAND au bruit des réacteurs nucléaires. Par contre, il semble que la région de Sudbury est plus riche en éléments radioactifs que le reste du Bouclier Canadien ce qui complique l'étude de la radioactivité mantellique.

L'objectif de ce travail

L'objectif principal de ce travail est de déterminer le flux de géo-neutrinos provenant de la croûte près de l'observatoire SNOLAB. En déterminant le flux de géo-neutrinos générés par la désintégration des éléments radioactifs dans la croûte, nous pourrons calculer la contribution du manteau au flux total qui sera observé par les expériences suivant la mise en oeuvre de la phase SNO+. Nous pourrons calculer la concentration en U et Th ainsi que leur apport au budget énergétique de la Terre. Par contre, il reste impossible d'obtenir des résultats pour K dont l'énergie (1.31 MeV) est sous le seuil de détection (1.8 MeV).

Le flux de géo-neutrinos et le flux de chaleur dépendent directement de la radioactivité de la croûte terrestre. Pour déterminer cette radioactivité, nous disposons de mesures sur échantillons de forages ou de surface, de mesures de flux de chaleur et de données radiométriques aéroportées. Nous calculerons la radioactivité crustale à partir de ces différentes

données. Nous utiliserons ces résultats pour prédire le flux de géo-neutrinos d'origine crustale dans la région de Sudbury.

Les études

Article 1

La première partie de ce mémoire est écrite sous la forme d'un article scientifique intitulé *Airborne radiometric surveys and crustal heat production near SNOLAB, Canada.*

Le but de cet article est de comparer la production de chaleur crustale déterminée à partir des données d'études radiométriques aéroportées avec des mesures de production de chaleur effectuées sur des échantillons par analyse géochimique.

Pour ce faire, nous avons comparé des données radiométriques recueillies lors d'une étude aéroportée dans région de Sudbury avec des mesures de production de chaleur sur échantillons. Les échantillons ont été recueillis en surface, le long d'un transect et dans des forages d'exploration minière. Les données de l'étude aéroportée proviennent de la banque de données géoscientiques (EDC) du secteur des sciences de la Terre du ministère des Ressources naturelles du Canada. Les mesures sur échantillons proviennent de travaux antérieurs de plusieurs chercheurs et de nos mesures.

Ce travail nous a permis de conclure que les données radioactives provenant de levés géophysiques aéroportés sous-estiment la radioactivité de la croûte. Par conséquent, ces données ne seront pas utiles pour calculer la radioactivité et prédire le flux de géo-neutrinos d'origine crustale.

Article 2

La seconde partie de ce mémoire est aussi présentée sous la forme d'un article scientifique. Le titre de ce deuxième article est *Estimating the crustal geo-neutrino flux, including a local study near SNOLAB, Canada* .

Dans ce travail, nous discutons des différentes approches qui ont été utilisées jusqu'à maintenant pour estimer la composante crustale du flux de géo-neutrinos. Nous présentons une nouvelle approche qui utilise des mesures de flux et de production de chaleur afin de calculer cette composante crustale. Nous comparons notre modèle avec celui de Fiorentini et al. (2005) qui est basé sur l'épaisseur de la croûte terrestre et sur des modèles géochimiques de distribution des radioéléments à l'intérieur de la Terre. Nous concluons que l'utilisation des mesures de flux et de production de chaleur est la meilleure méthode pour déterminer la composante crustale du flux de géo-neutrinos. Nous présentons des nouvelles mesures de flux et de production de chaleur provenant de deux nouveaux sites situés dans la région de Sudbury. En utilisant toutes les mesures disponibles, nous calculons la composante crustale du flux de géo-neutrinos dans le voisinage de SNOLAB.

CHAPITRE I (Article 1)

AIRBORNE RADIOMETRIC SURVEYS AND HEAT PRODUCTION NEAR SNOLAB, CANADA

Résumé

La production de chaleur crustale doit être estimée le plus précisément possible pour les futures expériences sur les géo-neutrinos envisagées à l'Observatoire de Neutrino de Sudbury (SNOLAB).

Nous comparons la production de chaleur crustale dans la région de Sudbury estimée à partir de levés radiométriques aéroportés, de mesures sur échantillons de carottes provenant de forages d'exploration minière, de mesures sur échantillons de surface et de mesures sur des échantillons prélevés le long d'une traverse. Les levés aéroportés ont une résolution spatiale élevée (1000 m) et montrent une bonne corrélation avec la géologie régionale, mais ces données sont sensibles qu'à la partie superficielle de la croûte. Ils donnent une production de chaleur moyenne de 0.87 ± 0.58 μW m^{-3} pour plus de 7,000 valeurs. Les mesures sur échantillons de surface prélevés le long de la traverse donnent une production de chaleur moyenne de 2.93 ± 2.42 μW m^{-3}, les mesures sur échantillons de carottes de forages donnent une moyenne de 1.79 ± 1.49 μW m^{-3} et les mesures sur échantillons de surface donnent une moyenne de 1.35 ± 1.63 μW m^{-3}. Ces valeurs élevées de production de chaleur obtenue sur les échantillons sont consistentes avec les mesures de flux de chaleur de la région de Sudbury qui sont plus élevées que la moyenne du Bouclier Canadien. La différence entre les résultats des levés aéroportés et des échantillons est probablement due à l'altération du mort-terrain.

Notre étude montre que les levés radiométriques ne sont pas susceptibles de fournir des estimations suffisament fiables pour calculer le flux de géo-neutrinos crustal, ainsi la production de chaleur crustale doit être calculée à partir des mesures de flux de chaleur et de production de chaleur sur des échantillons de surfaces et de carottes de forage.

Mots-clés : production de chaleur - flux de chaleur - flux de géo-neutrinos

Abstract

Crustal heat production must be estimated as precisely as possible for future experiments on geo-neutrinos envisaged at the Sudbury Neutrino Observatory (SNOLAB).

We compare estimates of crustal heat production in the Sudbury region from airborne radiometric surveys, from measurements on core samples from mining exploration drill holes, from measurements on surface samples and from measurements on samples collected on a transect. Airborne surveys have a high spatial resolution (1000 m) and they show a correlation with the regional geology but these data are only sensitive to the very shallow part of the crust. They give a mean heat production of 0.87 ± 0.58 μW m^{-3} for more than 7,000 values. Measurements on surface rock samples collected on the transect yield an average heat production of 2.93 ± 2.42 μW m^{-3}, measurements on core samples from drill holes give a mean of 1.79 ± 1.49 μW m^{-3}, and surface samples yield an average of 1.35 ± 1.63 μW m^{-3}. These high heat production values obtained on samples are consistent with heat flux measurements in the Sudbury area that are higher than the average Canadian Shield. The difference between results from airborne surveys and samples are perhaps due to the alteration of the overburden.

Our study shows that the airborne radiometric surveys are not likely to provide the reliable estimates needed to calculate the crustal geo-neutrino flux, and that crustal heat production must be calculated from heat flux and heat production measurements on rock and core samples.

Keywords : heat production - heat flux - geo-neutrino flux

1.1 Introduction

The global energy budget of the Earth and all its components has been studied for many decades. The Earth is a non-equilibrium system. The total outgoing flux of energy through the Earth's surface is not balanced by the internally produced energy. This difference is equal to the secular cooling of the Earth. To balance this budget and estimate the secular cooling rate, we need to obtain good estimates of each term that contributes to the Earth's energy budget.

The total energy loss of the Earth is well established at 46 ± 2 TW (Jaupart et al., 2007). This value is determined by the sum of the continental and oceanic heat fluxes of 14 and 32 TW, respectively. On the other hand we do not know precisely the relative contribution of all the components of this budget. The most important terms are the Earth radiogenic heat production, which is divided between the mantle and crust, and the secular cooling of the core and mantle. So far, the only well established term is the crustal heat production with 7 TW (Jaupart et al., 2007).

One approach to estimate the secular cooling rate is to constrain the mantle heat production contribution through different geochemical models of Bulk silicate Earth (BSE) (Hart and Zindler, 1986; McDonough and Sun, 1995; Palme and O'Neill, 2003; Arevalo et al., 2009). These have lead to a mantle contribution of 13 TW with an uncertainty of 20% (Jaupart et al., 2007). This uncertainty is high and leaves a large doubt on our understanding of the Earth's energy budget and its evolution. To improve our understanding of the energy budget of the Earth and to better assess the secular cooling rate, we need to obtain better estimates of the radiogenic mantle's contribution.

The recent improvement made in underground neutrino observatories might be the key for direct determination of the mantle heat production (Kobayashi and Fukao, 1991; Rothschild et al., 1998; Raghavan et al., 1998; Fiorentini et al., 2003; Mantovani et al., 2004; Fiorentini et al., 2005; Dye et al., 2006; Enomoto, 2006; Enomoto et al., 2007; Dye and Guillian, 2008; Dye, 2010). A neutrino observatory is located in Canada : the Sudbury Neutrino Observatory (SNOLAB). The upgrade and the launching of the SNO+ phase, which

consist of using a large liquid scintillator detector, will allow the observation of low energy geo-neutrinos (>1.8 MeV) from radioactive elements, uranium and thorium.

The first experimental geo-neutrino study was reported at the Kamioka observatory in Japan (Araki, T., and 86 collaborators, 2005). Their result is consistent with predictions made from Earth models, but the uncertainty on the heat production from U and Th remains very large. The geo-neutrino flux detected was low due to the low radioactivity of the Japan crust, strong noise of nearby nuclear reactors and the detector's radioactivity. However, this first result has demonstrated that geo-neutrinos have the ability to constrain the radioactivity of the Earth's interior. Other geo-neutrino experiments were conducted at the Laboratori Nazionali del Grande Sasso in Italie (Bellini, G., and 89 collaborators, 2010). They were able to observe a higher geo-neutrino rate compared to the first experiment since the Borexino detector is affected by a lower number of background events. They observed a higher geo-neutrino rate ($3.9^{+1.6}{}_{-1.3}$ events/(100 ton.yr)) than current BSE predictions of 2.5 ± 0.2 and 3.6 events/(100 ton.yr) from Fogli et al. (2005) and Rothschild et al. (1998), respectively. However the uncertainty is still too large to lead to definitive conclusions.

To determine the radioactivity and the composition of the mantle from results to be obtained during future experiments planned at SNOLAB, the geo-neutrino flux of the crust in the vicinity of SNOLAB must be estimated as accurately as possible.

Enomoto et al. (2007) have tried to constrain the crustal geo-neutrino component by summing the heat production contribution of the different geological units around KamLAND. Even with all the geological and geophysical studies that were made in the Sudbury region, the deep crustal composition around the observatory remains ambiguous and leaves high uncertainty on the crustal geo-neutrino flux calculation using this method (Perry et al., 2009). Another method from Fiorentini et al. (2005) relies on global crustal models along with geochemical studies on U, Th, and K distribution in the Earth's interior. Their model neglects lateral heterogeneities, since their estimate of geo-neutrino flux variation is generally associated with crustal thickness (Perry et al., 2009).

Perry et al. (2009) show how one can rely on heat flux and heat production measurements to calculate the crustal geo-neutrino flux. In the Sudbury region, some heat flux and

heat production data are available. But the density of these measurements is insufficient to precisely calculate the crustal geo-neutrino flux. Airborne radiometric surveys are also available in the Sudbury area. These surveys have high spatial resolution and they cover large areas. Using these data to calculate the heat production of the crust would greatly facilitate the task by reducing field and laboratory measurements. Before doing that we must determine whether these data are sufficiently reliable to assess the crustal heat production with the accuracy needed in order to calculate the crustal geo-neutrino flux?

The main objective of this work is to compare crustal heat production determined from airborne radiometric survey dataset with heat production measurements made on surface and core samples through geochemical analysis. To do so, we used radiometric dataset collected during an airborne survey over the Sudbury area, heat production measurements made on surface samples (Lewis and Bentkowski, 1988), heat production measurements made along a transect (Schneider et al., 1987) and heat production measurements made on core samples from mining exploration drill holes (Jessop and Lewis, 1978; Drury and Taylor, 1986; Pinet et al., 1991; Perry et al., 2009).

1.2 Geological context

The Sudbury Neutrino Observatory is located on the south range of the worlds largest preserved impact melt sheet, which is known as the Sudbury Igneous Complex (SIC), the host of important nickel deposits. More precisely, the SNOLAB detector is situated at 46.475^{o}N and 81.201^{o}W, 2039 meters below the surface in the Creighton's nickel mine owned by Vale INCO.

The SIC is the consequence of a meteoric impact that occurred at approximately 1.8 Ga in the PaleoProterozoic era (Krogh et al., 1984). Its extraterrestrial nature was long debated until the discovery of shock metamorphisms features (Dietz, 1964). The SIC is located at the contact of the Neo-Archean basement rocks of the Superior Province and the low grade metamorphosed sediments of the Huronian supergroup, part of the PaleoProterozoic Southern Province (Figure 1.1). Located about 15 kilometers southeast of the structure is the Grenville front. This late Proterozoic orogeny has given the basin its present elliptical

shape (Dietz, 1964).

The main geological units characterizing the Sudbury structure are the post impact sediments of Whitewater group, which filled the central depression, the underlying Sudbury Igneous Complex (SIC) and the footwall brecciated rocks (basement rocks) (Figure 1.2). Figure 1.2 was modified from Ames et al. (2006).

The Whitewater group is composed of three main sedimentary formations. From inside out are the Chelmsford, the Onwatin and the lowermost Onaping formations (Figure 1.2). The Chelmsford formation is composed of turbiditic wacke and siltstone while the Onwatin formation is mostly constituted of carbonaceous and pyritic argilite and siltstone. The Onaping formation originated from the fallback material excavated during the impact. It is composed of "glass-rich" breccias and many inclusions of granitic basement rocks (French, 1967). The SIC consists of an upper zone of granophyre, a thin middle layer (Transition Zone) of quartz gabbro and a lower zone of norite.

The northern footwall rocks comprise the Neoarchean Levack gneiss complex, which form a wide belt surrounding the north and east ranges of the SIC, and the intruding granite of the Cartier Batholith. About 20 km northwest of the structure, the Batholith is intruded by the metavolcanic and metasedimentary rocks of the Benny east-west-trending greenstone belt. South of the Benny belt are exposed, as isolated outliers, some Huronian rocks and some Nipissing diabase.

Meldrum et al. (1997) have shown that the Cartier Batholith is anomalously enriched in both U and Th; average values are over 5 and 33 ppm, respectively compare to the average continental crust concentration of 1.3 and 5.6 ppm (Rudnick and Gao, 2003). They propose that the Batholith was issued from partial melting of the Levack Gneiss Complex. They also reported that a detailed radiometric survey (unpublished) has also demonstrated the high level of radioactive elements present in the Batholith compared to the Levack Gneiss complex, SIC and Benny Belt rocks.

The southern footwall is located between the SIC and the Grenville front and is composed of the metasediment and metavolcanic rocks of the lower groups of the Huronian Supergroup,

lower and upper Elliot Lake and Hough Lake. Enclosed in the lower Elliot Lake group, on the south range of the structure, are found the Creigton and Murray granitic plutons. East of the SIC are found the Cobalt Lake and Quirke Lake groups. All these groups are intruded by the Nipissing diabases. The Chief Lake Igneous Complex (CLIC) is found about 20 km south of the structure, near the Grenville Front.

Meldrum et al. (1997) also proposed that uranium-rich paleoplacer deposits (Elliot Lake and Agnew Lake) as well as uraniferous detritus found in the Huronian Supergroup are due to the uplift and unroofing of the Batholith since they have mineralogical and geochemical characteristics in common. Easton (2009) reported the present of conglomerate units with uranium mineralization within the Elliot Lake group deposited by a northwest to southeast paleoflow. He suggested that these targets are not accessible to airborne surveys since due to their shallow to moderate dips.

1.3 Thermal regime

The Canadian Shield has been stable for > 1 Gy and its thermal regime is in steady state. heat flux below the upper crust is roughly constant with a value of 33 mW m^{-2} and the Moho heat flux varies in the narrow range of 12-18 mW m^{-2} (Jaupart and Mareschal, 1999; Mareschal and Jaupart, 2004). Thus, the lateral variations observed in surface heat flux measurements, which vary from 80 mW m^{-2} to 23 mW m^{-2} in the Canadian Shield, reflects the heat generated $< H >$ in the crustal layer as :

$$< H >= \frac{(Q - Q_m)}{Z_m} \tag{1.1}$$

where Q is the surface heat flux, Q_m is the Moho heat flux and Z_m is the crustal thickness.

So far, heat flux measurements were made at 13 sites in the Sudbury region (see Table 1.1 for an overview of measurements and Figure 1.4 for their location). The heat flux varies between 43 mW m^{-2} and 61 mW m^{-2}, and is considerably higher than the average heat flux of 42 mW m^{-2} of the Canadian Shield (Figure 1.3 and 1.4). This high heat flux is due to local upper crustal radio elements enrichment. This enrichment will have consequences

for the geo-neutrino studies planned at SNOLAB because of the high crustal geo-neutrino flux, perhaps as much as 50% higher than the average Shield (Perry et al., 2009).

The Sudbury heat flux values were obtained from a compilation of all the heat flow data available in the Sudbury region from (Perry et al., 2009) as well as three nearby sites, Elliot Lake (Sass et al., 1968), East Bull Lake (Drury and Taylor, 1986), and Sturgeon Falls (Pinet et al., 1991) (see Figure 1.1 for their location). The latter sites are located further away from Sudbury but they are worth mentioning because their high heat flux indicate that the crustal radioactivity is high in a wide area around Sudbury.

1.4 Airborne gamma-ray spectrometry and heat production

1.4.1 Airborne gamma-ray

Gamma-ray spectrometry is a powerful tool that permits to detect the environmental radioactivity. The method consists of measuring gamma-rays released during the spontaneous decay of radioactive elements (in particular, K, U, Th). Gamma-rays are high energy photons that can travel up to several hundred meters in air and more than 30 centimeters in rocks (Grasty et al., 1979). Thus, gamma-ray spectrometry provides an efficient tool for detecting and mapping the concentration of radioactive elements present at the Earth's surface but have no significant depth of penetration.

Gamma-ray spectrometry was first used for uranium exploration and with the latest instrumental and procedure advances, has become a general tool useful in several geoscience disciplines (IAEA, 2003). Radiometric surveys can be completed on the ground or in the air. Airborne radiometric surveys can quickly cover a broad region and can be accompanied by using a multi-sensory spectrometer, to measure other geophysical variables such as magnetic and electromagnetic data. Such methods are very effective for geological mapping, provided the superficial stratum has not been sheltered by transported sediments.

1.4.2 Previous studies

Data collected during airborne gamma-ray surveys were used to estimate the crustal heat production in the well exposed granite-greenstone terrane of the Achaean Pilbara Craton, Western Australia by Bodorkos et al. (2004). These authors investigated the accuracy and potential of these data to estimate crustal heat production by comparing results with heat production determined by geochemical analysis on ground samples. They found that airborne surveys lead to area-average heat production 10 to 50% lower than heat production calculated through geochemical analysis on bedrock samples. They concluded that the lower heat production from surveys is due to K depletion from weathering in the overburden and U enrichment or depletion due to a disequilibrium in the U-238 decay chain (Bodorkos et al., 2004).

Kukkonen (1989) has assessed the heat production of the bedrock in the Baltic Shield of Finland. The number of unperturbed heat flux measurements and core samples heat production measurements available in the region was insufficient for the purpose of its work. Consequently, an alternative approach was needed. Following Vaittinen (1986), he used glacial till samples instead of airborne radiometric dataset. In his work, Vaittinen has compiled apparent heat production maps for a few test areas using airborne gamma-ray spectrometry. He concluded that airborne measurements are highly sensitive to overburden and vegetation effects and are therefore very difficult to combine with drill hole data.

1.4.3 Factors perturbing gamma-ray spectrometry

Some environmental factors such as air density changes, temperature inversion layer or soil moisture can influence gamma-ray spectrometry but they can easily be avoided by not investigating in the early morning or just after a rainfall. Other effects are not escapable and must be considered in the interpretation of surveys. Weathering modifies the concentration and distribution of the radioelements relative to that of fresh bedrock. Knowledge of the specific behavior of K, Th and U elements in weathered environments is important for a good interpretation. The concentration of K generally decreases with increasing weathering.

K is a highly soluble element and gets easily leached from the weathering profile (Curtis, 1976). On the other hand, Th is normally retained. This is illustrated in very high weathered materials such as bauxitic soils, where a high-Th concentration is usually observed (Wilford, 1995). Uranium is relatively soluble under oxidizing conditions but is retained or precipates in reducing environments. Thus, U is easily leached from rocks, but may be deposited in sediments nearby. Usually in advanced stages of weathering U is leached from the profile relative to fresh rocks.

1.4.4 Interpretation of gamma-ray spectrometry

The interpretation of airborne radiometric surveys reposes on the variation of K, Th and U elements over the studied area. But in regions of varying level of alteration an examination of derived products such as ratios and ternary maps may reinforce understanding of radioelements concentration variation. The ternary RBG (Red, Blue, Green) image and ratios are useful for illustrating the relationship between weathered and unweathered areas. In the RBG image, regions of bright green color illustrates high level of weathering and in contrast red color indicates region poorly affected by weathering. Black to brown regions indicate low concentration in 3 radioelements (K, Th and U) while white regions illustrate a high level of these elements.

1.4.5 Application to our study

Since 1967, a Federal/Provincial cooperation program (Uranium reconnaissance program) has completed hundreds of surveys across Canada to support mapping and mineral exploration (Darnley et al., 1975). Data collected during these investigations are available in the Geoscience data repository of the Geological Survey of Canada as a series of open files.

Uranium reconnaissance program's surveys have, in general, been completed using a fixed wing sky van aircraft, at ground clearances of about 120 meters and at flight speed of 120 knots (about 155 m/s). Gamma-ray spectra were sampled at 1 second intervals using a

256 channels spectrometer accorded to a large detector volume (50 litres of NaI crystals). The standard procedure is detailed in Bristow (1983). The primary results obtained are displayed in the form of an energy spectrum within the energy range 0-3 MeV. These raw measurements are monitored over four spectral windows, three centered at 1.46 MeV for potassium (K), at 2.61 MeV for thorium (Th), at 1.76 MeV for uranium (U) and the total count covering the full spectral range of these elements. Raw acquisitions are then corrected from undesirable variables, stripped and adjusted for attenuation with height and finally converted to equivalent concentration of radioelement at ground level. Calibration and data processing procedure are detailed in Minty (1997).

In this work we used a airborne survey conducted in the Sudbury area, in 1989 with a resolution of 1000 meters. The survey covers the region comprise between -80.53 to -81.93 degrees in longitude and 46.22 to 47.03 degrees in latitude.

The data file for this survey contains the latitude, longitude, time, date, and altitude at which data were recorded and the following radiometric variables : Potassium (K, %), equivalent Uranium (eU, ppm), equivalent Thorium (eTh, ppm) and the total air absorbed dose rate (NADR, nGy/h) as well as five derived products (ratios, ternary and natural air absorbed dose rate).

From these data we calculated the heat generated from radioactive decay by summing the total contribution of each radioactive elements with the following formula :

$$H = 10^{11}(9.52[U] + 2.56[Th] + 3.48[K]) \tag{1.2}$$

where [U] and [Th] are the uranium and thorium concentration in ppm and [K] is the potassium concentration in %. Heat production is calculated in Wkg^{-1}. To calculate heat production per unit volume, A, we use an average crustal density of 2700 kg m^{-3}.

$$A = 0.257[U] + 0.069[Th] + 0.094[K] \tag{1.3}$$

where A is the heat production per unit volume in μW m^{-3}.

Resulting heat production calculated from gamma-ray measurements is shown on a map (Figure 1.5). This map was made by averaging airborne radiometric data over 0.01° x 0.01° cells over a region of 0.6 degrees in latitude and 1.5 degrees in longitude more or less centered on SNOLAB.

We found low heat production values within the Sudbury structure, the Southern and the Grenville Provinces, and higher values in the Superior Province, northwest and west of the structure. The average heat production within the Sudbury region determined from these data is $0.87 \pm 7.5 \times 10^{-5}$ μW m^{-3} with a standard deviation of 0.58 μW m^{-3} (Figure 1.6). This average was calculated from cell averages, over 7000 values.

Figure 1.7, 1.8 and 1.9 show the individual K, Th and U concentration maps, respectively. They correlate together as well as with the heat production map (Figure 1.5).

High heat production areas northwest and west of the structure, in the Superior Province, is associated with the granites of the Cartier Batholith. Heat production decreases north of the Batholith where lie the metasedimentary and metavolcanic rocks of the Benny belt and isolated outliers of the Huronian rocks and Nipissing diabase. The high heat production of the Superior Province is also marked at the border with the Southern Province southwest of the structure (well defined heat production contrasts fit the geological boundary).

In the Sudbury basin, the heat production within the Onaping formation is slightly higher than the heat production in the Onwatin and Chelmsford formations. This is probably due to the fact that many inclusions of granitic basement rocks are found within this formation. This is well marked in the U-concentration map where the Onaping formation shows a much greater concentration of uranium compared with the surrounding norite/granophyre of the SIC and the sediments of the Onwatin and Chelmsford formations (Figure 1.9). This effect is also observable on the thorium map (Figure 1.8). High heat production values are locally found just south of the structure, in two main areas located east and west of SNOLAB. These anomalies are well correlated with the granites of the Creigton-Murray plutons. A high heat production anomaly is found just north of the Grenville front, in the Southern Province. This anomaly is associated with the granitoid of the CLIC.

The mean Th/U ratio, determined from cell averages (1587 cell values), is 6.8 ± 1.6 with a standard deviation of 2.57 (Figure 1.11). We have calculated Th/U ratio since U has the most important impact in the heat generation. To do this, we have excluded all U values lower than 0.1 ppm so the result will not be biased by very high Th/U local anomalies. Th/U ratio was then calculated by averaging airborne radiometric data over 0.025° x 0.025° cells. The resulting map (Figure 1.10) show that Th/U ratio is on average constant within the structure and increases northwest and west of the structure. These high Th/U ratio anomalies are well correlated with the high heat production areas corresponding to the Cartier Batholith. Th/U ratio in the Batholith varies over a wide range; from 8 to more than 20. In the western part of the Batholith Th/U ratio is decreasing. The high Th/U anomaly in the Batholith seems to extend within the Levack complex. Higher Th/U ratio is also spotted in the CLIC.

Figure 1.12 shows the resulting K/Th ratio map. This map was made with the same procedure used to make the Th/U map. We observe that K/Th ratio is consistent with Th/U ratio (lower values within the Batholith and Chief Lake complex). On the other hand, the Creigton-Murray plutons show lower K/Th ratios, which do not appear on the Th/U map. The Onaping formation also seem to have slightly lower K/Th values. Mean K/Th ratio is 2871 with a standard deviation of 1099 based on 1586 values (Figure 1.13). The K/Th ratio in the Cartier Batholith is averaging 1000.

The ternary RGB image (Figure 1.14) confirms these observations. The Cartier Batholith is marked by a high level of thorium (bright green anomaly) relative to U and K. This is consistent with both, the Th/U and K/Th ratios observed in the Batholith. The western part of the Batholith contain many purple bluish spots which are consistent with the low Th/U ratio observed in this area. The CLIC and Creighton-Murray plutons are creamiest-white color representing a high level in three radioelements. Purple-bluish spots are found all over the Huronian rocks as well as the Onaping formation corresponding to a slightly higher level of uranium.

1.5 Heat production measurements from core and surface samples

In the Sudbury region many heat production measurements are available. Some of these measurements were made on core samples collected at heat flow sites or close by (Jessop and Lewis, 1978; Pinet et al., 1991; Drury and Taylor, 1986; Perry et al., 2009), some were made on surface samples from various locations (Lewis and Bentkowski, 1988), and others were made on surface samples collected along a SE-NW 17 km transect located in the Superior Province northwest of the structure (Schneider et al., 1987). For a general overview of all heat production measurements from core samples and surface samples (including the transect) refer to Table 1.2 and 1.3, respectively. The location of these measurements is shown on the heat production map from airborne survey (Figure 1.5). The map does not include the East Bull Lake and Sturgeon Falls sites which are located outside our study area.

From these samples, the concentration of U, Th and K was determined through laboratory analysis. The technique is described in Mareschal et al. (1989). Heat production was then calculated using the equation (1.3), which we previously used to determined the heat production from airborne gamma-ray spectrometry data in the above section.

1.5.1 Heat production distributions

Using all the available heat production measurements (Table 1.2 and 1.3) we examine how the heat production is distributed by rock type and by geological provinces (Table 1.4 and 1.5). We found that greywackes, granites and gneisses have higher heat production average than norites, gabbros, greenstones and anorthosites. These high heat production rocks are common in the Sudbury area, which is consistent with the high heat flux observed in the area. The Superior and Southern Provinces have high average heat production, which is consistent with their composition being granite and greywacke rich. Also, the mean heat production is higher outside the structure (2.1 μW m^{-3}) than inside (1.78 μW m^{-3}). This is consistent with the high heat production around the Sudbury structure in the Superior and Southern Provinces.

1.5.2 Heat production from core samples

From all the heat flow sites measured by the Geological Survey of Canada (Sudbury 1, Elliot Lake, Moose Lake, Onaping, Windy Lake, Victoria, Murray and Lockerby 1), heat production was determined only at Moose Lake (Jessop and Lewis, 1978). This site is located on the north range of the structure within the SIC. Average heat production of this site, determined from 11 core samples, is 1.43 μW m^{-3}. The lithology of these samples is not given. Other heat production measurements, from the Copper-Cliff and Sturgeon Falls sites, were published in Pinet et al. (1991). As mentioned above, the Sturgeon Fall site is located 80 km east from Sudbury in the Grenville Province. Its average heat production (1.55 μW m^{-3}) will not be included in the mean heat production calculation and the statistical analysis. Copper-Cliff is located in the Southern Province, between the structure and the Grenville front. The average heat production at this site is 3.2 μW m^{-3}. This value was determined from 7 core samples, which are all greywackes.

The East Bull Lake site is also located far from Sudbury (50 km west) in the Superior Province. Mean heat production determined at this site is 0.54 μW m^{-3}. This value was determined from 20 core samples, mostly consisting of anorthosite and gabbro (Drury and Taylor, 1986). As for the Sturgeon Falls, East Bull Lake average heat production will not be included in the analysis.

Recently heat production measurements were made at the Falconbridge, Lockerby Mine and Craig Mine sites (Perry et al., 2009). Craig Mine is located near Moose Lake (in the SIC). Its mean heat production value is 1.15 μW m^{-3} and was determined from 19 granophyre and norite core samples. Falconbridge is located just south of Wanapitei Lake, on the east rang of the structure within the SIC. Heat production at this site is 0.73 μW m^{-3} and was determined from 26 core samples, all norites. Finally, the Lockerby Mine site, which is located on the southern perimeter of the structure, just west of the Creighton pluton, exhibit a mean heat production of 3.53 μW m^{-3}. This value was determined from 20 core samples, all granites.

1.5.3 Heat production from surface samples

Surface heat production measurements were made by the Geological Survey of Canada. In majority, heat production at each site was determined from a single sample. Some values are an average of two or three samples. Most of the measurements are located within the structure. The heat production from these measurements varies from as low as 0.12 μW m^{-3} to as high as 3.32 μW m^{-3}. Lithological data are available for all samples, but one. They are either greenstones, gabbros, granites or gneisses. These data were published in Lewis and Bentkowski (1988).

There are two more surface heat production measurements published by Lewis and Bentkowski (1988), Windy Lake and Wanapitei Lake. Windy Lake is located at the border of the structure with the Superior Province within the Levack complex. Mean heat production, determined from three samples, is 3.33 μW m^{-3}. At Wanapitei Lake, which is located on the northeastern corner of the structure on the SIC and Onaping border, five samples were collected and the average heat production is 2.58 μW m^{-3}. Samples lithology from these two sites is unknown. These measurements will be discussed separately because their mean heat production is very high.

Other surface measurements were made along a SE-NW 17 km transect located in the Superior Province northwest of the structure. Sampling started at Windy Lake and extended to Cartier with samples collected at 0.5 km interval along highway 144. Along this transect, 34 granite/gneiss samples were collected and mean heat production obtained is 2.93 with a standard deviation of 2.42 μW m^{-3} (Schneider et al., 1987). Results show a systematic heat production increase with distance from the structure. The first dozen samples, located in the Levack Gneiss complex, have low heat production, usually lower than 1μW m^{-3}. In the middle of the transect, heat production varies greatly, from less than 1 μW m^{-3} to more than 7 μW m^{-3}. This seems to mark the transition between the Cartier Batholith and the Levack Complex. The last dozen of measurements in the Batholith are usually higher than 4 μW m^{-3} and exceed 8 μW m^{-3}at the far end of the transect. This low to high heat production transition is consistent with the Batholith being enriched in radioements relative to the Levack complex (Meldrum et al., 1997).

1.5.4 Heat production analysis

The average heat production calculated from all these measurements, for a total of 141 values, is 2.08 ± 0.013 μW m^{-3} with a standard deviation of 1.84 μW m^{-3} (Figure 1.15). This value seems high and we need to analyze the different groups of measurement separately. Although this high heat production average is consistent with the high heat flux of the region.

Mean heat production from all surface samples, which include the transect, Wanapitei Lake, and Windy Lake values, is 2.48 ± 0.04 μW m^{-3} with a standard deviation of 2.2 μW m^{-3}. This value was calculated from 58 samples (Figure 1.16a). Heat production measured on core samples yield an average of 1.79 ± 0.018 μW m^{-3} with a standard deviation of 1.49 μW m^{-3} for 83 samples (Figure 1.16b). The average heat production from surface samples is much higher than that of core samples. The average heat production calculated with samples from the transect, Wanapitei Lake, and Windy Lake is 2.91 ± 0.05 μW m^{-3} with a standard deviation of 2.26 μW m^{-3} for 42 samples (Figure 1.16a).

the mean heat production is higher outside the structure (2.1 μW m^{-3}) than inside (1.78 μW m^{-3})

Because the average heat production obtained from surface measurements from the transect, Wanapitei Lake and Windy Lake seems very high and perhaps biased, we have calculated the mean heat production from surface samples without these values. We obtained an average heat production of 1.35 ± 0.01 μW m^{-3} with a standard deviation of 1.63 μW m^{-3} (Figure 1.16c). This result seems more representative and is closer to the average determined from core samples (1.79 μW m^{-3}). Thus, the more accurate heat production measurements are given from core samples and surface samples (without the transect, Wanapitei Lake and Windy Lake values). Mean heat production from 99 core and surface samples is 1.81 ± 0.014 μW m^{-3} with standard deviation of 1.54 μW m^{-3} (Figure 1.15).

The same analysis was made for Th/U ratio values. Average Th/U ratio from all measurements (141 values) is 9.16 ± 0.08 with a standard deviation of 11.24. Mean Th/U ratio from the transect and Windy and Wanapitei Lake is very high (17.54± 0.41 with a standard

deviation of 17.38) and average was calculated from values varying over a wide range since the standard deviation is as high as the average. Average Th/U ratio excluding values from the transect, Wanapitei Lake and Windy Lake sites is 5.57 $\pm$ 0.03 with a standard deviation of 3.14 (Figure 1.17). Detailed histograms are shown in Figure 1.18.

1.6 Comparisons and conclusions

The average heat production in the Sudbury area estimated from airborne radiometric surveys dataset is 0.87 μW m^{-3}. Mean heat production determined from the core and surface samples, considered reliable, is 1.81 μW m^{-3}. This comparison demonstrates that airborne surveys underestimates the radioelements content. Since surveys are known to be only sensitive to the superficial layer, some process must have affected the level of radioelement contained in the upper layer. Weathering processes are likely to be responsible for heat production being underestimated within the superficial layer in the Sudbury region.

The best way to illustrate the level of weathering is the K/Th ratio since K is a mobile element easily leached while Th is immobile. In the K/Th ratio map (Figure 1.12), the Cartier Batholith, Levack complex and the Creighton-Murray Plutons are the areas most affected by weathering. This is also observed in the ternary map whereas the Batholith is marked by a bright green color anomaly. On the other hand the Levack complex white-greenish-blueish color illustrate a high level in Th and U and the Creighton-Murray Plutons white-pinkest color a high level in 3 radioelements. These regions have shown some sign of weathering but no obvious U loss compared to the Cartier Batholith. This illustrates the higher mobility of K compared to U. We found from airborne survey data an average K/Th of 2,871 which is consistent with the average crustal ratio of 2,500 McDonough and Sun (1995). Within the Cartier Batholith, the K/Th ratio is low with an average of 1000 and gets even lower north of the structure and in the western part of the Batholith.

The Th/U ratio map shows similiar trends but less pronounced in the western part of the Cartier Batholith and in the Levack complex (Figure 1.10). In contrast no Th/U anomalies are seen in the Creighton-Murray Plutons. These regions have been less affected by weathering than the Batholith and only have lost K content. Mean ratio calculated from

surveys dataset is 6.8 while Th/U ratio from core and surface samples measurements is 5.57.

It seems that the uranium content within the superficial layer has decreased more in the Cartier Batholith than in other units. This is consistent with the significantly lower heat production obtained from radiometric surveys since uranium is the radioactive element that contributes most to the heat generated by the rocks. Th/U ratio in the Batholith gets very high, over 20, much higher that the average crustal ratio of 4 (McDonough and Sun, 1995; Jaupart and Mareschal, 2003). This is coherent with geochemistry results illustrating that U loss has occurred in the Cartier Batholith, possibly through leaching, despite the already high estimates of U. (Meldrum et al., 1997).

On the ternary map we observe purple bluish color spots all over the Huronian rocks and the Onaping formation. The uranium rich conglomerates found in the Huronian Supergroups are attributed to uplift and unroofing of the Batholith. The eroded rocks were carried out by paleocurrents (Meldrum et al., 1997). These uranium rich conglomerates may be more abundant than indicated by the airborne survey maps because of their depth and their low to moderate dips (Easton, 2009). Within the Onaping formation, the slightly lower K/Th ratio indicates that the formation has been affected by some weathering, but the reducing nature of these sediments has prevented uranium from being leached. Overall U loss have affected mainly the Cartier Batholith.

Our study shows that the airborne radiometric surveys are not likely to provide the reliable estimates needed to calculate the crustal geo-neutrino flux. Mean heat production calculated from surveys is very low, half the average measured on core and surface samples. In the Sudbury region, the ground has been affected by weathering. Under such conditions, U and K are easily leached and their concentration and distribution is lower than in fresh rocks.

Therefore, to determine the crustal geo-neutrino flux, the crustal radioactivity must be calculated from heat flow and heat production measurements on rock and core samples.

The Sudbury region is well known and documented since it has been explored for its mineral potential. Hence, all the available drill holes in the region offer the opportunity to

well calculate the crustal radioactivity from heat flux measurements. A very good knowledge of the radioelement content in the crust will allow us to establish with high precision the crustal contribution to the geo-neutrino flux in the vicinity of SNOLAB. The majority of existing heat flux values are located in the impact structure and in the Southern Province; very few have been obtained farther away. Our next goal is to provide measurements in the area where the heat flux has not been measured, outside the structure and mostly within the Cartier Batholith.

Acknowledgements

This work was supported by NSERC discovery grants to Claire Perry and Jean-Claude Mareschal. We are grateful to the Geological Survey of Canada for providing and maintaining the Geoscience data repository.

References

Ames, D. E., Singhroy, V., Buckle, J., Molch, K., 2006. Geology, Integrated Bedrock Geology-Radarsat-Digital Elevation. Data of Sudbury, Ontario; Geol. Surv. Can., Open File Report 4571.

Araki, T., and 86 collaborators, 2005. Experimental investigation of geologically produced antineutrinos with KamLAND. Nature 436, 499–503.

Arevalo, R., McDonough, W. F., Luong, M., Feb. 2009. The K/U ratio of the silicate Earth : Insights into mantle composition, structure and thermal evolution. Earth Planet. Sci. Lett. 278, 361–369.

Bellini, G., and 89 collaborators, 2010. Observation of geo-neutrinos. Phys. Lett. B 687, 299–304.

Bodorkos, S., Sandiford, M., Minty, B. R. S., Blewett, R. S., 2004. A high-resolution, calibrated airborne radiometric dataset applied to the estimation of crustal heat production in the Archaean northern Pilbara Craton, Western Australia. Precambrian Res. 128, 57–82.

Bristow, Q., 1983. Airborne gamma-ray spectrometry in uranium exploration. Principles and current practice. Int. J. Appl. Radiat. Isot. 32 (1), 199–229.

Chouinard, C., Mareschal, J.-C., Jan. 2009. Ground surface temperature history in southern Canada : Temperatures at the base of the Laurentide ice sheet and during the Holocene. Earth Planet. Sci. Lett. 277, 280–289.

Curtis, C. D., 1976. Chemistry of rock weathering : fundamental reactions and controls. In : Derbyshire, E. (Ed.), Geomorphology and Climate. Vol. 48. John Wiley Sons, Ltd, London, pp. 25–57.

Darnley, A. G., Cameron, E. M., Richardson, K. A., 1975. The Provincical-Federal Uranium Reconnaissance Program. In : Uranium exploration 1975. Geol. Surv. Can., Paper 75–26, pp. 49–68.

Dietz, R. S., 1964. Sudbury structure as an astrobleme. J. Geol. 72, 412–434.

Drury, M., Taylor, A., 1986. Some new measurements of heat flow in the Superior Province of the Canadian Shield. Can. J. Earth Sci. 24, 1486–1489.

Dye, S. T., Aug. 2010. Geo-neutrinos and silicate Earth enrichment of U and Th. Earth Planet. Sci. Lett. 297, 1–9.

Dye, S. T., Guillian, E., Learned, J. G., Maricic, J., Matsuno, S., Pakvasa, S., Varner, G., Wilcox, M., Dec. 2006. Earth Radioactivity Measurements with a Deep Ocean Anti-neutrino Observatory. Earth Moon and Planets 99, 241–252.

Dye, S. T., Guillian, E. H., Jan 2008. Estimating terrestrial Uranium and Thorium by antineutrino flux measurements. Proc. Nat. Acad. Sci. USA 105, 44–47.

Easton, R. M., 2009. Compilation mapping, Pecors-Whiskey Lake area, Superior and Southern Provinces ; in Summary of Field Work and Other Activities. Ont. Geol. Surv., Open File Report 6240, 10.1–10.21.

Enomoto, S., 2006. Experimental Study of Geoneutrinos with KamLAND. Earth Moon and Planets 99, 131–146.

Enomoto, S., Ohtani, E., Inoue, K., Suzuki, A., 2007. Neutrino geophysics with KamLAND and future prospects. Earth Planet. Sci. Lett. 258, 147–159.

Fiorentini, G., Lissia, M., Mantovani, F., Vannucci, R., 2005. Geo-neutrinos : a new probe of Earth's interior [rapid communication]. Earth Planet. Sci. Lett. 238, 235–247.

Fiorentini, G., Mantovani, F., Ricci, B., Apr. 2003. Neutrinos and energetics of the Earth. Physics Letters B 557, 139–146.

Fogli, G. L., Lisi, E., Palazzo, A., Rotunno, A. M., 2005. KamLAND neutrino spectra in energy and time : Indications for reactor power variations and constraints on the georeactor. Phys. Lett. B 623, 80–92.

French, B. M., May 1967. Sudbury structure, Ontario : Some petrographic evidence for origin by meteorite impact. Science 156, 1094–1098.

Grasty, R. L., Kosanke, K, L., Foote, R. S., Aug. 1979. Fields of view of airborne gamma-ray detectors. Geophysics 44 (8), 1447–1457.

Hart, S. R., Zindler, A., 1986. In search of a bulk-Earth composition. Chem. Geol. 57, 247–267.

IAEA, 2003. Guidelines for radioelement mapping using gamma-ray spectrometry data. IAEA-TECDOC-1363, Vienna, Austria. 173 pp.

Jaupart, C., Labrosse, S., Mareschal, J.-C., 2007. Temperatures, heat and energy in the mantle of the Earth. In : Bercovici, D. (Ed.), Treatise on Geophysics, The Mantle. Vol. 7. Elsevier, New York, pp. 253–303.

Jaupart, C., Mareschal, J.-C., 1999. The thermal structure and thickness of continental roots. Lithos 48, 93–114.

Jaupart, C., Mareschal, J.-C., 2003. Constraints on crustal heat production from heat flow data. In : Rudnick, R. L. (Ed.), Treatise on Geochemistry, The Crust. Vol. 3. Permagon, New York, pp. 65–84.

Jessop, A. M., Jan. 1971. The distribution of glacial perturbation of heat flow in Canada. Canadian Journal of Earth Sciences 8, 162–166.

Jessop, A. M., Lewis, T. J., 1978. Heat flow and heat generation in the Superior Province of the Canadian Shield. Tectonophysics 50, 55–57.

Kobayashi, M., Fukao, Y., Apr. 1991. The Earth as an antineutrino star. Geophys. Res. Lett. 18, 633–636.

Krogh, T. E., Davis, D. W., Corfu, F., 1984. Precise U-Pb zircon and baddeleyite ages for the Sudbury ares. In : Pye, E. G., Naldrett, A. J., Gilbin, P. E. (Eds.), The Geology and Ore Deposits of the Sudbury Structure. Vol. Special 1. Ont. Geol. Surv., pp. 431–446.

Kukkonen, I. T., 1989. Terrestrial heat flow and radiogenic heat production in Finland, the central Baltic Shield. Tectonophysics 164, 219–230.

Lewis, T. J., Bentkowski, W. H., 1988. Potassium, uranium and thorium concentrations of crustal rocks : a data file. Geol. Surv. Can., Open File Report 1744, 165 pp.

Mantovani, F., Carmignani, L., Fiorentini, G., Lissia, M., Jan. 2004. Antineutrinos from Earth : A reference model and its uncertainties. Phys. Rev. D 69 (1), 013001.

Mareschal, J.-C., Jaupart, C., Jun. 2004. Variations of surface heat flow and lithospheric thermal structure beneath the North American craton. Earth Planet. Sci. Lett. 223, 65–77.

Mareschal, J.-C., Pinet, C., Gariepy, C., Jaupart, C., Bienfait, G., Dalla-Coletta, G., Jolivet, J., Lapointe, R., 1989. New heat flow density and radiogenic heat production data in the Canadian Shield and the Quebec Appalachians. Can. J. Earth Sci. 26, 845–852.

McDonough, W. F., Sun, S. S., 1995. The composition of the Earth. Chem. Geol. 120, 223–253.

Meldrum, A., Abdel-Rahman, A.-F. M., Wodicka, N., 1997. Documentation of a 1450 Ma contractional orogeny preserved between the 1850Ma Sudbury impact structure and the 1 Ga Grenville orogenic front, Ontario, Canada. Precambrian Res. 82, 265–285.

Minty, B. R. S., 1997. Fundamentals of airborne gamma-ray spectrometry. AGSO J. Aust. Geol. Geophys. 17, 39–50.

Misener, A., Thompson, L., Uffen, R., 1951. Terrestrial heat flow in Ontario and Quebec. Trans. Am. Geophys. Union 36, 1055–1060.

Palme, H., O'Neill, H. S. C., 2003. Cosmochemical estimates of mantle composition : Mantle and Core. In : Holland, H., Turekian, K. K. (Eds.), Treatise on Geochemistry. Vol. 2. Elsevier, New York, pp. 1–38.

Perry, H. K. C., Mareschal, J.-C., Jaupart, C., Oct. 2009. Enhanced crustal geo-neutrino production near the Sudbury Neutrino Observatory, Ontario, Canada. Earth Planet. Sci. Lett. 288, 301–308.

Pinet, C., Jaupart, C., Mareschal, J.-C., Gariepy, C., Bienfait, G., Lapointe, R., Nov. 1991. Heat flow and structure of the lithosphere in the eastern Canadian shield. J. Geophys. Res. 96, 19,941–19,963.

Raghavan, R. S., Schoenert, S., Enomoto, S., Shirai, J., Suekane, F., Suzuki, A., Jan. 1998. Measuring the Global Radioactivity in the Earth by Multidetector Antineutrino Spectroscopy. Phys. Rev. Lett. 80, 635–638.

Rothschild, C. G., Chen, M. C., Calaprice, F. P., Apr. 1998. Antineutrino geophysics with liquid scintillator detectors. Geophys. Res. Lett. 25, 1083–1086.

Rudnick, R. L., Gao, S., 2003. Composition of the continental crust. In : Rudnick, R. L. (Ed.), Treatise on Geochemistry, The Crust. Vol. 3. Permagon, New York, pp. 1–64.

Sass, J. H., Killeen, P. G., Mustonen, E. D., Dec. 1968. Heat flow and surface radioactivity in the Quirke Lake Syncline near Elliot Lake, Ontario, Canada. Can. J. Earth Sci. 5, 1417–1428.

Schneider, R. V., Roy, R. F., Smith, A. R., 1987. Investigations and interpretations of the vertical distribution of U, TH, and K : South Africa and Canada. Geophys. Res. Lett. 14, 264–267.

Vaittinen, T., 1986. Regional radiogenic heat production in Finland as determined with the help of airborne gamma ray measurements. M. Sc. thesis, Helsinki university of technology, department of mining and metallurgy, 62 pp.

Wilford, J. R., 1995. Airborne gamma-ray spectrometry as a tool for assessing relative landscape activity and weathering development of regolith, including soils. AGSO Res. Newslett. 22, 12–14.

Table 1.1
Location and heat flux for all the Sudbury sites

Site hole	Latitude North	Longitude West	Q (mW m^{-2})	Reference
Sudbury 1	46°28	81°11	51	(1)
Elliot Lake	46°30	82°30	60	(2)
67001 Moose Lake	46°39	81°18.2	49	(3)
67002 Onaping	46°37.7	81°23.3	56	(3)
67003 Windy Lake	46°36.6	81°25.8	43	(3)
67005 Victoria	46°24.8	81°23.7	55	(3)
67006 Murray	46°30.9	81°05.1	51	(3)
67007 Lockerby 1	46°26	81°19.3	61	(3)
East Bull Lake	46°26	82°13	56	(4)
Copper-Cliff	46°26.4	81°03.93	59	(5)
Sturgeon Falls	46°26.6	79°56.8	44	(5)
Falconbridge	46°39.1	80°47.5	49	(6),(7)
Lockerby Mine	46°26	81°18.92	59	(6),(7)

Q is the site averaged heat flux value. These values were adjusted for post glacial warming following the model of Jessop (1971).
References : (1) Misener et al. (1951), (2) Sass et al. (1968), (3) Jessop and Lewis (1978), (4) Drury and Taylor (1986), (5) Pinet et al. (1991), (6) Chouinard and Mareschal (2009), (7) Perry et al. (2009).

Table 1.2
Heat production at the heat flow sites

Site	Rocktype	Province	U (ppm)	Th (ppm)	K (%)	Th/U	A (μW)	σ_A (m^{-3})	N_A	Ref
67001 Moose Lake	-	in structure	2.1	10.0	1.7	4.47	1.43	0.98	11	(1)
Copper-Cliff	Greywacke	Southern	6.8	16.5	2.2	2.37	3.2	0.8	7	(2)
Sturgeon Falls	Granite/Gneiss	Grenville	1.05	6.45	3.7	6.14	1.55	0.28	2	(2)
East Bull Lake	↓	**Superior**	**0.74**	**4.23**	**0.61**	**3.52**	**0.54**	**0.57**	**20**	**(3)**
"	Anorthosite	"	0.49	1.65	0.64	3.42	0.3	0.17	10	(3)
"	Gabbro	"	0.97	7.87	0.53	7.05	0.86	0.8	9	(3)
"	Granite	"	1.28	2.46	1.43	1.92	0.64	-	1	(3)
Craig Mine[a]	↓	**in structure**	**1.72**	**8.07**	**1.62**	**5.83**	**1.15**	**0.79**	**19**	**(4)**
"	Granophyre	"	2.95	13.8	2.71	5.28	1.97	0.19	9	(4)
"	Norite	"	0.76	3.68	0.78	6.32	0.52	0.12	10	(4)
Falconbridge	Felsic norite	in structure	1.1	5.4	0.9	5.66	0.73	0.2	26	(4)
Lockerby Mine	Granite porphyry	in structure	5.4	26.5	3.2	5.44	3.53	1.4	20	(4)

[a] Craig Mine is located near the Moose Lake site.
U and Th are Uranium and Thorium concentration in ppm, K is Potassium concentration in per cent, A and σ_A are the heat production and its standard deviation in μW m^{-3}, respectively and N_A is the number of samples. Bold characters indicate the average value of the site (for all rocktypes), for sites where more than one type of rock is encountered.
References : (1) Jessop and Lewis (1978), (2) Pinet et al. (1991), (3) Drury and Taylor (1986), (4) Perry et al. (2009).

Table 1.3
Heat production from surface samples and Cartier transect

Site		Rocktype	Province	U	Th	K	Th/U	A	σ_A	N_A	Ref
Lat (N)	Long (W)			(ppm)	(ppm)	(%)		(μW)	(m^{-3})		
46°25	81°24	Greenstone	in structure	0.36	0.95	0.28	2.64	0.19	-	1	(1)
46°25	81°28	Greenstone	in structure	0.17	0.88	0.35	5.18	0.14	-	1	(1)
46°41	81°20	Gabbro	in structure	0.41	3.54	0.79	8.63	0.43	-	1	(1)
46°41	80°49	Granite/Gneiss	in structure	0.7	10.33	1.17	14.76	1.02	-	1	(1)
46°39	80°46	Granite/Gneiss	in structure	1.82	5.45	3	3	1.14	-	1	(1)
46°26	81°04	Gabbro	Southern	2.97	6.45	0.86	2.17	1.3	-	1	(1)
46°39	81°21	Diorite	in structure	0.18	0.56	0.31	3.11	0.12	-	1	(1)
46°39	81°02.3	Gabbro	in structure	0.5	4	0.69	8	0.48	-	1	(1)
46°34	81°00	-	in structure	0.76	3.59	0.92	4.72	0.63	-	1	(1)
46°45	81°06	Gneiss	in structure	3.56	18.39	2.62	5.17	2.46	-	2	(1)
46°46	80°52	Gabbro	Grenville	0.44	5.05	1.56	12.7	0.62	-	2	(1)
46°30	81°05	Granite/Gneiss	in structure	5.41	23.67	2.74	4.84	3.32	-	3	(1)
Windy Lake											
46°37.5	81°26.7	-	Superior	0.95	38.67	3.85	40.42	3.33	-	3	(1)
Wanapitei Lake											
46°44.4	80°56.4	-	in structure	3.78	17.56	3.91	8.61	2.58	1.34	5	(1)
Cartier transect[a]		Granite/Gneiss	Superior	2.15	28.8	3.3	16.84	2.93	2.41	34	(2)

U and Th are Uranium and Thorium concentration in ppm, K is potassium concentration in per cent, A and σ_A are the heat production and its standard deviation in μW m^{-3}, respectively and N_A is the number of samples.
[a] Cartier transect is located just on the northwest edge of the structure (see Figure 1.4).
References : (1) Lewis and Bentkowski (1988), (2) Schneider et al. (1987).

Table 1.4
Average heat production distributed by rocktype

Rocktype	N_A^a	A^b (μW m^{-3})	σ_A^c (μW m^{-3})
Greywacke	7	3.2	0.8
Gabbro/Norite	50	0.7	0.36
Granite/Gneiss	71	2.93	1.98
Greenstone	2	0.17	0.04
Anorthosite	10	0.31	0.17

[a] Number of samples
[b] Mean heat production (μW m^{-3})
[c] Standard deviation on the heat production distribution (μW m^{-3})

Table 1.5
Average heat production distributed by geological provinces

	Province	N_A^a	A^b (μW m^{-3})	σ_A^c (μW m^{-3})
in structure		**94**	**1.78**	**1.55**
out stucture	↓	**67**	**2.1**	**2.17**
"	Grenville	2	0.62	0.04
"	Superior	57	2.11	2.25
"	Southern	8	2.6	11.1

[a] Number of samples
[b] Mean heat production (μW m^{-3})
[c] Standard deviation on the heat production distribution (μW m^{-3})

Figures captions

Table Page

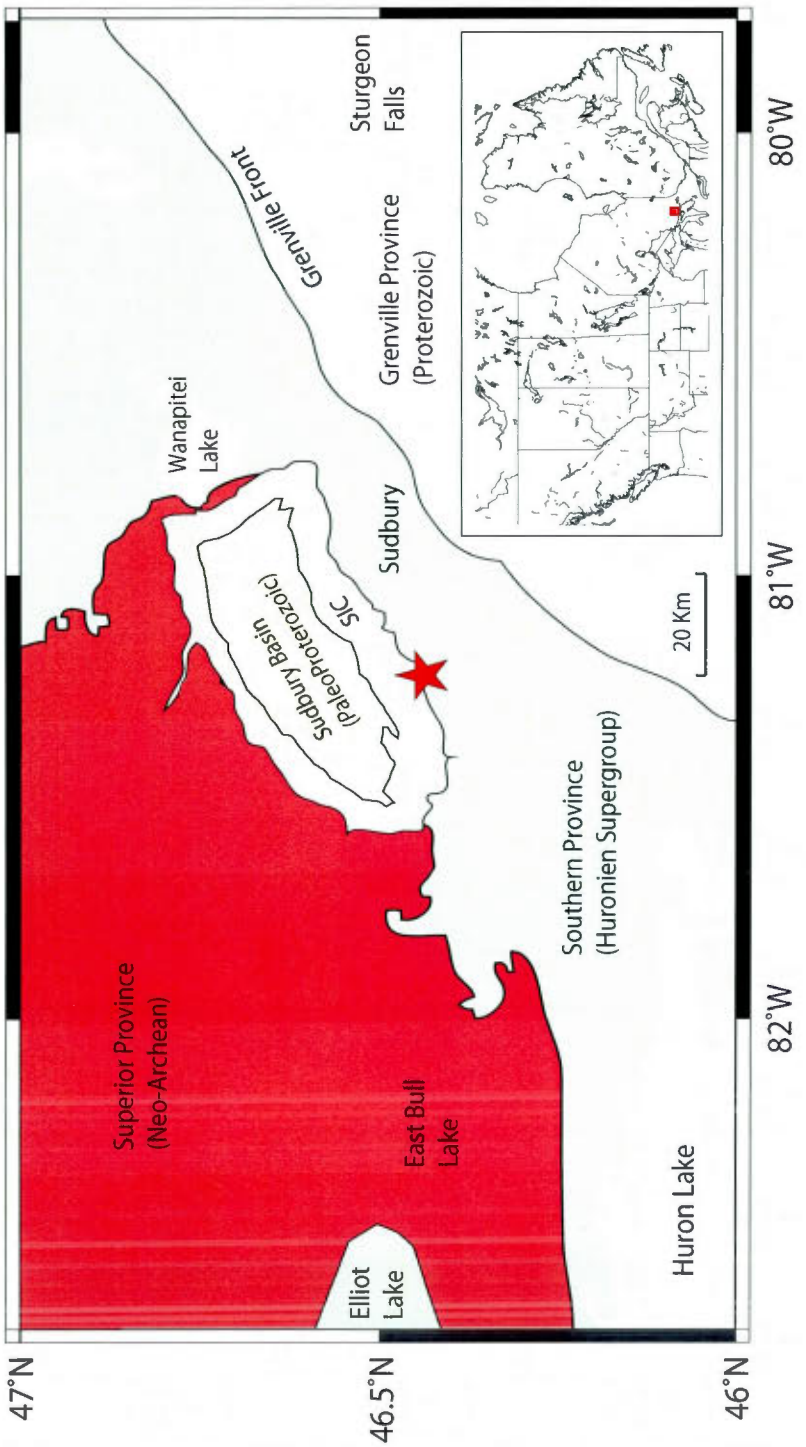
47°N
46.5°N
46°N
82°W
81°W
80°W
Superior Province
(Neo-Archean)
East Bull
Lake
Elliot
Lake
Huron Lake
Southern Province
(Huronien Supergroup)
Sudbury
SIS
Sudbury basin
(Paleoproterozoic)
Wanapitei
Lake
Grenville Front
Grenville Province
(Proterozoic)
Sturgeon
Falls
20 Km

Figure 1.1

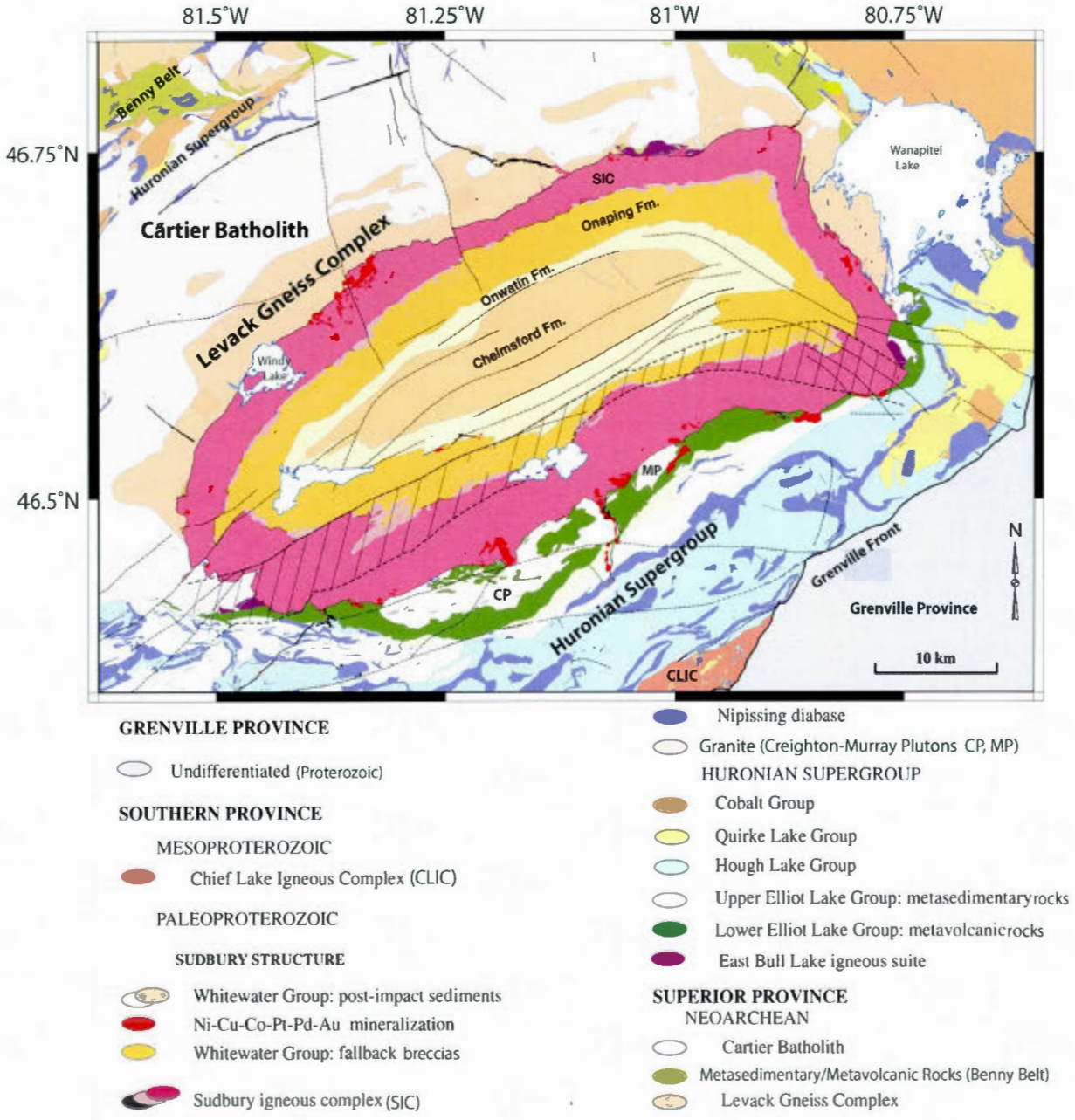
81.5°W
81.25°W
81°W
80.75°W
46.75°N
46.5°N
Benny Belt
Huronian Supergroup
Cartier Batholith
Levack Gneiss Complex
SIC
Onaping Fm.
Onwatin Fm.
Chelmsford Fm.
Windy Lake
Wanapitei Lake
MP
CP
CLIC
Huronian Supergroup
Grenville Front
Grenville Province
N
10 km
GRENVILLE PROVINCE
Undifferentiated (Proterozoic)
SOUTHERN PROVINCE
MESOPROTEROZOIC
Chief Lake Igneous Complex (CLIC)
PALEOPROTEROZOIC
SUDBURY STRUCTURE
Whitewater Group: post-impact sediments
Ni-Cu-Co-Pt-Pd-Au mineralization
Whitewater Group: fallback breccias
Sudbury igneous complex (SIC)
Nipissing diabase
Granite (Creighton-Murray Plutons CP, MP)
HURONIAN SUPERGROUP
Cobalt Group
Quirke Lake Group
Hough Lake Group
Upper Elliot Lake Group: metasedimentary rocks
Lower Elliot Lake Group: metavolcanic rocks
East Bull Lake igneous suite
SUPERIOR PROVINCE
NEOARCHEAN
Cartier Batholith
Metasedimentary/Metavolcanic Rocks (Benny Belt)
Levack Gneiss Complex

Figure 1.2

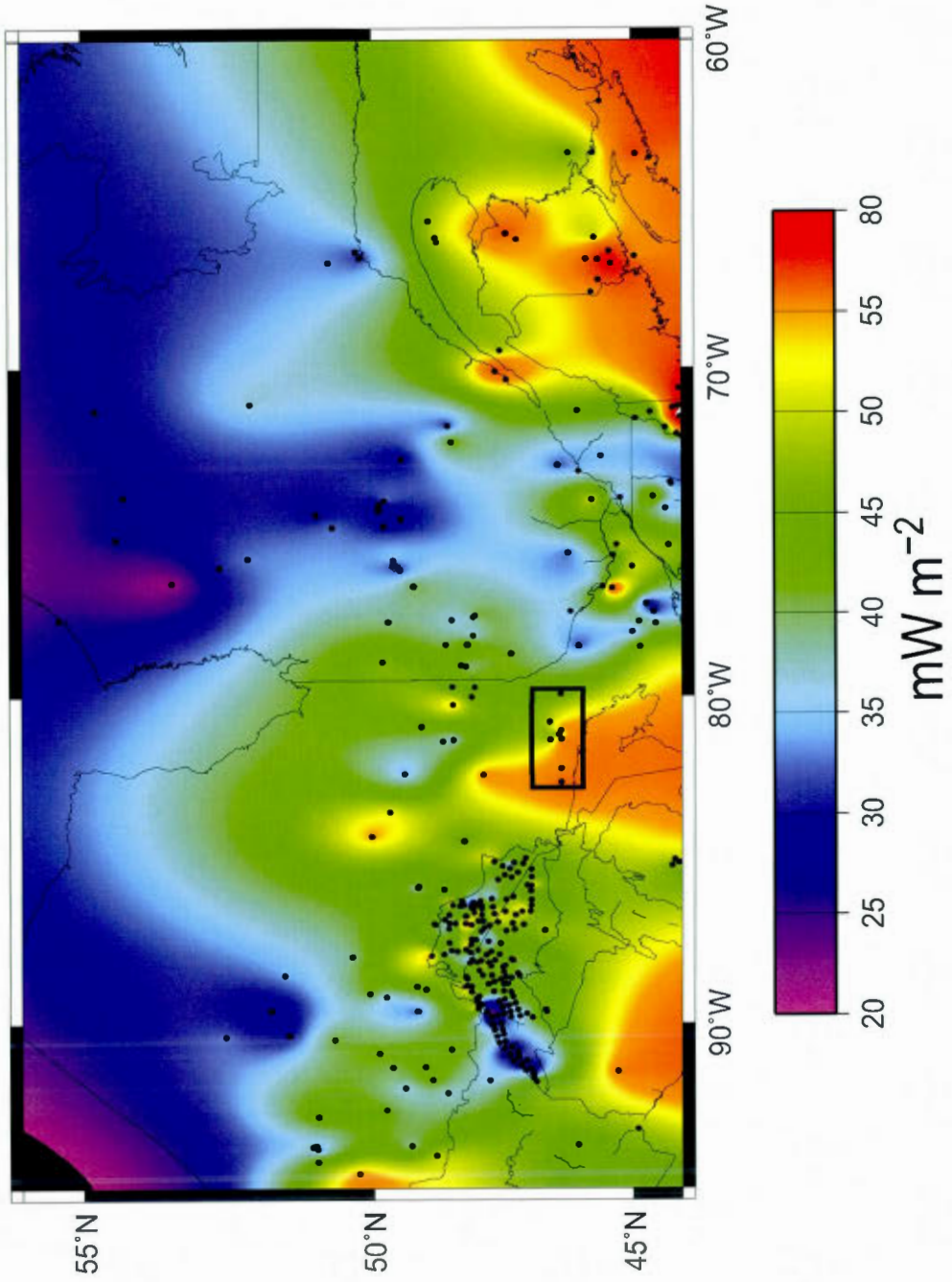

Figure 1.3

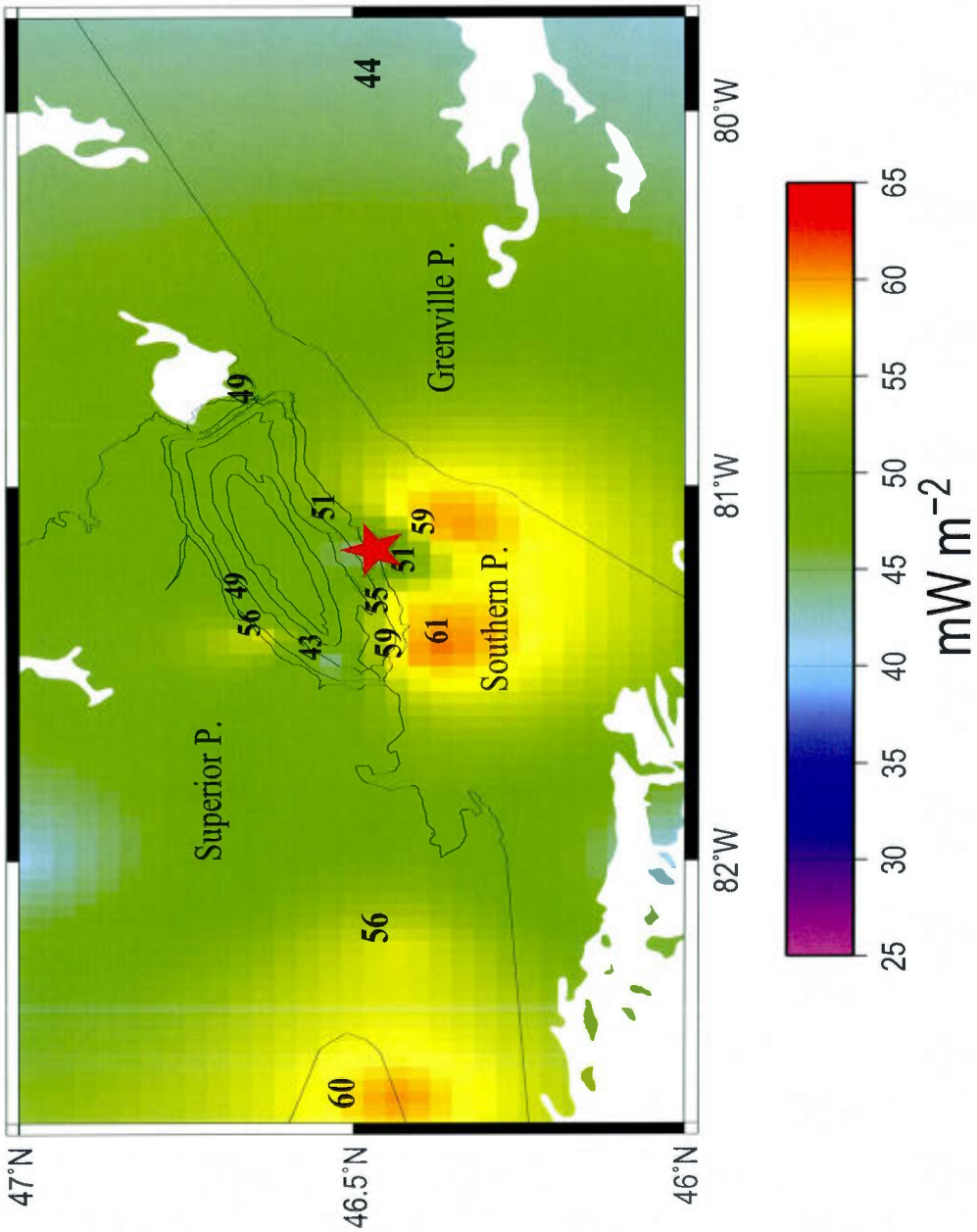
47°N
46.5°N
46°N
82°W
81°W
80°W
Superior P.
Southern P.
Grenville P.
44
49
51
59
51
56
49
55
43
59
61
56
60
25
30
35
40
45
50
55
60
65
mW m^{-2}

Figure 1.4

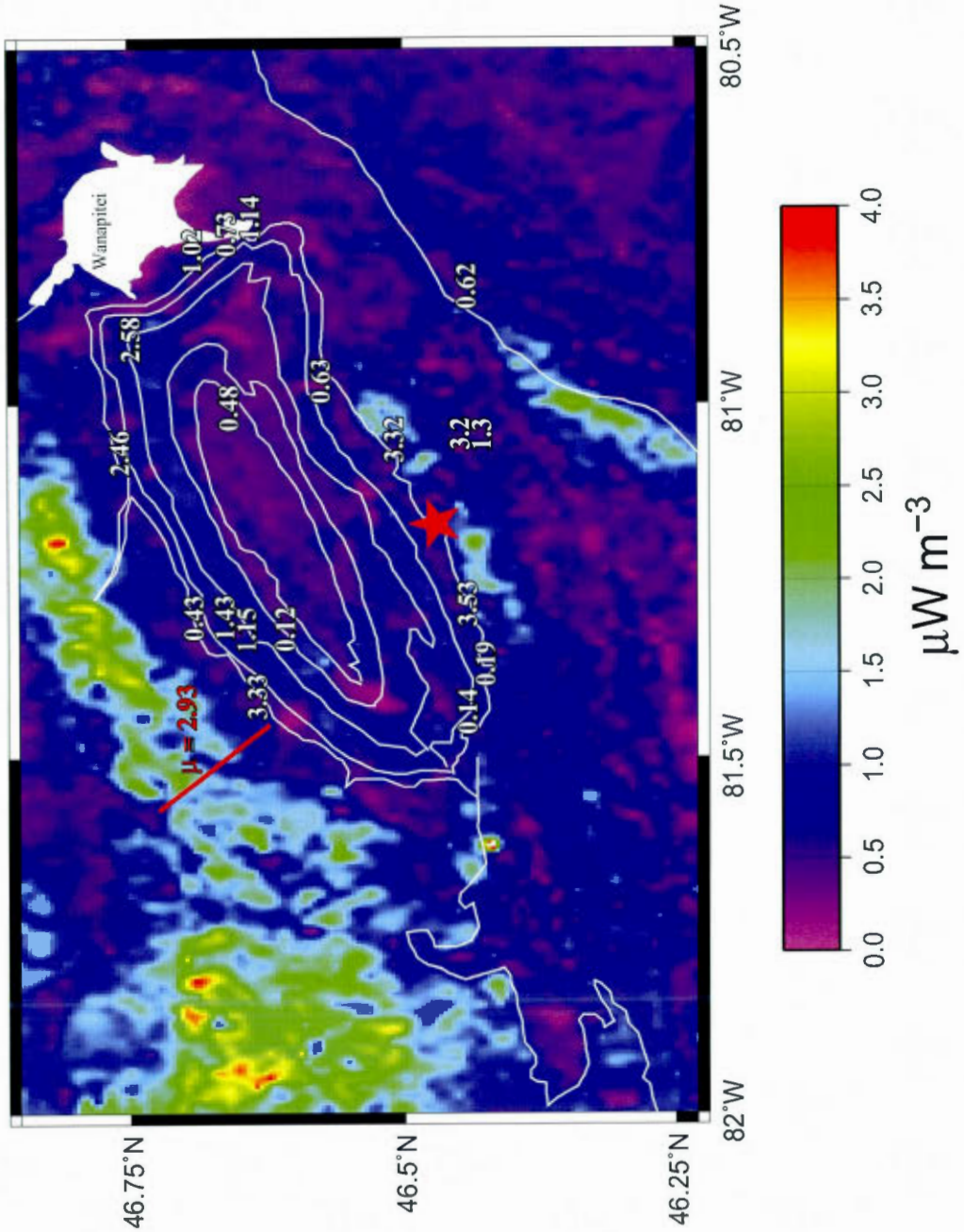
Wanapitei
2.58
2.46
0.48
0.63
0.62
3.32
3.2
1.3
0.43
1.43
1.15
0.12
3.33
μ = 2.93
3.53
0.14
0.19
1.07
0.73
1.14
46.75°N
46.5°N
46.25°N
82°W
81.5°W
81°W
80.5°W
0.0
0.5
1.0
1.5
2.0
2.5
3.0
3.5
4.0
μW m⁻³

Figure 1.5

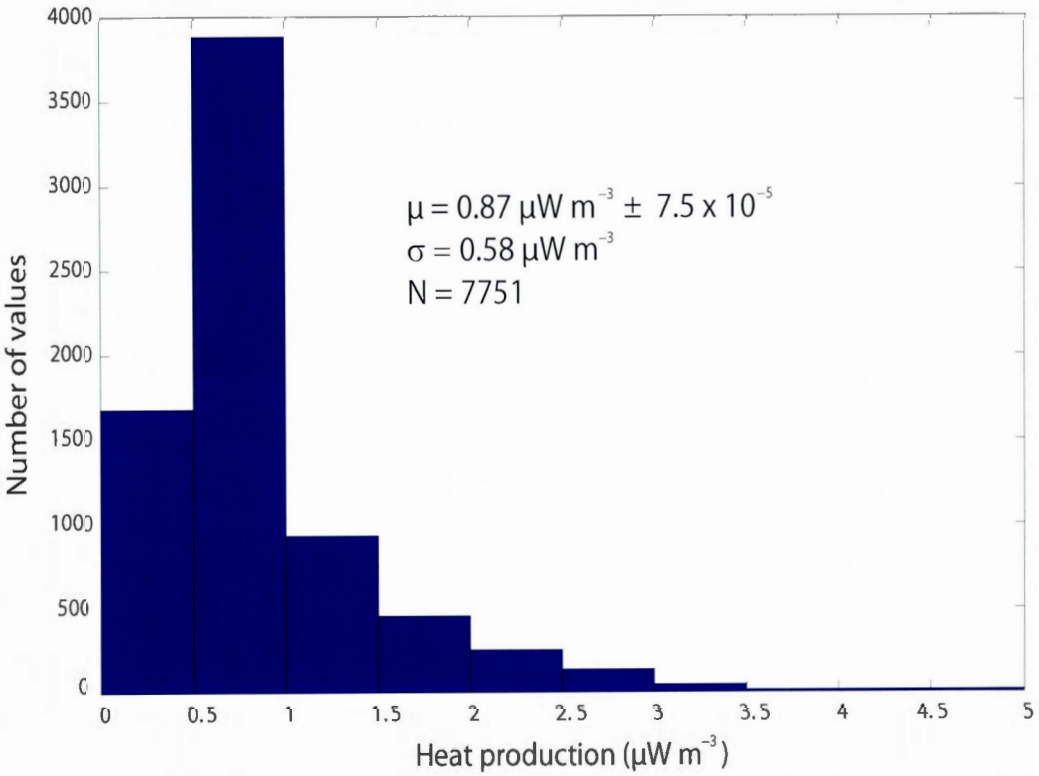
4000
3500
3000
2500
2000
1500
1000
500
0
Number of values
μ = 0.87 μW m⁻³ ± 7.5 x 10⁻⁵
σ = 0.58 μW m⁻³
N = 7751
0
0.5
1
1.5
2
2.5
3
3.5
4
4.5
5
Heat production (μW m⁻³)

Figure 1.6

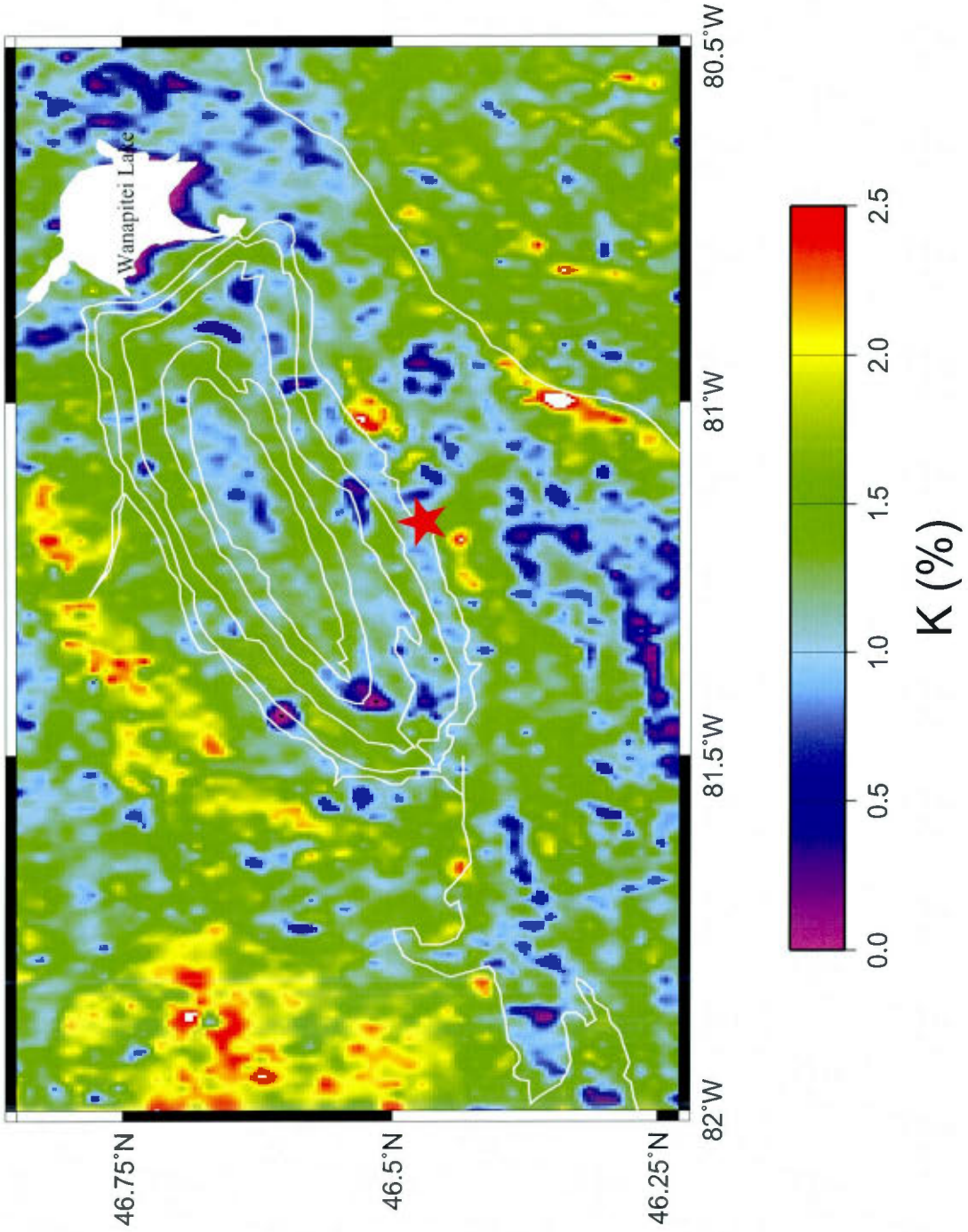
Wanapitei Lake
80.5°W
81°W
81.5°W
82°W
46.75°N
46.5°N
46.25°N
0.0
0.5
1.0
1.5
2.0
2.5
K (%)

Figure 1.7

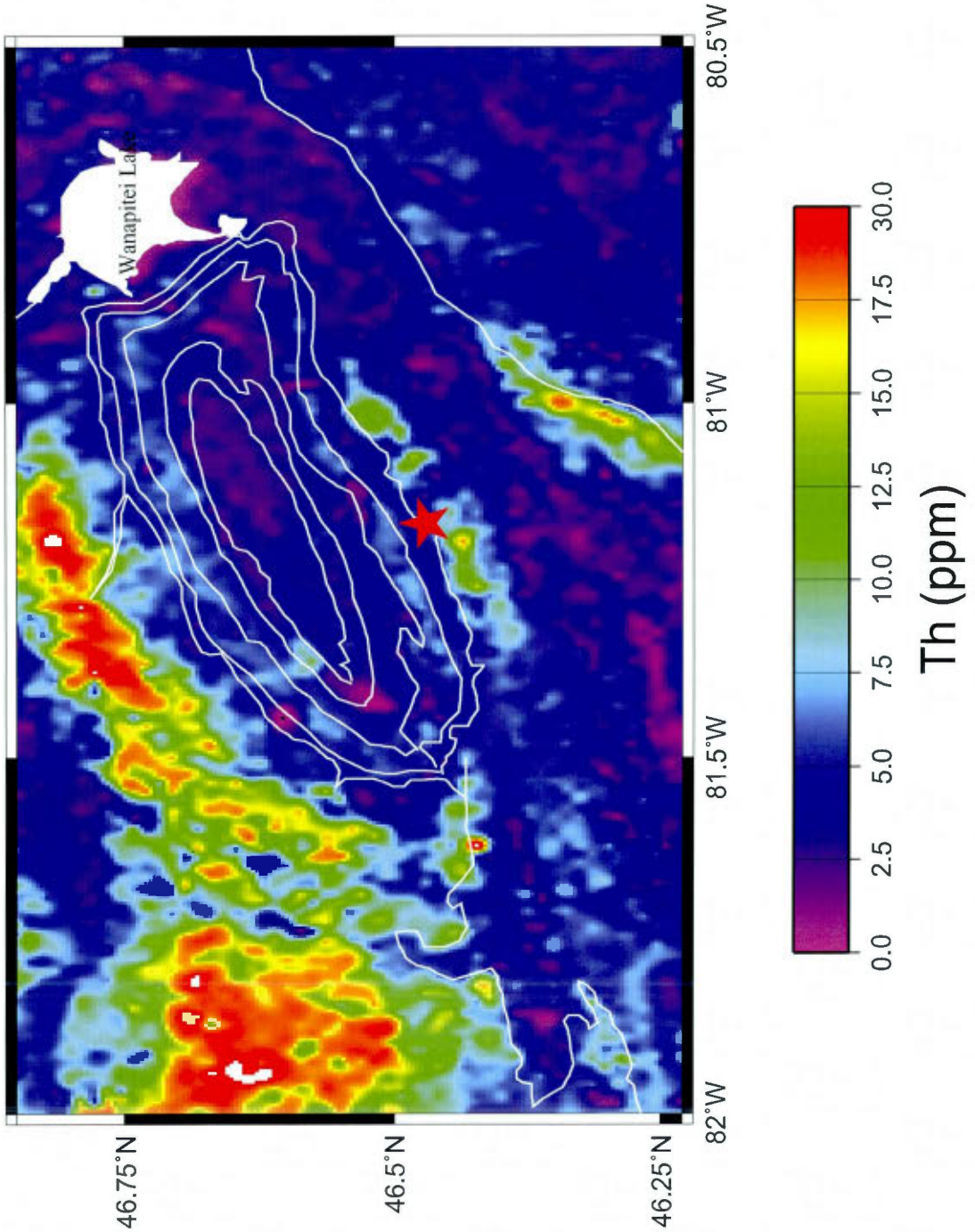
Wanapitei Lake
80.5°W
81°W
81.5°W
82°W
46.75°N
46.5°N
46.25°N
0.0
2.5
5.0
7.5
10.0
12.5
15.0
17.5
30.0
Th (ppm)

Figure 1.8

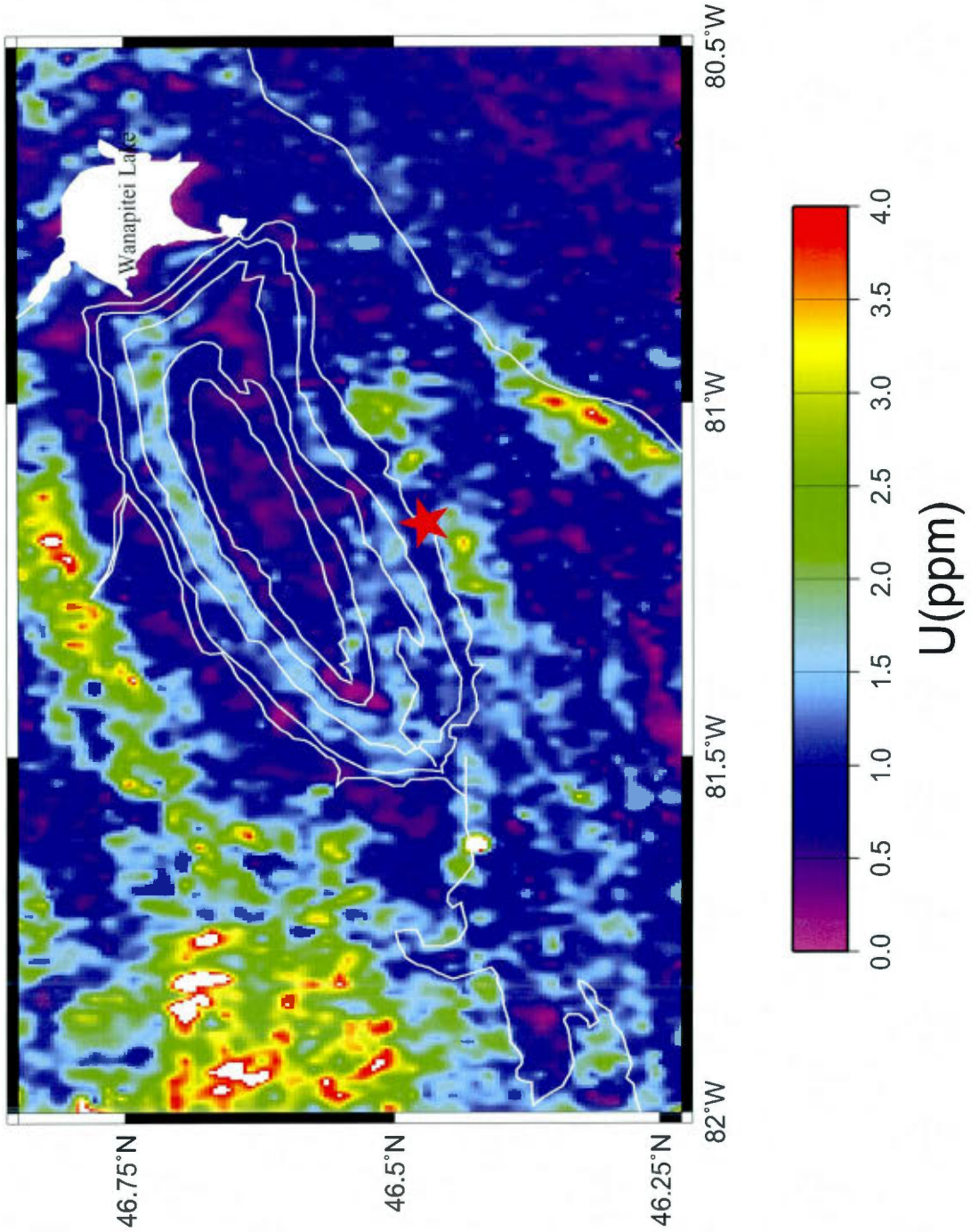
Wanapitei Lake
80.5°W
81°W
81.5°W
82°W
46.75°N
46.5°N
46.25°N
0.0
0.5
1.0
1.5
2.0
2.5
3.0
3.5
4.0
U(ppm)

Figure 1.9

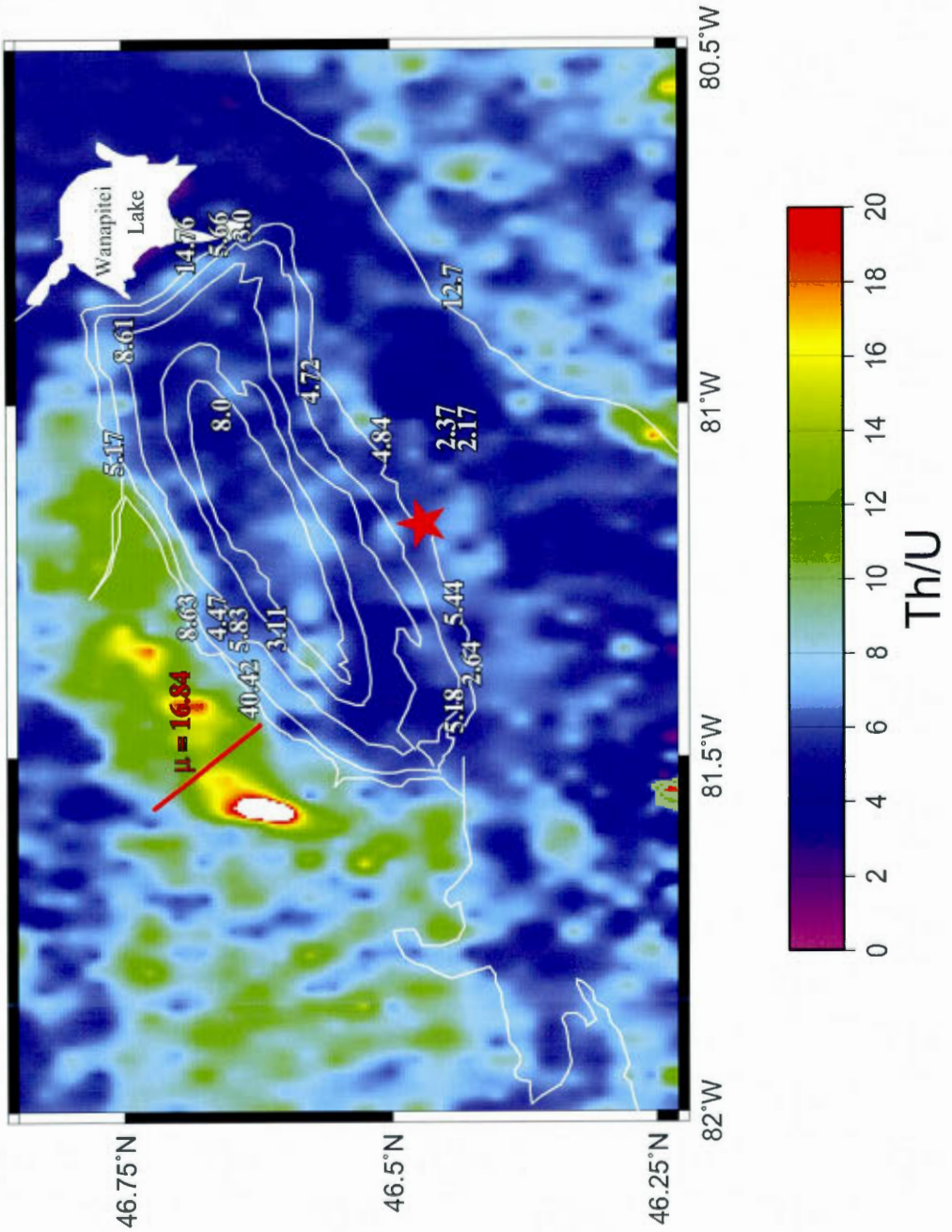
Wanapitei
Lake
μ = 16.84
14.76
5.66
3.0
8.61
12.7
5.17
8.0
4.72
4.84
2.37
2.17
8.63
4.47
5.83
3.11
40.42
5.44
5.18
2.64
82°W
81.5°W
81°W
80.5°W
46.75°N
46.5°N
46.25°N
0
2
4
6
8
10
12
14
16
18
20
Th/U

Figure 1.10

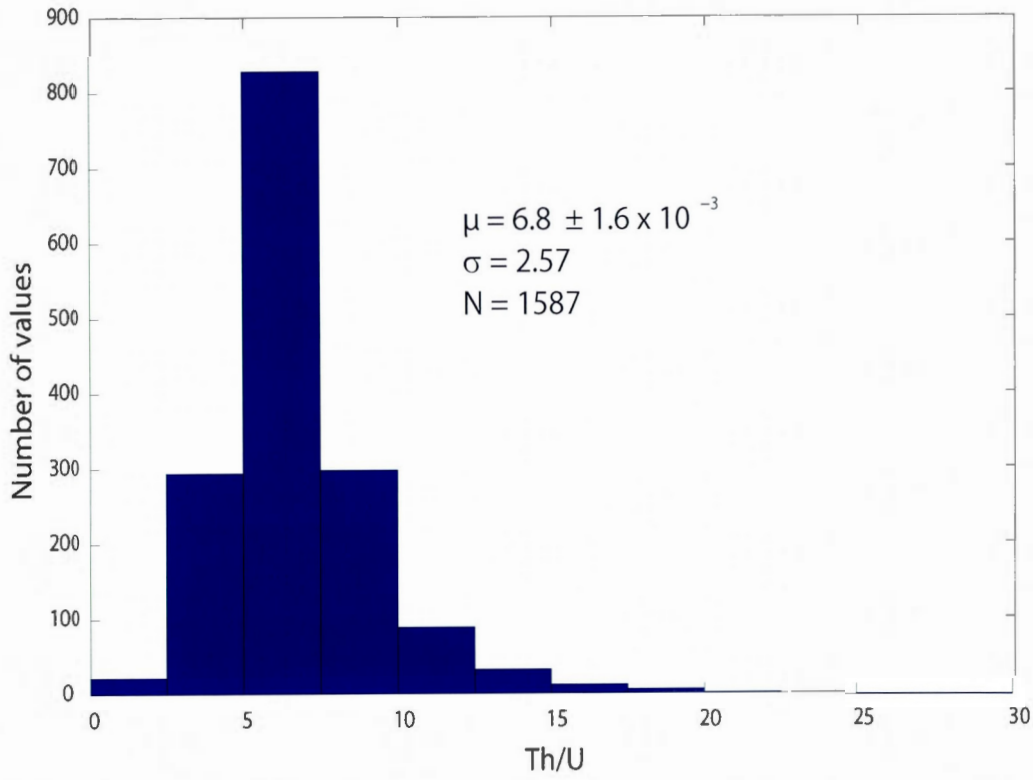
900
800
700
600
500
400
300
200
100
0
Number of values
μ = 6.8 ± 1.6 x 10 −3
σ = 2.57
N = 1587
0
5
10
15
20
25
30
Th/U

Figure 1.11

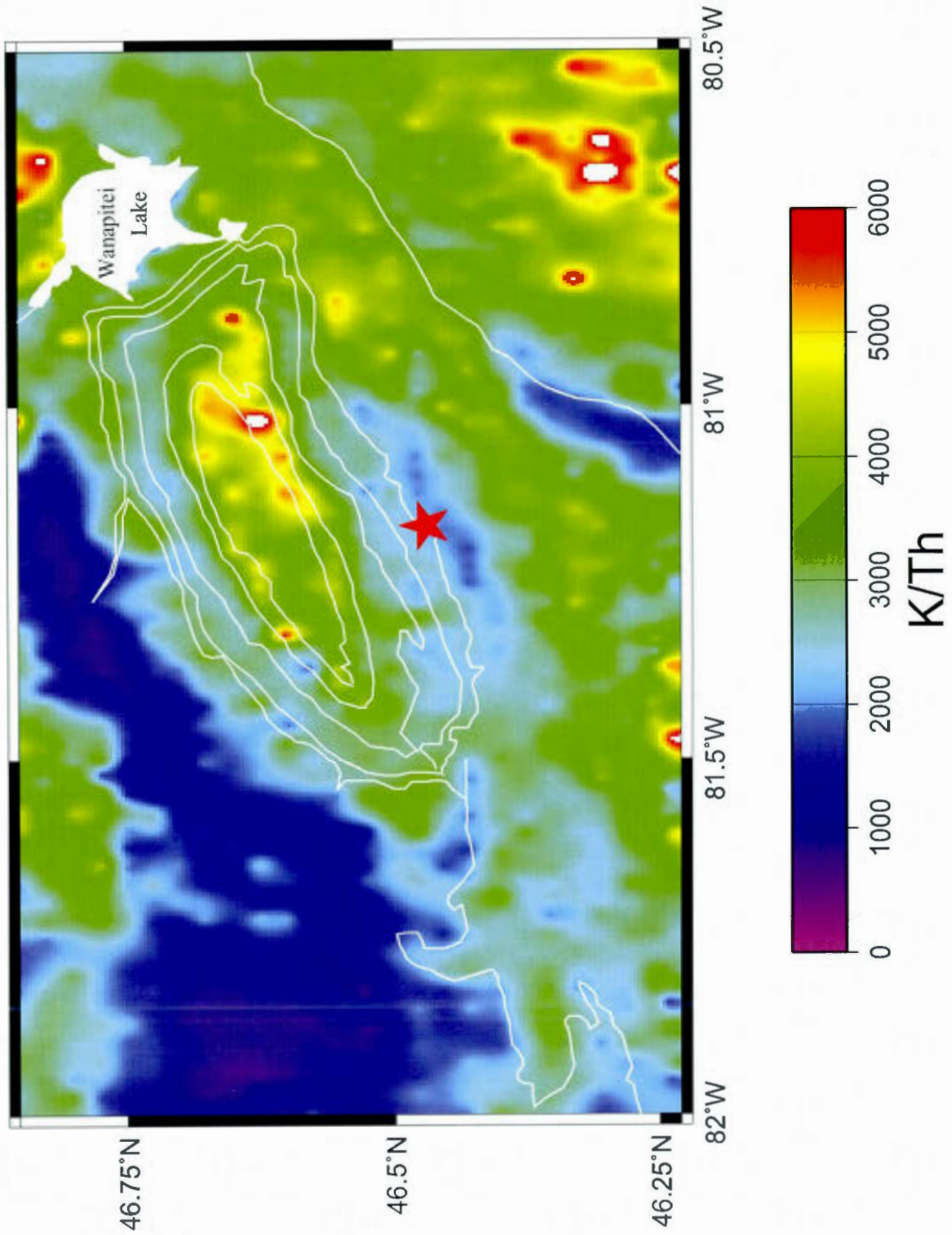
Wanapitei
Lake
80.5°W
81°W
81.5°W
82°W
46.75°N
46.5°N
46.25°N
0
1000
2000
3000
4000
5000
6000
K/Th

Figure 1.12

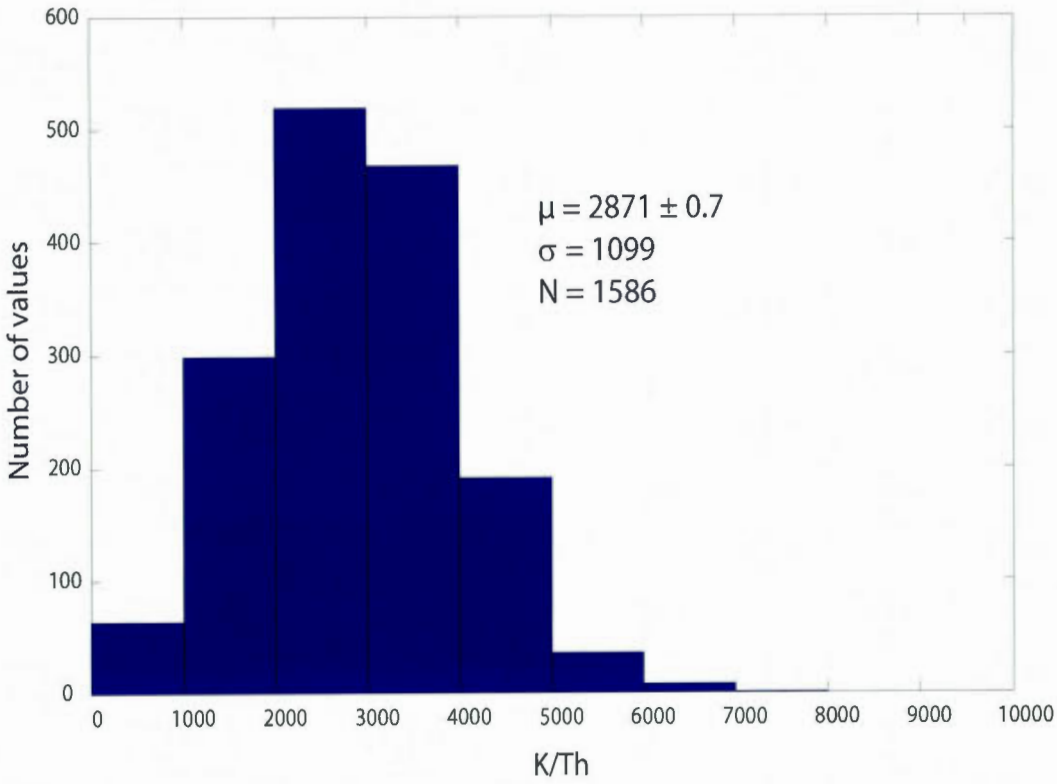
600
500
400
300
200
100
0
Number of values
μ = 2871 ± 0.7
σ = 1099
N = 1586
0
1000
2000
3000
4000
5000
6000
7000
8000
9000
10000
K/Th

Figure 1.13

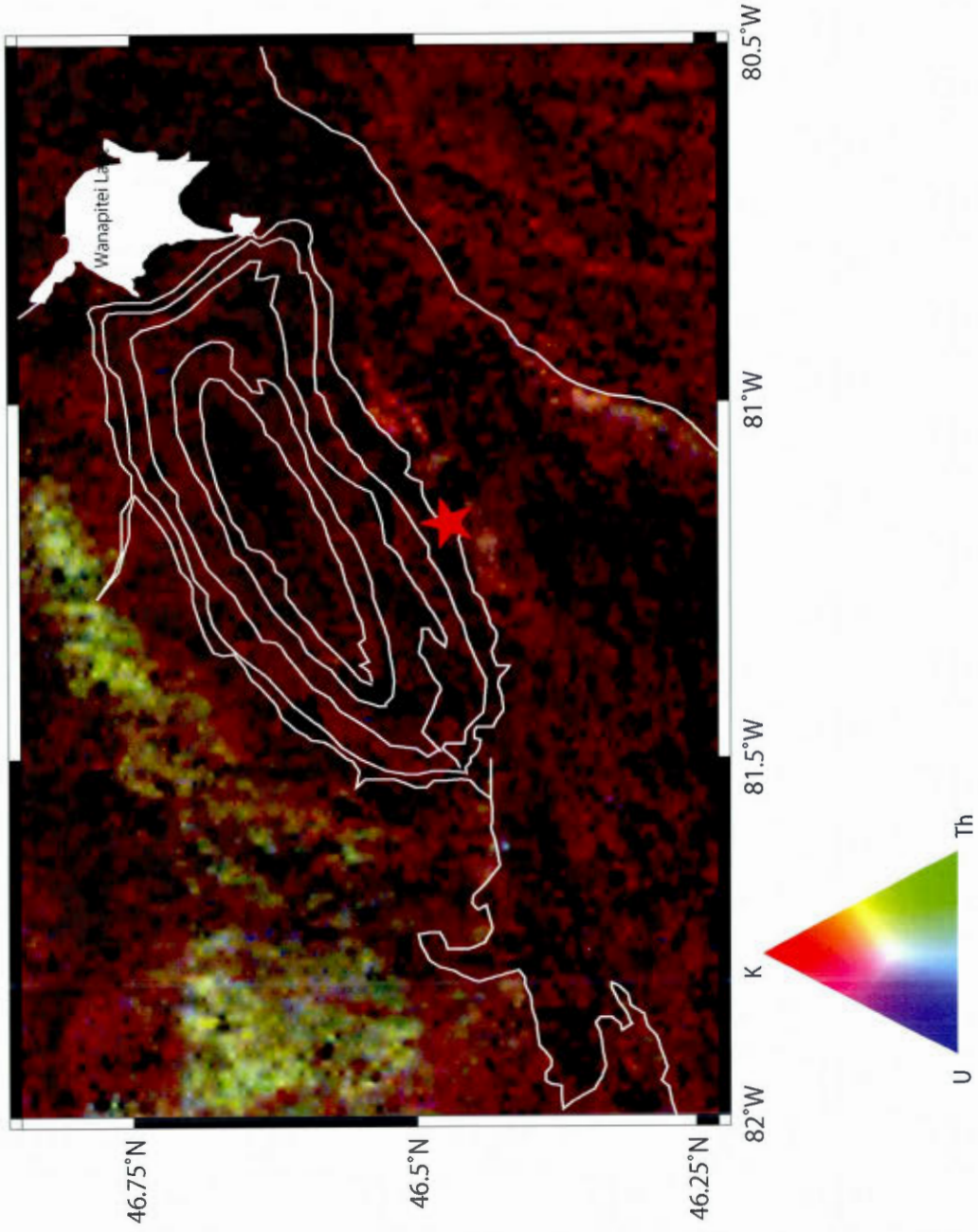

Figure 1.14

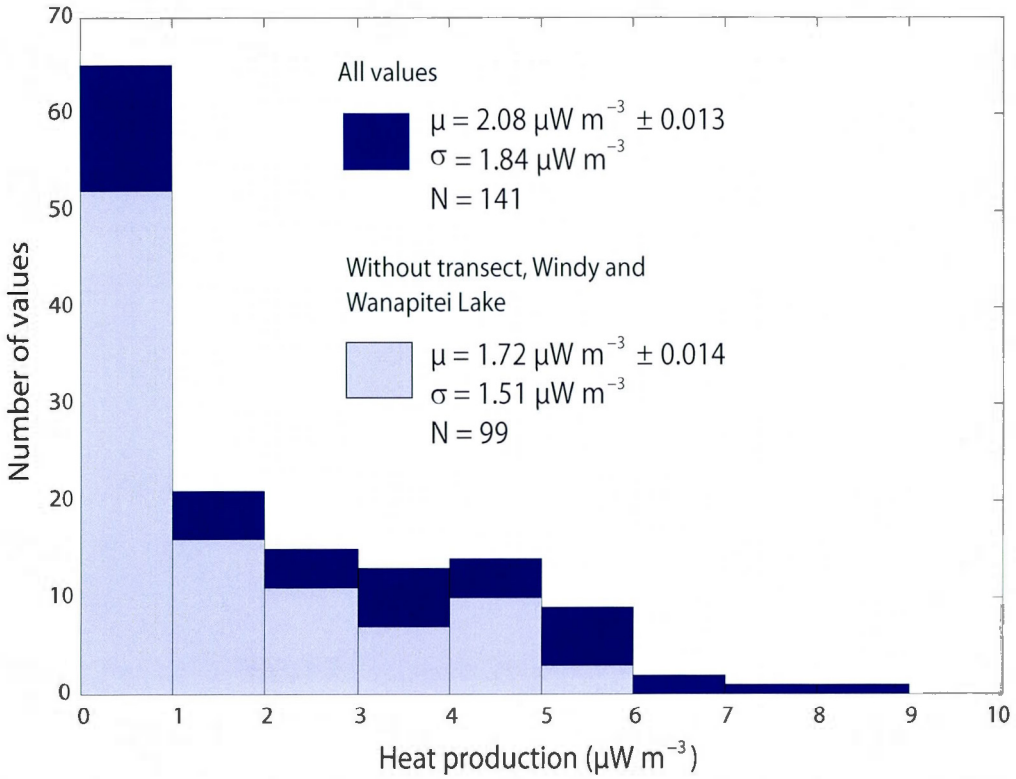
All values
μ = 2.08 μW m^{-3} ± 0.013
σ = 1.84 μW m^{-3}
N = 141
Without transect, Windy and Wanapitei Lake
μ = 1.72 μW m^{-3} ± 0.014
σ = 1.51 μW m^{-3}
N = 99
Number of values
Heat production (μW m^{-3})
0
10
20
30
40
50
60
70
0
1
2
3
4
5
6
7
8
9
10

Figure 1.15

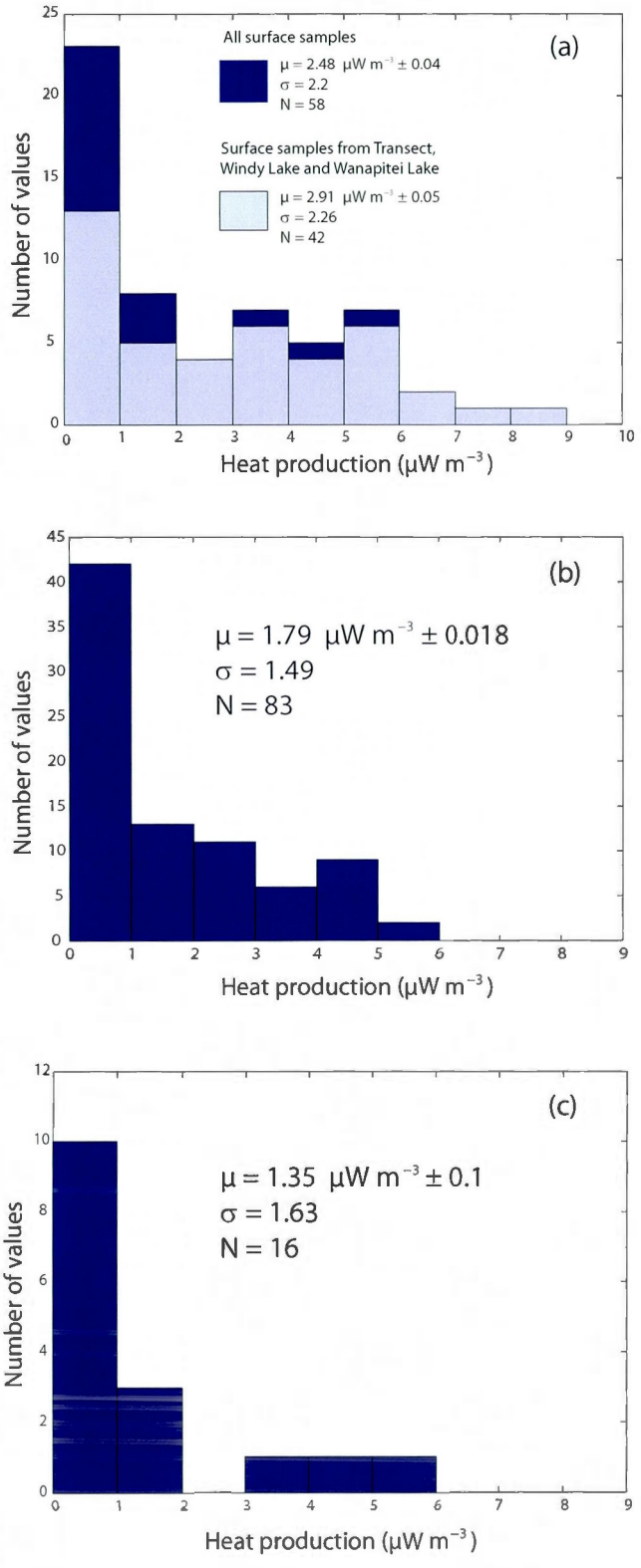
All surface samples
μ = 2.48 μW m⁻³ ± 0.04
σ = 2.2
N = 58
Surface samples from Transect, Windy Lake and Wanapitei Lake
μ = 2.91 μW m⁻³ ± 0.05
σ = 2.26
N = 42
(a)
Number of values
Heat production (μW m⁻³)
(b)
μ = 1.79 μW m⁻³ ± 0.018
σ = 1.49
N = 83
Number of values
Heat production (μW m⁻³)
(c)
μ = 1.35 μW m⁻³ ± 0.1
σ = 1.63
N = 16
Number of values
Heat production (μW m⁻³)

Figure 1.16

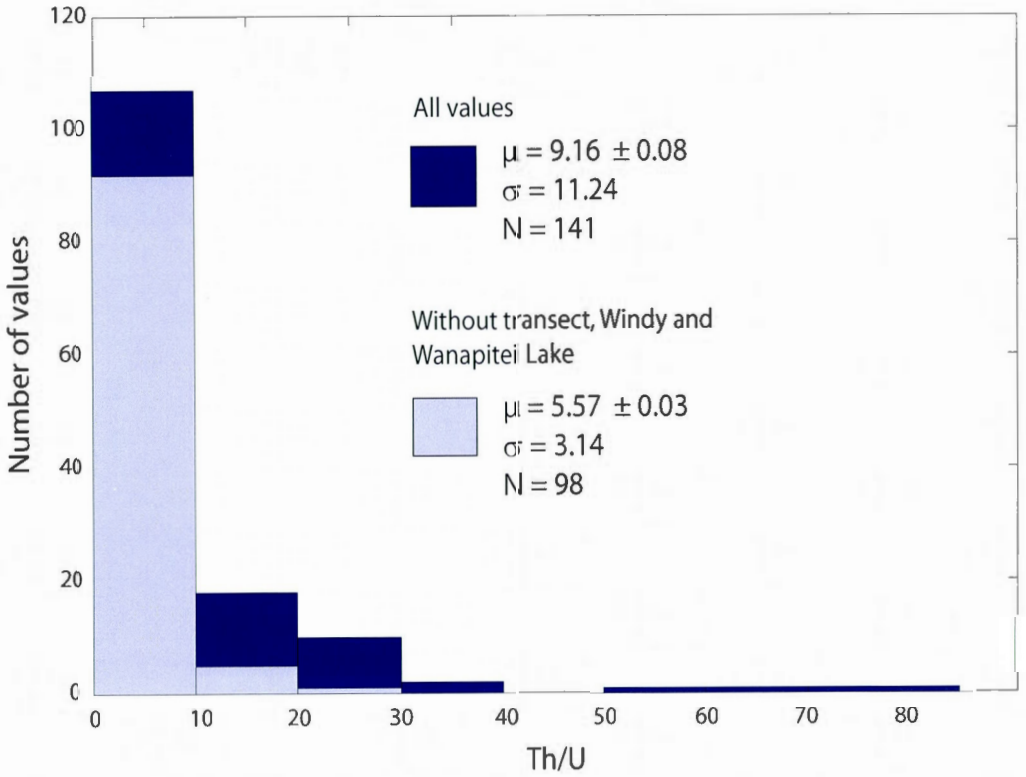
120
100
80
60
40
20
0
Number of values
0
10
20
30
40
50
60
70
80
Th/U
All values
μ = 9.16 ± 0.08
σ = 11.24
N = 141
Without transect, Windy and
Wanapitei Lake
μ = 5.57 ± 0.03
σ = 3.14
N = 98

Figure 1.17

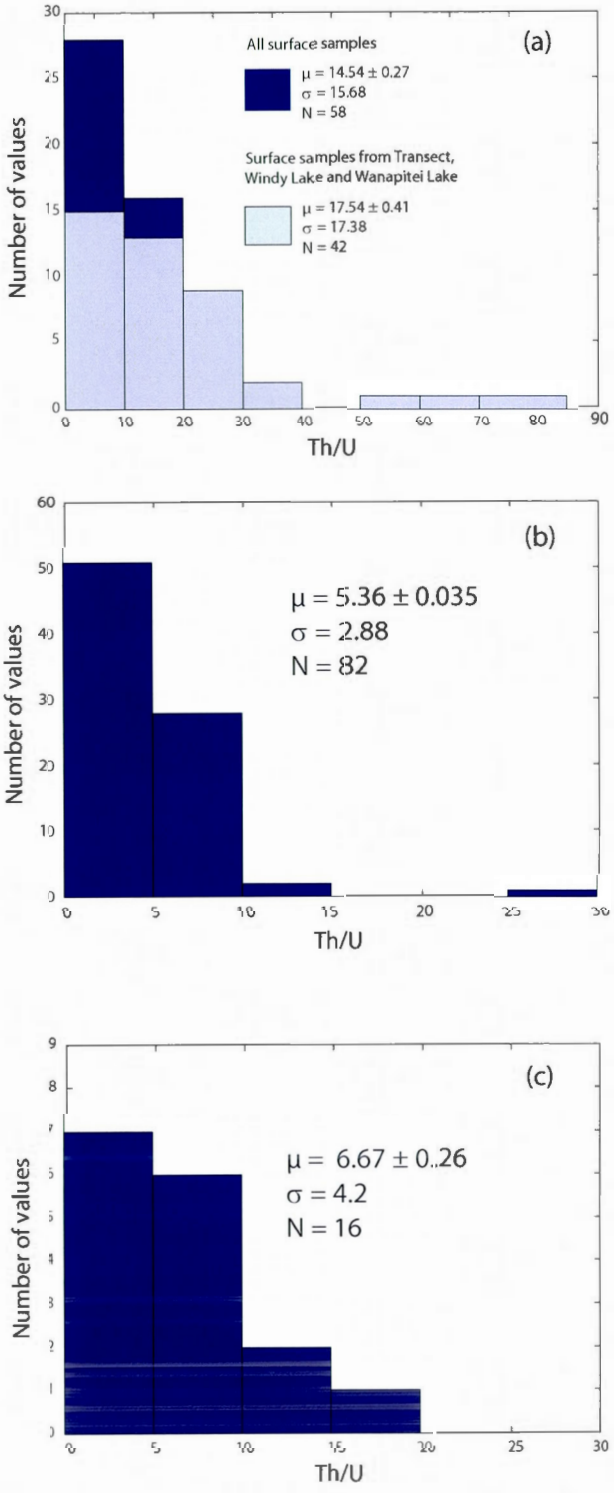
(a)
All surface samples
μ = 14.54 ± 0.27
σ = 15.68
N = 58
Surface samples from Transect,
Windy Lake and Wanapitei Lake
μ = 17.54 ± 0.41
σ = 17.38
N = 42
Number of values
Th/U
(b)
μ = 5.36 ± 0.035
σ = 2.88
N = 82
Number of values
Th/U
(c)
μ = 6.67 ± 0..26
σ = 4.2
N = 16
Number of values
Th/U

Figure 1.18

CHAPITRE II (Article 2)

ESTIMATING THE GLOBAL CRUSTAL GEO-NEUTRINO FLUX, INCLUDING A LOCAL STUDY NEAR SNOLAB, CANADA

Résumé

Les géo-neutrinos peuvent nous aider à déterminer l'abondance de U et Th dans la croûte et le manteau terrestre ainsi que leur contribution au budget énergétique de la Terre. Afin de déterminer la radioactivité du manteau, la composante crustale du flux de géo-neutrino doit être déterminée très précisément. Les estimations actuelles, fondées sur des modèles globaux tels que CRUST 2.0, sont inadéquats, puisqu'ils contraignent mal les fluctuations locales et régionales due aux changements géologiques et structurales. Nous proposons d'utiliser des mesures de flux et de production de chaleur pour calculer les variations régionales du flux de géo-neutrino crustale. La carte du flux de géo-neutrino qui en résulte est bien corrélée avec la carte du flux de chaleur de surface en région continentale stable, là où la majeure partie du flux de chaleur de surface provient de la radioactivité de la croûte. Dans plusieurs régions les prédictions entre les 2 modèles diffèrent par un facteur de 2. Pour déterminer précisément la contribution de la croûte au flux de géo-neutrino, des études locales du flux et de la production de chaleur sont nécessaires à proximité des observatoires.

De telles études sont actuellement en cours autour de l'observatoire de neutrinos de Sudbury au Canada (SNOLAB). Nous présentons de nouvelles données de flux et de production de chaleur recueillies à deux endroits autour de la structure de Sudbury. Le flux de chaleur moyen dans la région de Sudbury (52 mW m^{-2}) et est plus élevé que la moyenne du Bouclier Canadien (41 mW m^{-2}). L'augmentation du flux de chaleur autour de Sudbury est due à un enrichissement local de la radioactivité et provoque une augmentation locale du flux de géo-neutrino. Les mesures de flux de chaleur disponibles dans la région de Sudbury proviennent, pour la plupart, en bordure de la structure là où les activités d'exploration minérale ont été concentrées. D'autres mesures sont nécessaires pour déterminer la radioactivité de la croûte en dehors de la structure, notamment dans le sous-sol Archéen (Batholithe de Cartier), afin de bien estimer sa contribution au flux de géo-neutrinos.

Mots-clés : radioactivité - flux de chaleur - flux de géo-neutrinos

Abstract

Geo-neutrinos can help us determine the abundance of U and Th in the Earth's crust and mantle and as well as the contribution of these elements to the Earth's energy budget. In order to determine the mantle's radioactivity, the crustal component of the geo-neutrino flux must be determined very precisely. Current estimates, based on global models such as CRUST 2.0, are inadequate because they fail to sufficiently account for local and regional fluctuations generated by geological and structural changes. We propose to use heat flux and heat production measurements to calculate the regional variations in the crustal geo-neutrino flux. The resulting map of estimated geo-neutrino flux is well correlated with the surface heat flux map in stable continental regions, where most of the surface heat flux comes from crustal radioactivity. In several regions, estimates of these two models differ by a factor of two. To precisely determine the crustal contribution to the geo-neutrino flux, local heat flux and heat production studies are needed, which are to be conducted in the proximity of observatories.

Such studies are currently underway around the Sudbury Neutrino Observatory (SNO-LAB) in Canada. We present new heat flux and heat production data collected at two sites around the Sudbury structure. The average surface heat flux in the Sudbury region is (52 mW m^{-2}), which is higher than in the average Canadian Shield (41 mW m^{-2}). The higher heat flux around Sudbury, which also causes a local increase in the geo-neutrino flux, is due to local enrichment in crustal radioactivity. The available heat flux measurements are mostly on the edge of the structure, where most of mineral exploration activity was focused. More measurements are necessary to determine the crustal radioactivity outside the structure, especially in the Archean basement (Cartier Batholith), in order to properly estimate the crustal contribution to the geo-neutrino flux.

Keywords : radioactivity - heat flux - geo-neutrino flux

2.1 Introduction

The energy budget of the Earth is balanced between an outgoing flux of energy and internal sources. The outgoing flux of energy is fairly well ascertainable, with current estimates falling within a narrow range of 42 and 47 TW (Sclater et al., 1980; Pollack et al., 1993; Jaupart et al., 2007; Davies and Davies, 2010). The main source of internally produced energy comes from the decay of radioactive elements. So far, the radioactive heat production of the Earth has been determined with geochemical models such as the Bulk Silicate Earth (BSE) model. Crustal heat production is well known since it can be determined directly from different sampling methods and heat flux measurements. However, considerable uncertainty exists as to the heat production of the mantle since the mantle radioactivity is estimated from models. Reducing this uncertainty would be a first step in finding ways to balance the Earth energy budget and to lead to a better understanding of mantle convection, magmatic and volcanic systems, and the Earth's thermal history and evolution.

The recent improvements made to underground neutrino observatories may be the key to a direct determination of the mantle heat production and a test for the geochemical models. This would result from direct observation of low energy anti-neutrinos, also called geo-neutrinos, produced during the inverse β decay of the radioactive isotopes, uranium and thorium. Such experiments are underway at the Kamioka and Gran Sasso observatories. Preliminary results have already been published in Araki, T., and 86 collaborators (2005); Enomoto et al. (2007); Bellini, G., and 89 collaborators (2010); Gando, A. and 65 collaborators (2011). While their interpretations have led to estimates of the mantle radioactivity, the uncertainties remain significant. Identifying mantle radioactivity with geo-neutrino studies calls for a very accurate estimate of the crustal radioactivity, since the crustal radioactivity component dominates (> 80 %) the total geo-neutrino signal in continental observatories (Raghavan et al., 1998; Fiorentini et al., 2005; Chen, 2006; Enomoto et al., 2007). The high uncertainty on geo-neutrino-based mantle radioactivity estimates is in part due to the unreliable assessment of the crustal geo-neutrino flux near observatories. So far, the crustal geo-neutrino flux near observatories is calculated using global models such as CRUST 2.0. These models not even suitable on a global scale, are inadequate for local studies given their

inability to sufficiently account for geological and structural changes. Perry et al. (2009) and Mareschal et al. (2012) have discussed the efficiency of heat flux measurements in order to determine the crustal geo-neutrino flux in stable continental regions where the Moho heat flux is well established and varies only slightly.

A new geo-neutrino detector at SNOLAB was put in operation this year. SNOLAB is located in the Creighton mine, near Sudbury, within the Canadian Shield, an old stable craton where thermal regime is in steady state and where the Moho heat flux has been fairly well estimated (15 ± 3 mW m^{-2}) (Jaupart and Mareschal, 1999; Mareschal and Jaupart, 2004). The Sudbury region has been well researched and documented in exploration of its mineral potential. Available drill holes offer the opportunity to make heat flux and heat production measurements and accurately calculate the crustal radioactivity. The crustal radioactivity will then allow us to precisely calculate the crustal contribution to the geo-neutrino flux in the vicinity of SNOLAB. It should be pointed out that SNOLAB is located in a region where the crust is abnormally radioactive.

In this work, we review the crustal geo-neutrino flux model of Mantovani et al. (2004) and Fiorentini et al. (2005), which we then compare with a model based on heat flux data. We shall argue that heat flux measurement is the optimal method for determining the crustal component of the geo-neutrino flux in stable continental regions. We present new heat flux and heat production measurements located in the Sudbury region. Finally, using all available measurements, we calculate a first estimate of the crustal contribution to the geo-neutrino flux in the vicinity of SNOLAB.

2.2 Crustal geo-neutrino flux predictions

In this study, we will focus on determining the crustal geo-neutrino flux. We refer to Annexe 2.A for a basic review on the physics and detection of geo-neutrinos.

The crustal component of the geo-neutrino flux, Φ, can be calculated at any point on the Earth's surface by integrating the crustal heat production, H, over the entire volume of

the Earth's crust :

$$\Phi(\theta,\phi) = \frac{\gamma a^2}{4\pi} \int_0^{z_m} dz' \int_0^{2\pi} d\phi' \int_0^{\pi} d\ cos\theta' \ \frac{H(z',\theta',\phi')}{R^2_{pp'}} \tag{2.1}$$

Where the factor γ is the ratio of crustal radioactivity to neutrino luminosity, a is the Earth's radius, θ and ϕ are the colatitude and longitude of the observation point, respectively, z is the depth, z_m is the Moho depth, $R_{pp'}$ is the distance between the source (p') and the observation point (p) and H is the crustal heat production.

The above equation assumes that the mass ratio of the heat producing elements is constant and that a single factor γ can be used to calculate the neutrino luminosity to heat production ratio. For Th/U = 4 and K/U =12,000, we obtain $\gamma = 0.65 \times 10^{12}$ J^{-1}.

2.2.1 Seismic crustal model

Estimates of the crustal component of the geo-neutrino flux calculated by Fiorentini et al. (2005) rely on global seismic crustal models along with geochemical studies on U, Th, and K distribution in the Earth's interior. More precisely, the crustal structure is inferred from a global crustal model parameterized on a 2 x 2 degree grid, namely CRUST 2.0 (Mooney et al., 1998), while the crustal heat production is calculated from U, Th and K abundances obtained by averaging the best geochemical compilations (Taylor and McLennan, 1995; Shaw et al., 1986; Rudnick and Fountain, 1995; Wedepohl, 1995).

The crustal component of the geo-neutrino flux based on the CRUST 2.0 model was calculated using a procedure similar to that of Fiorentini et al. (2005) (Figure 2.1). The geo-neutrino flux is given in TNU assuming 100 % efficiency and a survival probability of 0.56 (see Appendix 2.A). TNU refers to Terrestrial Neutrino Unit and represents the total number of events recorded per unit detector exposure (10^{32} protons/year).

This resulting geo-neutrino flux is higher where the crust is thicker, for example in the Himalayas and the Andes (compare model with the Earth's crustal thickness map shown in Figure 2.2). Also, the geo-neutrino flux seems to increase within the interior of continents, where the crust is generally thicker. In the Baltic and Siberian shields, crustal heat

production is quite low, which should yield a low crustal geo-neutrino flux. However, given the thick crust of these regions, the model predicts high geo-neutrino fluxes. Conversely, the model predicts a low geo-neutrino flux in western Europe, where the crust is thin but crustal heat production high. Since this model is based on the world average abundance of radiogenic material, it neglects the lateral heterogeneities caused by geological and structural changes. Most of the flux of geo-neutrino comes from the decay of radioactive elements in the immediate vicinity of the observatory (<200 km). Given that observatories may be located in regions where crustal radioactivity differs from the world average, this model may not provide the precise estimate of the crustal geo-neutrino sources we need to calculate the mantle radioactivity.

2.2.2 Heat flux model

In stable continents, where the thermal regime is in steady state, the Moho heat flux is quite constant at 15 mW $m^{-2} \pm 3$ mW m^{-2} and on the same order as the mean surface heat flux. Consequently, lateral variations in surface heat flux reflect the heat generated <H> within the crustal layer as :

$$< H >= \frac{Q - Q_M}{Z_M} \tag{2.2}$$

where Q is the surface heat flux and Q_M the Moho heat flux. Z_M is crustal thickness.

The crust is vertically differentiated and the upper 10-km-thick layer is enriched in radio-elements. Perry et al. (2009) have demonstrated that this upper enrichment affects the geo-neutrino flux within a radius of less than $5z_M$ from the observatory. Thus, this upper enrichment must be considered in the crustal geo-neutrino flux calculation.

This stratification is determined with a differentiation index, D_i, that measures the ratio of the surface to the average crustal heat production (Perry et al., 2006a).

$$DI = \frac{HZ_M}{Q - Q_M} \tag{2.3}$$

where H is the average surface heat production.

Figure 2.3 shows the world average heat flux on a 2 x 2 degree grid. This map was constructed with all available heat flux measurements made on land (> 35,000 values) (http ://www.heatflow.und.edu/). Average heat flux in cells with no data was interpolated except in two regions for which no data are available (Greenland and Antarctica). The oceans have been greyed out because their heat flux represents the ocean floor cooling and are not related to crustal radioactivity.

Since the surface heat flux in stable continental regions reflects the radioactivity of the crust, one expects a strong correlation between the estimated geo-neutrino flux and the measured surface heat flux. However, the map of the predicted crustal geo-neutrino flux based on CRUST 2.0 (Figure 2.1) does not show this correlation. Heat flux measurements that integrate radioactivity over the total crustal column allow us to ascertain the heat generated near each measurement site. Thus, these data allow the identification of lateral variations caused by geological or structural changes that are not accounted for by the crustal model.

We made use of all the available heat flux data, to calculate the crustal heat production and the geo-neutrino flux. The resulting map of the estimated global geo-neutrino flux is shown in Figure 2.4. In active regions, the geo-neutrino flux is estimated from crustal models, since the surface heat flux is perturbed by magmatic and tectonic activity and does not reflect crustal radioactivity. These regions include the western part of north America, the Andes, Japan and the subduction zones of the Western Pacific and the Alpine Himalayan Belt. The geo-neutrino flux in Greenland and Antarctica is also estimated from crustal thickness. In stable continental regions, the geo-neutrino flux correlates well with the surface heat flow.

Figure 2.5 shows the differences between the crust-derived and heat-flux derived estimates of geo-neutrino flux. The most significant differences between models are found in stable continental regions. In the Canadian, Siberian and Baltic shields, where the crust is thick but heat production is low, the estimated geo-neutrino flux from heat flux data is significantly lower than the estimate based on crustal thickness (by a factor higher than two). The same differences, but less pronounced, are observed in the West African craton, East

Saharan metacraton and in the Dharwar craton. In western Europe, northeastern Australia and the eastern part of China, where the crust is thin but heat production high, the opposite is observed : the heat flux model predicts a higher geo-neutrino flux than the crustal model. This points to the reliability of heat flux and heat production data to determine the crustal geo-neutrino flux in stable continental regions.

Unfortunately, out of the three geo-neutrino observatories that are now in operation, only SNOLAB is located in a stable continental region (Canadian Shield). The other two observatories, KamLAND and Borexino are located in tectonically active regions and surface heat flux measurements cannot be used to estimate the crustal radioactivity.

2.3 New heat flux and heat production data in the Sudbury region

In this section, we present new heat flux and heat production data located in the Sudbury region. We describe the environment and location of sites where measured boreholes are situated, and we give details on the new heat flux and heat production values obtained. For measurement methods refer to Appendix 2.B.

2.3.1 New sites description

Four new boreholes were logged during our field campaign in October 2011. These boreholes are located on two different sites in the Sudbury region : two boreholes are located on the Victor Mine property owned by Vale/Inco and two on the Parkin property owned by Xstrata Nickel. For site locations see Figure 2.6, and Figure 2.7 and 2.8 for details on Victor Mine and Parkin property, respectively. A summary of the new heat flux and heat production data is presented in Table 2.1 and 2.2, respectively. Temperature gradient and heat flux profiles for each borehole are shown in Figure 2.9, 2.10, 2.11 and 2.12.

Victor Mine

Boreholes 1101 and 1102, are located on the Victor Mine property about 500 meters away from each other (Figure 2.7). This property is located on the east range of the Sudbury structure southwest of Wanapitei Lake, some 25 km northeast of Sudbury and 5 km north of the Sudbury airport (Figure 2.6).

Boreholes 1101 is located in a large open area surrounded by forest. The area is accessible via a short drive (about 100 meters) that goes east from Victor Mine road (Figure 2.7). This hole sits at an elevation of 377 meters and has a collar dip of 88°. Underground, its dip gradually inclines until it reaches 83.5° at the end of the hole, over 2000 meters deep. This hole was logged up to 1300 meters deep. Over the first 200 meters, the temperature gradient is perturbed by recent warming and/or other surface effects. The average temperature gradient below this perturbed topmost 200 meters is 14.6 mK m^{-1}. The average thermal conductivity value of 2.59 W $m^{-1}K^{-1}$ was determined from 8 unidentified segments of the core (measurements vary from 2.33 to 2.89 W $m^{-1}K^{-1}$). This average value was used to determine heat flux (Figure 2.9). Below the first 200 meters, the gradient is steady and heat flux equal 38 mW m^{-2} until approximately 1000 meters deep. In the last portion of the borehole, the gradient increases and heat flux raises to 41 mW m^{-2}. Post-glacial warming correction of 4 mW m^{-2} is almost entirely seen in the heat flux profile. Mean radioactivity determined from 6 unidentified segments of the core is 0.78 μW m^{-3}.

Borehole 1102 is located in a wooded area close to a steep incline of about 50 meters. This borehole is located within walking distance (about 200 meters via an ill-defined path), of Victor Mine road (Figure 2.7). The hole sits at an elevation of 430 meters and is vertical over its entire length (1740 meters). In this borehole measurements were made down to 930 meters. Over the first 250 meters, the temperature gradient is perturbed whereas below the temperature gradient is steady, averaging 14.5 mK m^{-1}. The average thermal conductivity value of 2.72 W $m^{-1}K^{-1}$, determined from 7 unidentified segments of the core (2.5 to 3.0 W $m^{-1}K^{-1}$), was used to determined heat flux (Figure 2.10). Below the perturbed 250 meters, heat flux is steady over the entire length of the hole and equal 39 mW m^{-2}. Measurements are not sufficiently deep to observe the post-glacial warming correction of 7

mW m^{-2}. Mean radioactivity determined from 9 unidentified segments of the core is 0.78 μW m^{-3}.

This site mean heat flux (after climatic correction) and heat production values are 44 mW m^{-2} and 0.78 μW m^{-3} , respectively. The lithology throughout both boreholes is very homogeneous, consisting of gabbro and/or norite.

Parkin

Boreholes 1103 and 1104 are located on the Parkin property about one km away from each other (Figure 2.8). This property is situated about 35 km northeast of the city of Sudbury and about 10 km northeast from the town of Capreol (Figure 2.6). This site is located in the Superior Province north of the northeastern corner of the Sudbury structure. Both holes were drilled in 1998.

Hole 1103 is located just off Portelance road, in a semi-wooded area at an elevation of 337 meters (Figure 2.8). The borehole dip starts at 75° and increases up to 65° at its end, 1000 meters deep. Below the first 200 meters the average temperature gradient is steady and equal 15 mK m^{-1} (Figure 2.11). Thermal conductivity varies from 2.8 to 3.8 W $m^{-1}K^{-1}$ and seems to decrease with depth. The average thermal conductivity value determined from all 10 core samples is 3.26 W $m^{-1}K^{-1}$. Mean heat flux obtained over this borehole is 49 mW m^{-2} before correction.

In this profile (Figure 2.11) we observed that heat flux is steady between 200 and 400 meters and amounts approximately 54 mW m^{-2} and decreases to an average value of 47 mW m^{-2} in the last portion of the borehole. The thermal conductivity decreases with depth may explain the decreases in heat flux. The borehole is not deep enough to observe the post-glacial effect of 7 mW m^{-2}. Mean radioactivity determined from 7 core samples is 0.73 μW m^{-3}. Lithology throughout this borehole consists mostly of rhyolite along with some basalts.

Hole 1104 is located in a wooded area about 750 meters, along a walking path, from Portelance road (Figure 2.8). The hole sits at an altitude of 342 meters. Its colar dip is

70° and decreases up to 58° at 850 meters deep. The hole dips toward a small hill of about 10 meters. The temperature gradient is perturbed over the first 200 meters of the borehole and below the mean temperature gradient is 14.9 mK m^{-1} (Figure 2.12). Average thermal conductivity over the borehole is 3.31 W $m^{-1}K^{-1}$. This value was determined from 8 core samples giving values from 2.8 to 3.8 W $m^{-1}K^{-1}$. Thermal conductivity increases with depth; this is observed in the heat flux profile where heat flux increases at around 650 meters deep. The overall mean heat flux value obtain in this borehole is 49 mW m^{-2}. The borehole is not deep enough to observe the effect of post-glacial warming, 7 mW m^{-2}. Mean radioactivity determined from 10 core samples is 0.93 μW m^{-3}. According to the lithological log of Xstrata this borehole cuts through basalt along the first 400 meters, followed by an alternation of diorite and granite from 400 to 570 meters deep and rhyolite down to the end.

This site mean heat flux (after climatic correction) and heat production values are 56 mW m^{-2} and 0.81 μW m^{-3}, respectively. Samples for thermal conductivity and heat production measurements were collected from core stored on Xstrata's core farm.

2.4 Heat flow, heat production and the crustal structure of the Sudbury region

Many high-quality heat flux measurements are available in the Canadian shield. Studies of these data along with other geophysical methods have allowed for a fairly accurate identification of the crustal structure of this vast Precambrian craton. Within the shield, surface heat flux varies from 80 to 23 mW m^{-2} and average 42 mW m^{-2}(Mareschal and Jaupart, 2004). The mantle and lower crustal heat fluxes are roughly constant with values of 15 and 33 mW m^{-2}, respectively (Mareschal and Jaupart, 2004). The near-absence of fluctuations within these fluxes is due to the smoothing effects of heat diffusion and the small amount of radio-elements found in the lower crust and the lithospheric mantle. Thus, variations in surface heat flux are linked to variations of heat production occurring in the crustal layer.

The Sudbury Neutrino Observatory is located within the Canadian Shield. Subsequently, heat flux data can be used to ascertain the crustal heat production and accurately determine the local geo-neutrino sources, as discussed in section 2.2.

The 15 heat flux values that have been identified so far in the Sudbury region are listed in Table 2.3, and their location is shown in the heat flux map in Figure 2.13. In the Sudbury region, surface heat flux varies between 43 mW m^{-2} and 61 mW m^{-2} with an average of 53 mW m^{-2}, which is significantly higher than the average heat flow of the Canadian shield (42 mW m^{-2}) (Figure 2.14). This local high heat flux anomaly is due to local enrichment in radioactive elements. Heat flux values located outside the structure, in the Superior and Southern Provinces, are usually higher than those located inside the structure. The highest values are found just south of the structure in the Southern Province, south and southwest of SNOLAB. Other high heat flux values were obtained farther west of the structure in the Superior and Southern Provinces at the East Bull Lake and Elliot Lake sites, respectively. In the Grenville Province, the only nearby heat flux measurement reported is located at Sturgeon Falls (44 mW m^{-2}). Variations in surface heat flux across the Sudbury region correlate well with the local geology. The post-impact sediments filling the structure as well as the underlying Sudbury Igneous Complex (SIC) are mostly composed of norite, gabbro, greenstone and anorthosite. These rock types are slightly radioactive. On the other hand, the Southern and Superior Provinces are rich in highly radioactive rocks such as granite, gneiss and greywacke (see Table 1.4 and 1.5 in Chapter 1). For details on the geology around SNOLAB, see section 1.2 in Chapter 1.

Many heat production measurements are also available in the Sudbury region. Some of these measurements were made on core samples at heat flow sites (Table 2.4), others were made on surface samples from many locations, and still others were made along a 17-km-long transect located in the Superior Province northwest of the structure (see Table 1.3 in Chapter 1). The locations of all available heat production measurements are plotted on the Sudbury heat production map (Figure 2.15). Crustal heat production varies significantly in the Sudbury region (0.12 to as high as 8 μW m^{-3} in the last portion of the Cartier transect). A high heat production anomaly is found south of the structure, surrounding SNOLAB. Heat production, as observed with heat flux measurements, is lower within the structure. A high heat production anomaly is also found north of the structure. This anomaly is not marked on the heat flux map, probably due to the lack of measurements. Moreover, Meldrum et al. (1997) have shown that the batholith is enriched in both U and Th, with average values

above 5 and 33 ppm, respectively. This high heat production was also indicated in the heat production map based on airborne radiometric survey (Figure 1.5 in Chapter 1).

The heat flux measurement coverage is not uniform and most measurements were conducted on the perimeter of the structure with the highest concentration of exploration wells. More heat flux measurements are needed to increase the resolution for the crustal component of the geo-neutrino flux calculation. The Cartier Batholith is an important target. Additional measurements in the batholith will allow to better identify the impact of this high heat production unit as well as its contribution to the crustal geo-neutrino flux.

2.5 Crustal geo-neutrino component near SNOLAB

So far, two different approaches have been tested to estimate the crustal radioactivity for calculating the crustal component of the geo-neutrino flux near a geo-neutrino observatory.

Enomoto et al. (2007) identified the crustal geo-neutrino component by adding up the heat production contribution of the different geological units around KamLAND. This method required intensive sampling and a good understanding of the underground structure. Perry et al. (2009) showed the limitation of this method for determining the crustal geo-neutrino component in the vicinity of SNOLAB. After examining all available geological and geophysical studies conducted in the Sudbury region, Perry et al. (2009) concluded that current knowledge of the underground structure near SNOLAB is still insufficient to reliably calculate the crustal geo-neutrino flux.

In the first chapter of this work, we calculated the crustal heat production in the Sudbury region from airborne radiometric data. A Comparison of these data with direct heat production measurements made on core and surface samples then demonstrated that airborne radiometric data underestimate the radioelement concentration, because of the poor penetration depth of the method. The superficial layer is depleted in radio-elements as a result of weathering processes. We concluded that airborne radiometric data will not provide the reliable heat production estimate we need to calculate the crustal component of the geo-neutrino flux.

As discussed above, heat flux measurements are the best method to estimate the crustal heat production in stable continental regions. We used all available heat flux and heat production measurements to calculate the crustal geo-neutrino component in the Sudbury region. To do so, we constructed two different grids of heat flux and crustal heat production : the near field (distance $< 5z_M$), in which the vertical differentiation of the HPEs is considered ; and the far field. The near field is calculated in an area of < 2 degrees in latitude and < 3 degrees in longitude of SNOLAB with a spatial resolution of 0.25 x 0.25 km. The far field is calculated on a grid of 2 x 2 degree cells as used to built the global model above. To fill the near field empty cells we considered two end-member scenarios resulting in three possible estimates of geneutrino flux : (1) averaging heat flux by interpolation between all the data points (Figure 2.16) (2) assigning the cells a low heat flux value (24 mW m^{-2}) (Figure 2.17) and (3) assigning the cells a high heat flux value (54 mW m^{-2}) (Figure 2.18). By interpolation, we obtain a geo-neutrino flux of about 50 TNU at SNOLAB (Figure 2.16). By assigning a high and a low heat flux value, the resulting geo-neutrino fluxes at SNOLAB are 44 and 52 TNU, respectively (Figure 2.17 and 2.18).

2.6 Conclusions

The crustal model of Fiorentini et al. (2005) obviously neglects local and regional fluctuations caused by geological and structural changes, since the geo-neutrino flux variation is generally associated with crustal thickness changes. The model based on heat flux seems to correlate better with the crustal radioactivity.

All available heat flux data in the Sudbury region, including new measurements presented in this work, have allowed to estimate a range for the crustal component of the geo-neutrino flux near SNOLAB. This result in a geo-neutrino flux of 44 TNU (lower limit) and of 52 TNU (upper limit). The uncertainty is still higher that the desirable precision of 1 TNU, but it could be reduced by adding more heat flux measurements.

Next step is to increase the heat flux measurement density and the uniformity of coverage in the Sudbury region. The Cartier batholith is an important target. Surface heat

production measurements made along the transect (Schneider et al., 1987), the heat production map from airborne gamma-ray spectrometry (Figure 1.5 in Chapter 1) and the study by (Meldrum et al., 1997) all suggest that the batholith is abnormally radioactive. This could have important consequences for the geo-neutrino observations at SNOLAB.

Acknowledgements

We are grateful to Claude Jaupart and John Armitage for field measurements, as well as to Hélène Bouquerel and Thierry Rivet for thermal conductivity measurements. Vale Inco and Xstrata Nickel have given us permission to perform measurements in their boreholes and to access their core samples. This work was supported by the NSERC Discovery Grants program to Claire Perry and Jean-Claude Mareschal.

References

Araki, T., and 86 collaborators, 2005. Experimental investigation of geologically produced antineutrinos with KamLAND. Nature 436, 499–503.

Bellini, G., and 89 collaborators, 2010. Observation of geo-neutrinos. Phys. Lett. B 687, 299–304.

Chen, M. C., 2006. Geo-neutrinos in SNO+. Earth Moon and Planets 99, 221–228.

Chouinard, C., Mareschal, J.-C., Jan. 2009. Ground surface temperature history in southern Canada : Temperatures at the base of the Laurentide ice sheet and during the Holocene. Earth Planet. Sci. Lett. 277, 280–289.

Davies, J. H., Davies, D. R., Feb. 2010. Earth's surface heat flux. Solid Earth 1, 5–24.

Drury, M., Taylor, A., 1986. Some new measurements of heat flow in the Superior Province of the Canadian Shield. Can. J. Earth Sci. 24, 1486–1489.

Enomoto, S., Ohtani, E., Inoue, K., Suzuki, A., 2007. Neutrino geophysics with KamLAND and future prospects. Earth Planet. Sci. Lett. 258, 147–159.

Fiorentini, G., Lissia, M., Mantovani, F., Vannucci, R., 2005. Geo-neutrinos : a new probe of Earth's interior [rapid communication]. Earth Planet. Sci. Lett. 238, 235–247.

Fourier, 1822. Theorie Analytique de la Chaleur. Paris.

Gando, A. and 65 collaborators, Sep. 2011. Partial radiogenic heat model for Earth revealed by geoneutrino measurements. Nature Geoscience 4, 647–651.

Gonzalez-Garcia, M. C., Nir, Y., Mar. 2003. Neutrino masses and mixing : evidence and implications. Rev. Modern Phys. 75, 345–402.

Jaupart, C., Labrosse, S., Mareschal, J.-C., 2007. Temperatures, heat and energy in the mantle of the Earth. In : Bercovici, D. (Ed.), Treatise on Geophysics, The Mantle. Vol. 7. Elsevier, New York, pp. 253–303.

Jaupart, C., Mareschal, J.-C., 1999. The thermal structure and thickness of continental roots. Lithos 48, 93–114.

Jessop, A. M., Jan. 1971. The distribution of glacial perturbation of heat flow in Canada. Canadian Journal of Earth Sciences 8, 162–166.

Jessop, A. M., Lewis, T. J., 1978. Heat flow and heat generation in the Superior Province of the Canadian Shield. Tectonophysics 50, 55–57.

Lewis, T. J., Bentkowski, W. H., 1988. Potassium, uranium and thorium concentrations of crustal rocks : a data file. Geol. Surv. Can., Open File Report 1744, 165 pp.

Mantovani, F., Carmignani, L., Fiorentini, G., Lissia, M., Jan. 2004. Antineutrinos from Earth : A reference model and its uncertainties. Phys. Rev. D 69 (1), 013001.

Mareschal, J.-C., Jaupart, C., Jun. 2004. Variations of surface heat flow and lithospheric thermal structure beneath the North American craton. Earth Planet. Sci. Lett. 223, 65–77.

Mareschal, J.-C., Jaupart, C., Phaneuf, C. Perry, C., 2012. Geoneutrinos and the energy budget of the Earth. Journal of Geodynamics 54, 43–54.

Meldrum, A., Abdel-Rahman, A.-F. M., Wodicka, N., 1997. Documentation of a 1450 Ma contractional orogeny preserved between the 1850Ma Sudbury impact structure and the 1 Ga Grenville orogenic front, Ontario, Canada. Precambrian Res. 82, 265–285.

Misener, A., Thompson, L., Uffen, R., 1951. Terrestrial heat flow in Ontario and Quebec. Trans. Am. Geophys. Union 36, 1055–1060.

Misener, A. D., Beck, A. E., 1960. The Measurement of heat flow over land. Methods and Techniques in Geophysics, Volume 1, 10.

Mooney, W. D., Laske, G., Guy Masters, T., Jan. 1998. CRUST 5.1 : A global crustal model at $><$ 5 deg $\times$ 5 deg. J. Geophys. Res. (Solid Earth) 103, 727–748.

Perry, H. K. C., Jaupart, C., Mareschal, J.-C., Bienfait, G., 2006a. Crustal heat production in the Superior Province, Canadian Shield, and in North America inferred from heat flow data. J. Geophys. Res. (Solid Earth) 111, B04401, doi :10.1029/2005JB003893.

Perry, H. K. C., Mareschal, J.-C., Jaupart, C., Oct. 2009. Enhanced crustal geo-neutrino production near the Sudbury Neutrino Observatory, Ontario, Canada. Earth Planet. Sci. Lett. 288, 301–308.

Pinet, C., Jaupart, C., Mareschal, J.-C., Gariepy, C., Bienfait, G., Lapointe, R., Nov. 1991. Heat flow and structure of the lithosphere in the eastern Canadian shield. J. Geophys. Res. 96, 19,941–19,963.

Pollack, H. N., Hurter, S. J., Johnston, J. R., 1993. Heat flow from the Earth's interior : analysis of the global data set. Rev. Geophys. 31, 267–280.

Raghavan, R. S., Schoenert, S., Enomoto, S., Shirai, J., Suekane, F., Suzuki, A., Jan. 1998. Measuring the Global Radioactivity in the Earth by Multidetector Antineutrino Spectroscopy. Phys. Rev. Lett. 80, 635–638.

Rudnick, R. L., Fountain, D. M., 1995. Nature and composition of the continental crust : A lower crustal perspective. Rev. Geophys. 33, 267–310.

Sass, J. H., Killeen, P. G., Mustonen, E. D., Dec. 1968. Heat flow and surface radioactivity in the Quirke Lake Syncline near Elliot Lake, Ontario, Canada. Can. J. Earth Sci. 5, 1417–1428.

Schneider, R. V., Roy, R. F., Smith, A. R., 1987. Investigations and interpretations of the vertical distribution of U, TH, and K : South Africa and Canada. Geophys. Res. Lett. 14, 264–267.

Sclater, J. G., Jaupart, C., Galson, D., 1980. The heat flow through oceanic and continental crust and the heat loss of the Earth. Rev. Geophys. Space Phys. 18 (1), 269–311.

Shaw, D., Cramer, J., Higgins, M., Truscott, M., 1986. Composition of the Canadian Precambrian Shield and the continental crust of the Earth. In : Dawson, J. e. a. (Ed.), Nature of the Lower Continental Crust. Geol. Soc. London., pp. 257–282.

Taylor, S. R., McLennan, S. M., 1995. The continental crust : Its composition and evolution. Blackwell.

Wedepohl, K. H., 1995. The composition of the continental crust. Geochim Cosmochim. Acta 59, 1217–1239.

Table 2.1
Details on new heat flux measurements

Site hole #	Lat North	Long West	Dip °	Δh m	N_λ	$<\lambda>$ ($Wm^{-1}\ K^{-1}$)	Γ ($mK\ m^{-1}$)	Q ($mW\ m^{-2}$)	σ_Q	ΔQ	Q_c	Ref
Victor Mine	**46°40.68**	**80°49.58**									**44**	**(1)**
1101(855-151)	46°40.58	80°49.6	88	1300	8	2.59	14.6	38	1.86	4	42	(1)
1102(885-170)	46°40.78	80°49.55	90	930	7	2.72	14.5	39	0.93	7	46	(1)
Parkin	**46°48.19**	**80°52.68**									**56**	**(1)**
1103(P-60)	46°48.37	80°52.57	75	1000	10	3.26	15	49	1.32	7	55	(1)
1104(P-61)	46°48	80°52.79	70	850	8	3.31	14.9	49	1.52	7	56	(1)

Dip is the borehole inclination at the collar, Δh is the borehole depth, $<\lambda>$ is the thermal conductivity, N_λ is the number of conductivity determinations, Γ is the temperature gradient and Q is the heat flux with σ_Q standard deviation, and ΔQ is the adjustment for post glacial warming (Jessop, 1971). Site averaged heat flux values are in bold characters. Standard characters show individual heat flux values that were determined at each borehole. Hole numbers in bracket are the company's hole reference numbers.
Reference : (1) This report.

Table 2.2
Details on new heat production measurements

Site hole #	Rocktype	Province	U (ppm)	Th (ppm)	K (%)	Th/U	A (μW)	σ_A (m^{-3})	N_A	Ref
Victor Mine	**Gabbro/Norite**	**in structure**	**1.10**	**5.46**	**1.32**	**5.13**	**0.78**	**0.25**	**15**	**(1)**
1101	"	"	1.11	5.42	1.32	5.96	0.78	0.27	6	(1)
1102	"	"	1.09	5.52	1.32	5.38	0.78	0.24	9	(1)
Parkin	**Rhyolite/Basalt**	**Superior**	**1.13**	**5.09**	**1.82**	**4.5**	**0.81**	**0.23**	**17**	**(1)**
1103	"	"	1.09	4.70	1.31	4.35	0.73	0.2	7	(1)
1104	"	"	1.19	5.6	2.6	4.72	0.93	0.23	10	(1)

U and Th are Uranium and Thorium concentration in ppm, K is potassium concentration in per cent, A and σ_A are the heat production and its standard deviation in μW m^{-3}, respectively and N_A is the number of samples. Site averaged heat production values are in bold characters. Standard Characters show the average values of heat production determined from samples from each borehole.
References : (1) This report.

Table 2.3
Location and heat flux for all the Sudbury sites

Site hole	Latitude North	Longitude West	Q (mW m^{-2})	Reference
Sudbury 1	46°28	81°11	51	(1)
Elliot Lake	46°30	82°30	60	(2)
67001 Moose Lake	46°39	81°18.2	49	(3)
67002 Onaping	46°37.7	81°23.3	56	(3)
67003 Windy Lake	46°36.6	81°25.8	43	(3)
67005 Victoria	46°24.8	81°23.7	55	(3)
67006 Murray	46°30.9	81°05.1	51	(3)
67007 Lockerby 1	46°26	81°19.3	61	(3)
East Bull Lake	46°26	82°13	56	(4)
Copper-Cliff	46°26.4	81°03.93	59	(5)
Sturgeon Falls	46°26.6	79°56.8	44	(5)
Falconbridge	46°39.1	80°47.5	49	(6),(7)
Lockerby Mine	46°26	81°18.92	59	(6),(7)
new sites (2011)				
Victor Mine	46°40.68	80°49.58	44	(8)
Parkin	46°48.19	80°52.68	56	(8)

Q is the site averaged heat flux value. These values were adjusted for post glacial warming following the model of Jessop (1971).
References : (1) Misener et al. (1951), (2) Sass et al. (1968), (3) Jessop and Lewis (1978), (4) Drury and Taylor (1986), (5) Pinet et al. (1991), (6) Chouinard and Mareschal (2009), (7) Perry et al. (2009), (8) This report.

Table 2.4
Heat production at from all Sudbury heat flow sites

Site	Rocktype	Province	U (ppm)	Th (ppm)	K (%)	Th/U	A (μW)	σ_A (m^{-3})	N_A	Ref
67001 Moose Lake	-	in structure	2.1	10.0	1.7	4.47	1.43	0.98	11	(1)
Copper-Cliff	Greywacke	Southern	6.8	16.5	2.2	2.37	3.2	0.8	7	(2)
Sturgeon Fall	Granite/Gneiss	Grenville	1.05	6.45	3.7	6.14	1.55	0.28	2	(2)
East Bull Lake	↓	**Superior**	**0.74**	**4.23**	**0.61**	**3.52**	**0.54**	**0.57**	**20**	**(3)**
"	Anorthosite	"	0.49	1.65	0.64	3.42	0.3	0.17	10	(3)
"	Gabbro	"	0.97	7.87	0.53	7.05	0.86	0.8	9	(3)
"	Granite	"	1.28	2.46	1.43	1.92	0.64	-	1	(3)
Craig Mine[a]	↓	**in structure**	**1.72**	**8.07**	**1.62**	**5.83**	**1.15**	**0.79**	**19**	**(4)**
"	Granophyre	"	2.95	13.8	2.71	5.28	1.97	0.19	9	(4)
"	Norite	"	0.76	3.68	0.78	6.32	0.52	0.12	10	(4)
Falconbridge	Felsic norite	in structure	1.1	5.4	0.9	5.66	0.73	0.2	26	(4)
Lockerby Mine	Granite porphyry	in structure	5.4	26.5	3.2	5.44	3.53	1.4	20	(4)
new sites (2011)										
Victor Mine	Gabbro/Norite	in structure	1.10	5.46	1.32	5.13	0.78	0.25	15	(5)
Parkin	Rhyolite/Basalt	Superior	1.13	5.09	1.82	4.5	0.81	0.23	17	(5)

[a] Craig Mine is located near the Moose Lake site.
U and Th are Uranium and Thorium concentration in ppm, K is potassium concentration in per cent, A and σ_A are the heat production and its standard deviation in μW m^{-3}, respectively and N_A is the number of samples. Bold characters indicate the average value of the site (for all rocktypes), for sites where more than one type of rock is encountered.
References : (1) Jessop and Lewis (1978), (2) Pinet et al. (1991), (3) Lewis and Bentkowski (1988), (4) Perry et al. (2009), (5) This report.

Figures captions

Table Page

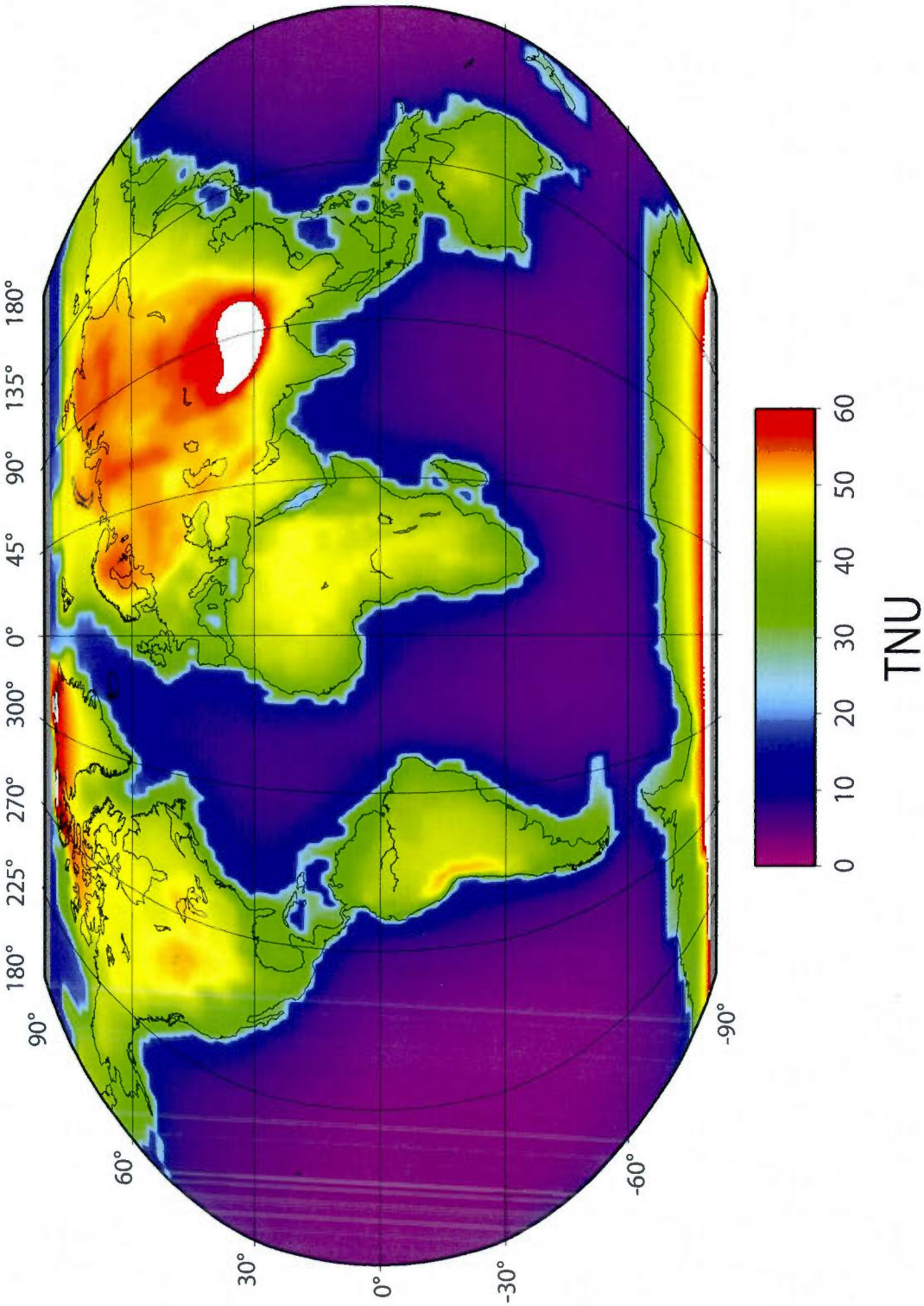
180°
225°
270°
300°
0°
45°
90°
135°
180°
90°
60°
30°
0°
-30°
-60°
-90°
0
10
20
30
40
50
60
TNU

Figure 2.1

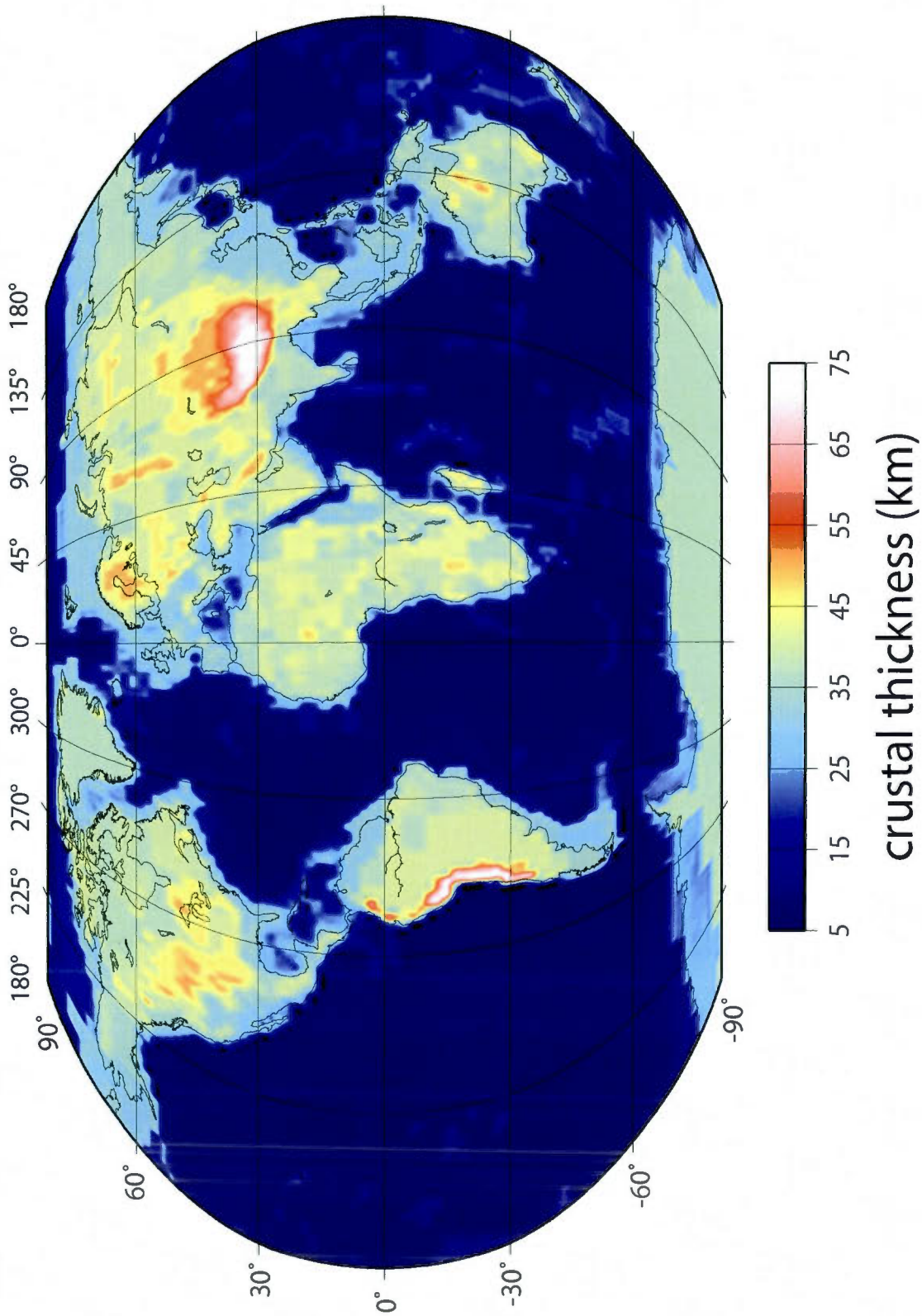
180°
225°
270°
300°
0°
45°
90°
135°
180°
90°
60°
30°
0°
-30°
-60°
-90°
5
15
25
35
45
55
65
75
crustal thickness (km)

Figure 2.2

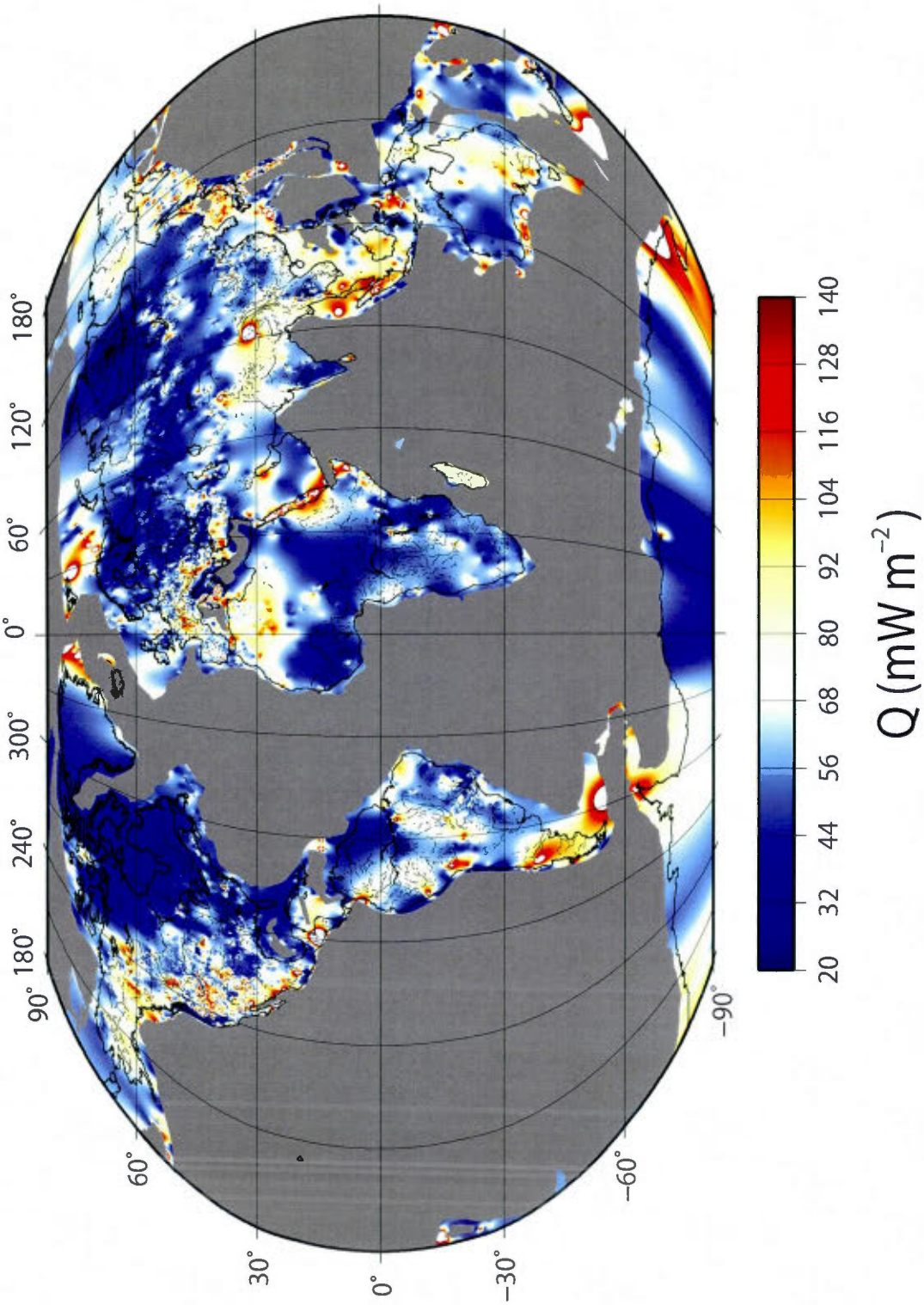
180°
120°
60°
0°
300°
240°
180°
90°
60°
30°
0°
−30°
−60°
−90°
20
32
44
56
68
80
92
104
116
128
140
Q (mW m^{-2})

Figure 2.3

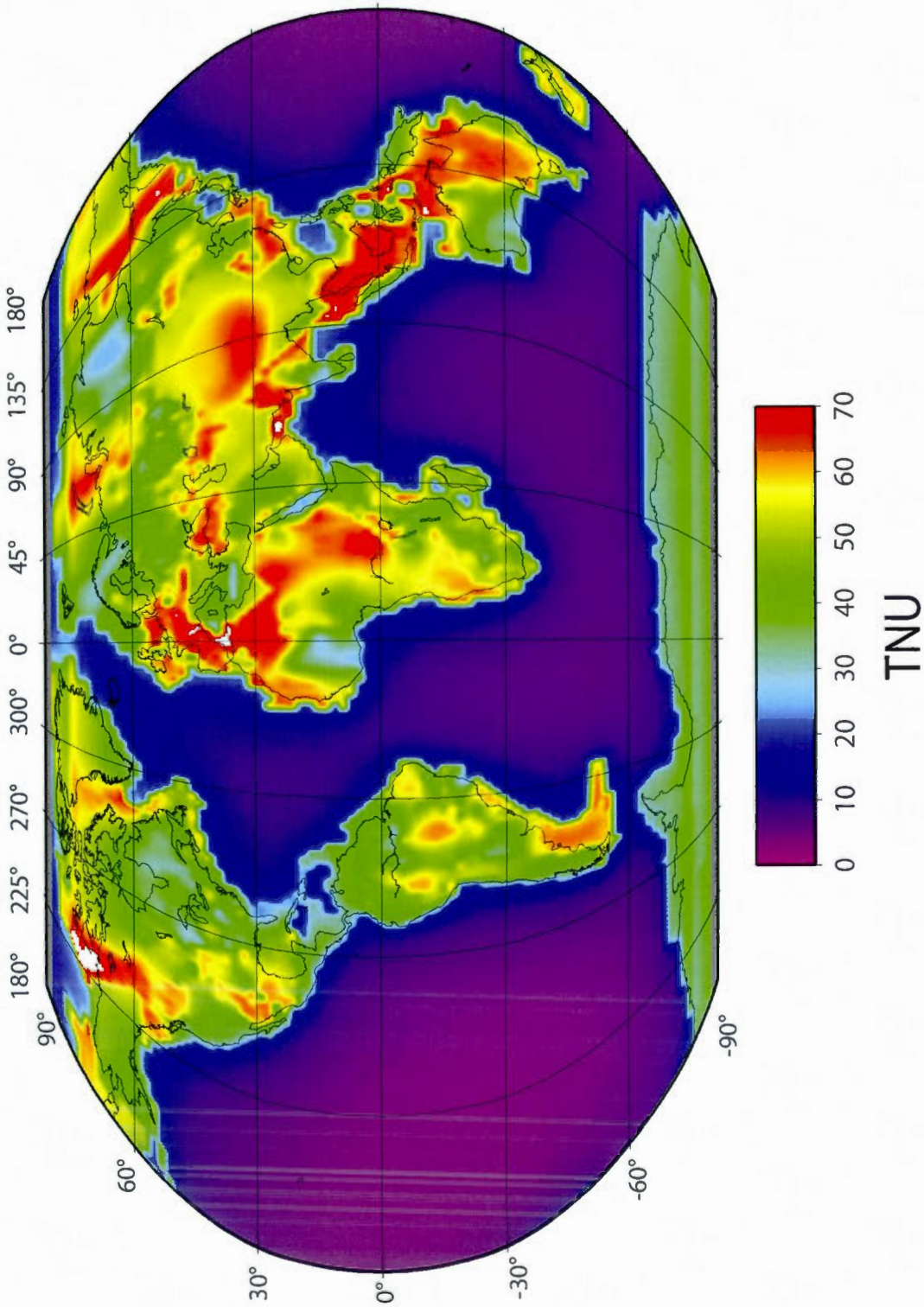
180°
225°
270°
300°
0°
45°
90°
135°
180°
90°
60°
30°
0°
-30°
-60°
-90°
0
10
20
30
40
50
60
70
TNU

Figure 2.4

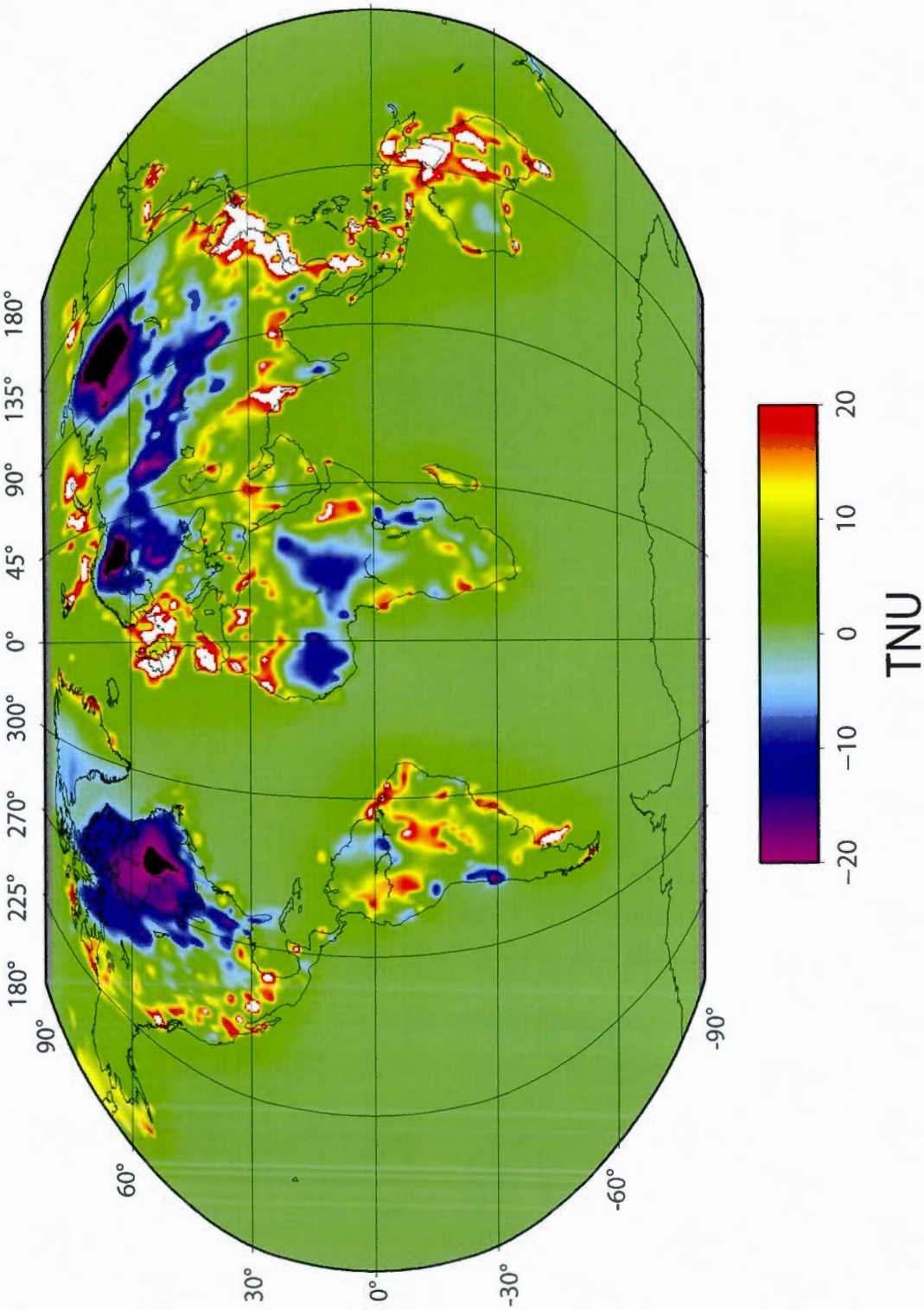

Figure 2.5

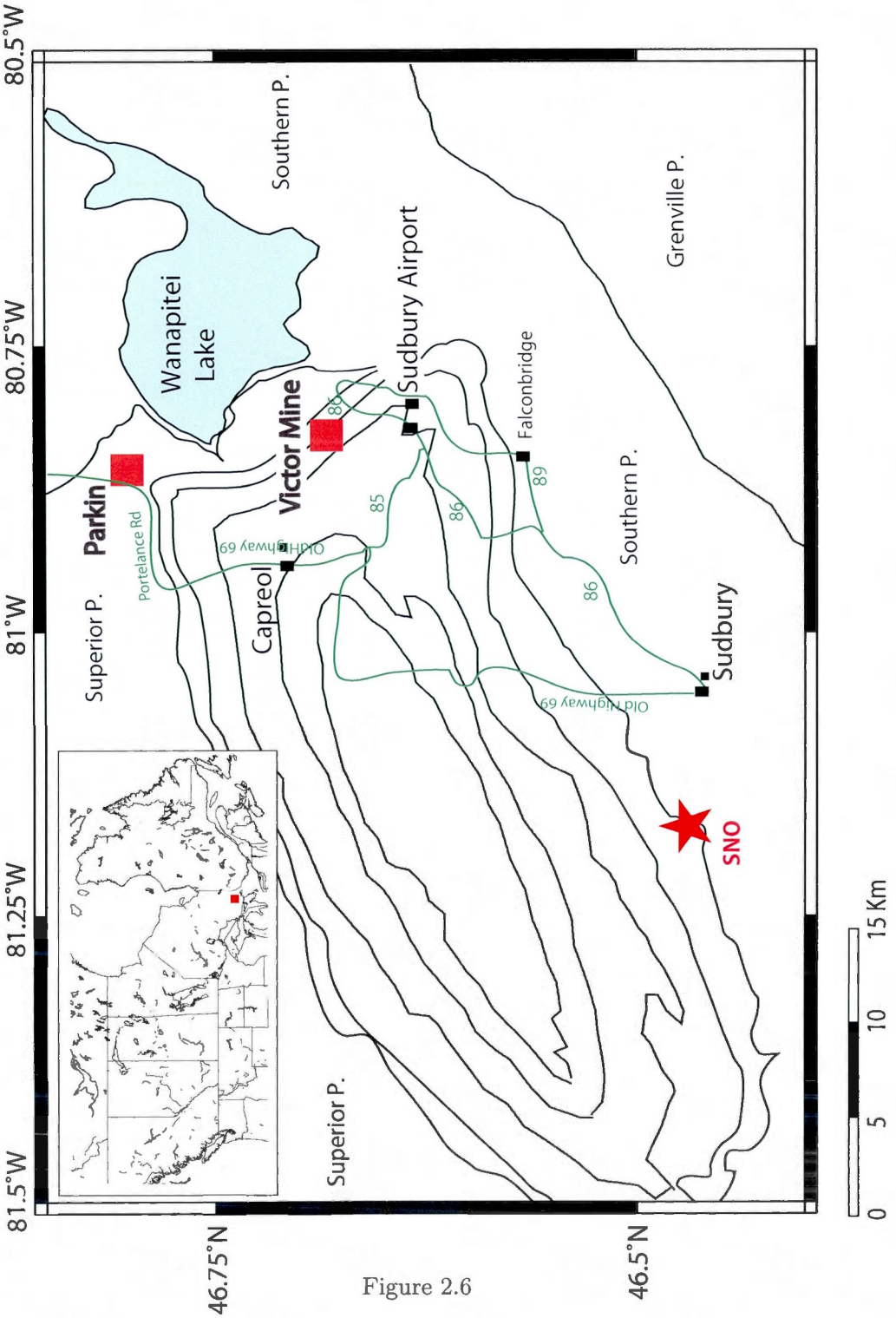
81.5°W
81.25°W
81°W
80.75°W
80.5°W
46.75°N
46.5°N
Superior P.
Parkin
Portelance Rd
Wanapitei Lake
Southern P.
Victor Mine
Capreol
Old Highway 69
Sudbury Airport
Falconbridge
Grenville P.
Southern P.
Sudbury
Old Highway 69
SNO
Superior P.
85
86
89
86
0
5
10
15 Km

Figure 2.6

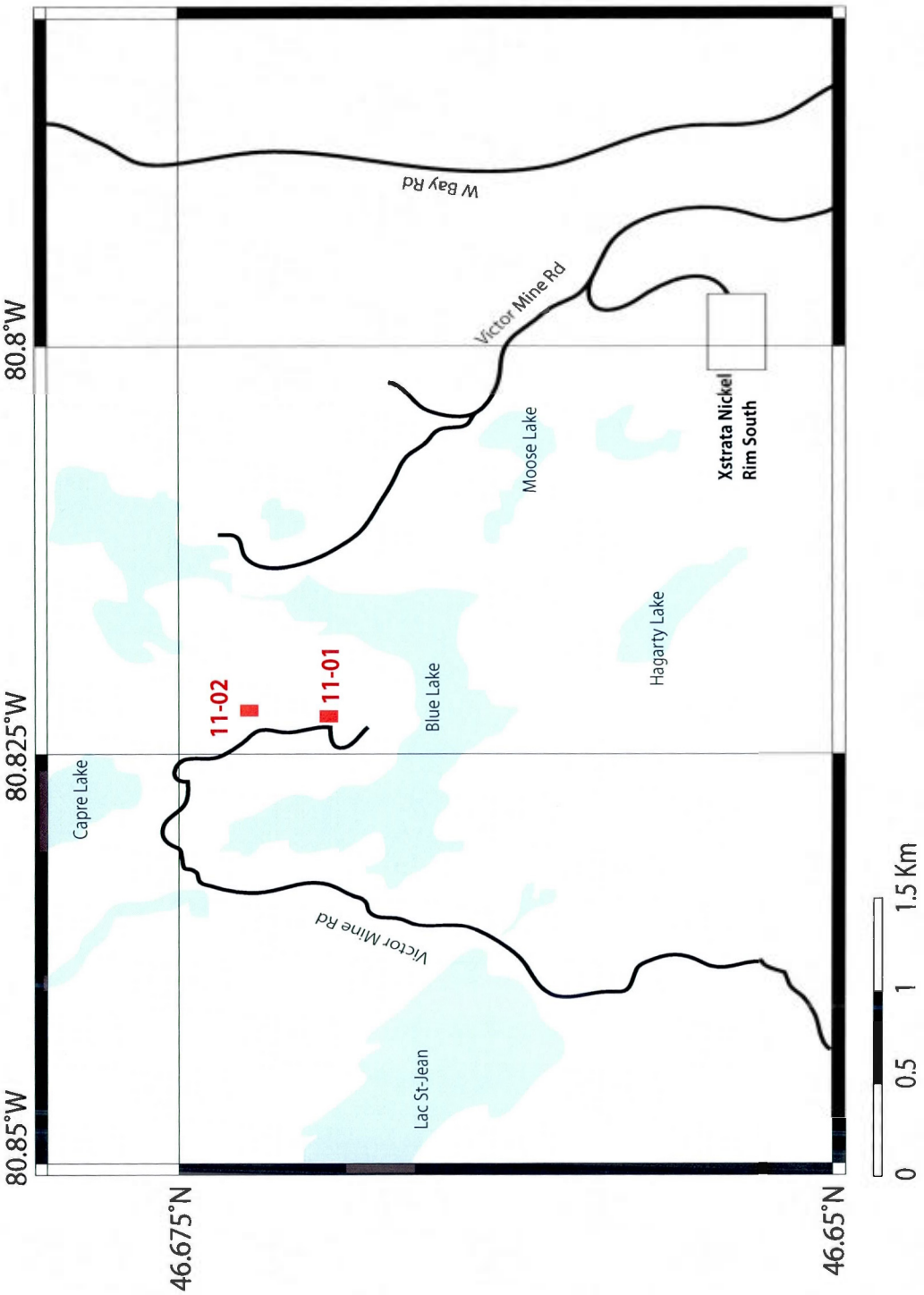
80.85°W
80.825°W
80.8°W
46.675°N
46.65°N
W Bay Rd
Victor Mine Rd
Victor Mine Rd
Xstrata Nickel
Rim South
Moose Lake
Hagarty Lake
Blue Lake
Capre Lake
Lac St-Jean
11-02
11-01
0
0.5
1
1.5 Km

Figure 2.7

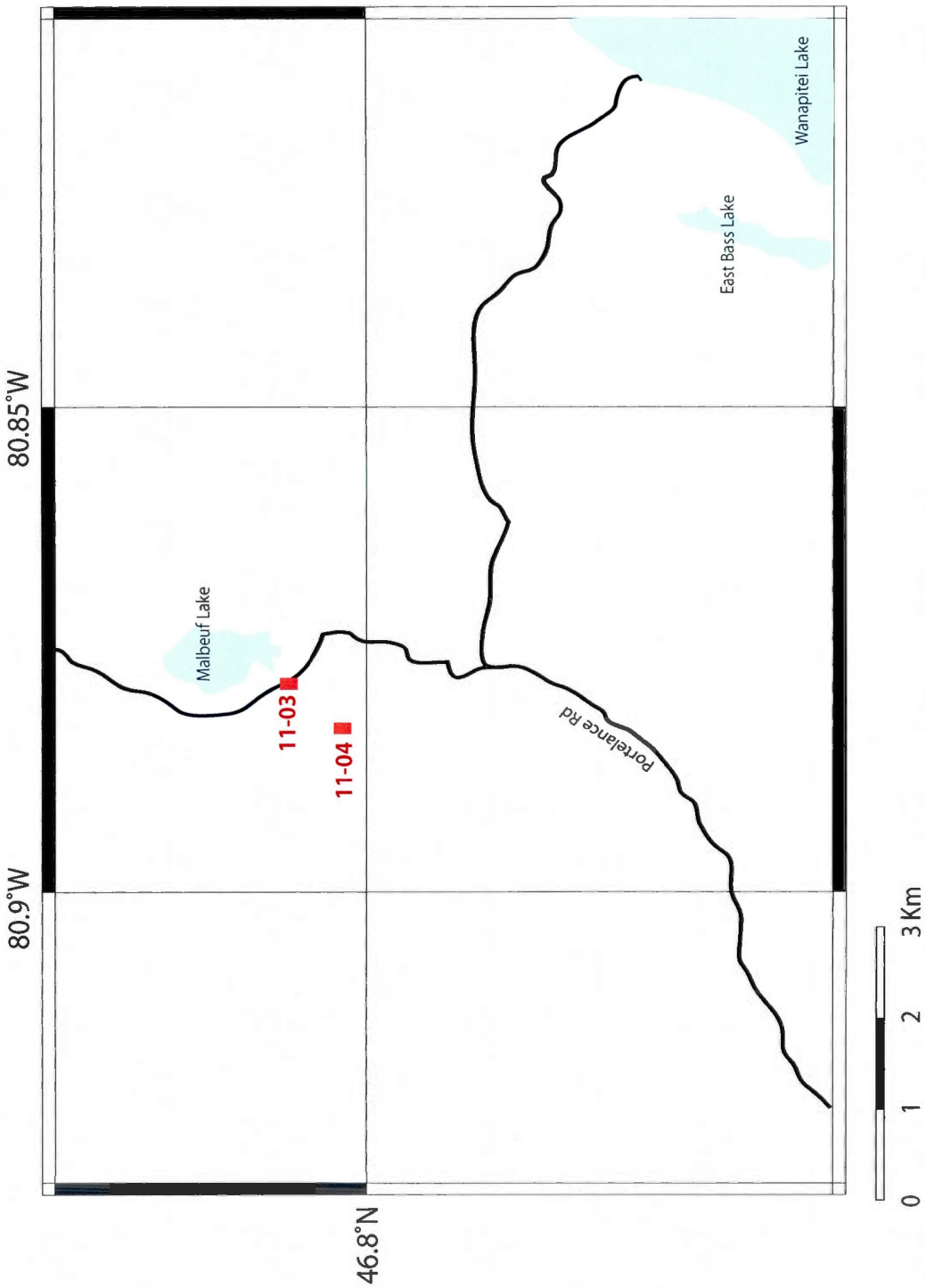
80.85°W
80.9°W
46.8°N
Malbeuf Lake
11-03
11-04
Portelance Rd
East Bass Lake
Wanapitei Lake
0
1
2
3 Km

Figure 2.8

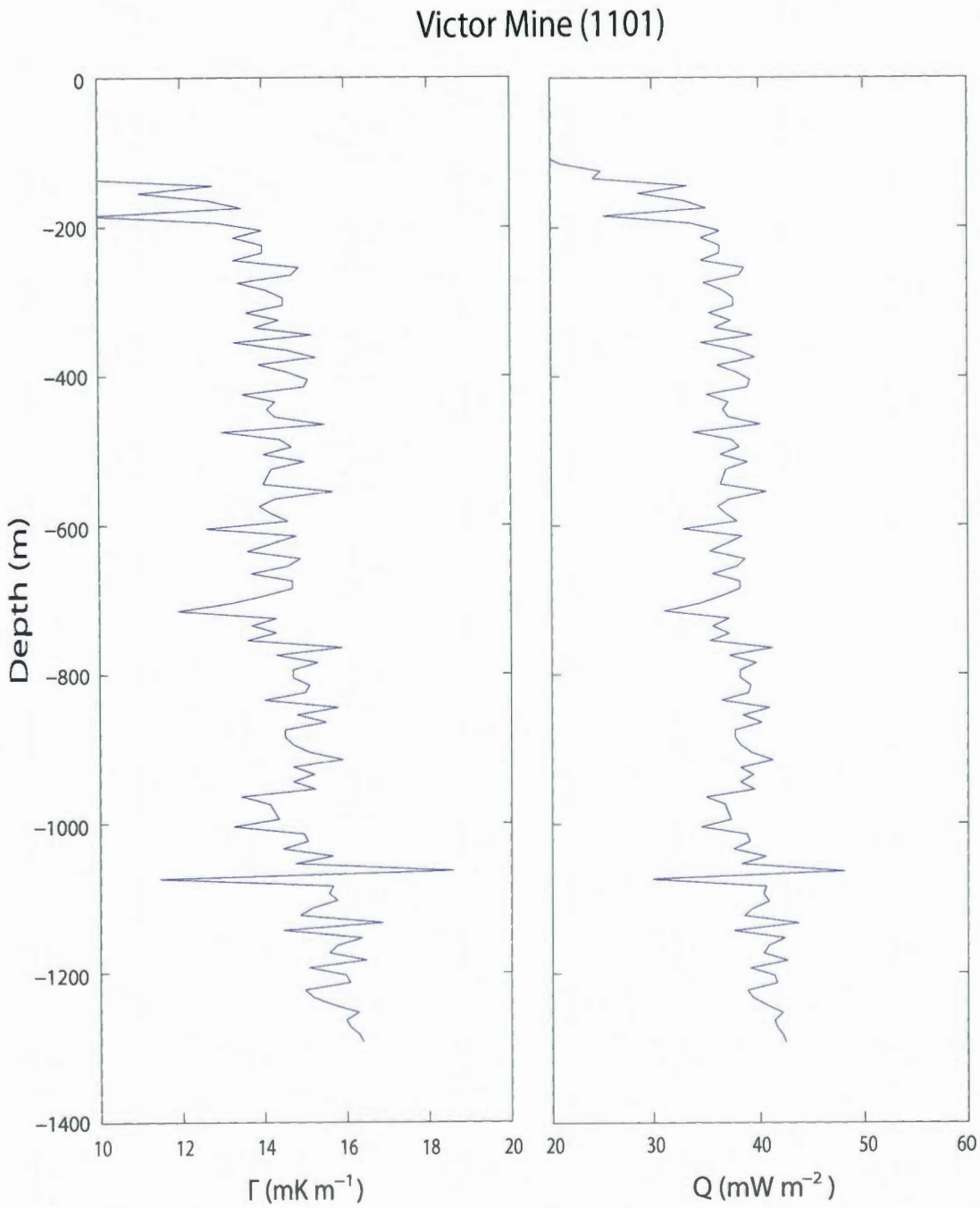
Victor Mine (1101)
Depth (m)
0
−200
−400
−600
−800
−1000
−1200
−1400
10
12
14
16
18
20
Γ (mK m^{-1})
20
30
40
50
60
Q (mW m^{-2})

Figure 2.9

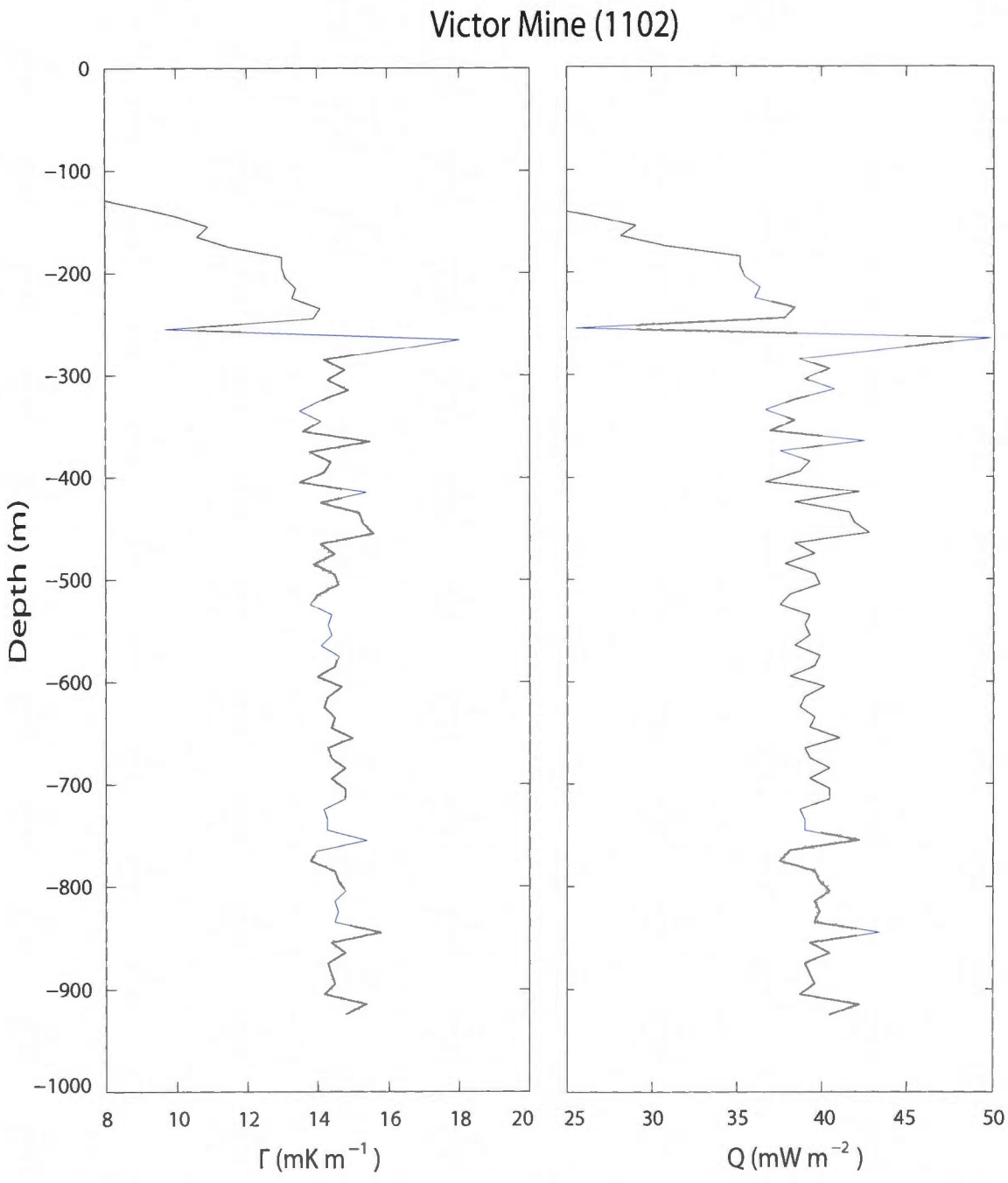
Victor Mine (1102)
Depth (m)
0
−100
−200
−300
−400
−500
−600
−700
−800
−900
−1000
8
10
12
14
16
18
20
Γ (mK m^{-1})
25
30
35
40
45
50
Q (mW m^{-2})

Figure 2.10

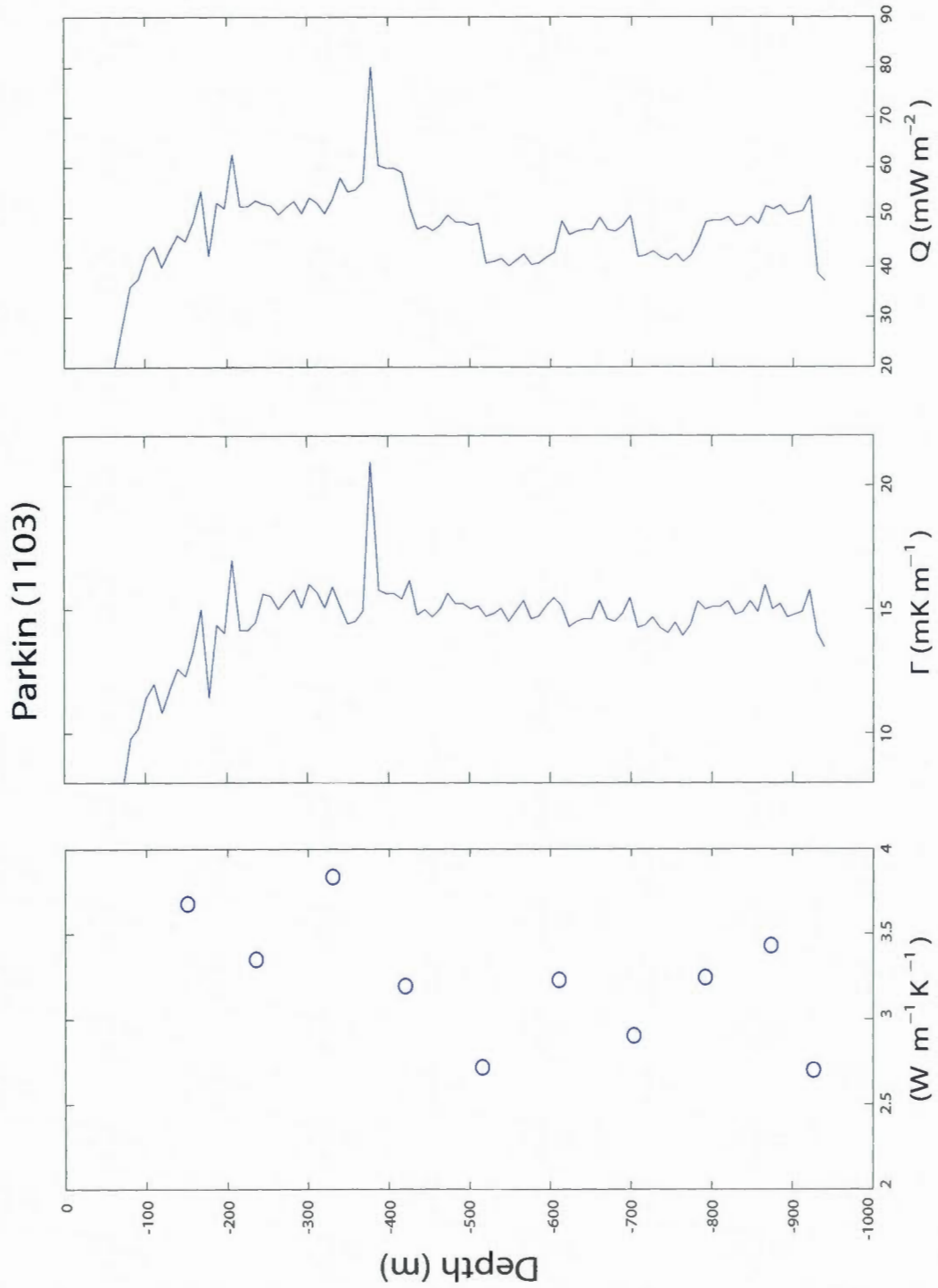
Parkin (1103)
Depth (m)
0
-100
-200
-300
-400
-500
-600
-700
-800
-900
-1000
2
2.5
3
3.5
4
(W m^{-1} K^{-1})
10
15
20
Γ (mK m^{-1})
20
30
40
50
60
70
80
90
Q (mW m^{-2})

Figure 2.11

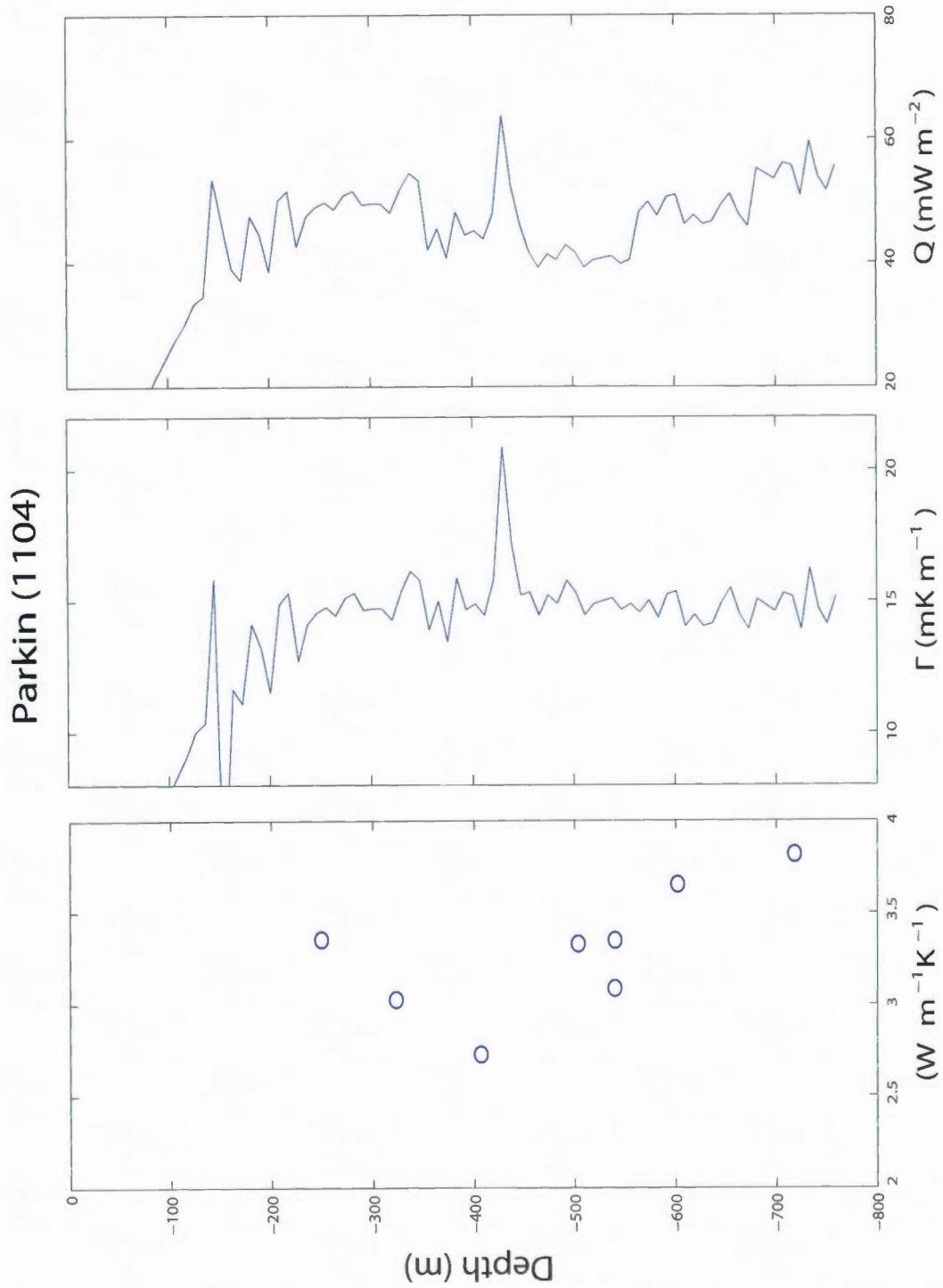
Parkin (1104)
Depth (m)
0
-100
-200
-300
-400
-500
-600
-700
-800
(W m^{-1}K^{-1})
2
2.5
3
3.5
4
Γ (mK m^{-1})
10
15
20
Q (mW m^{-2})
20
40
60
80

Figure 2.12

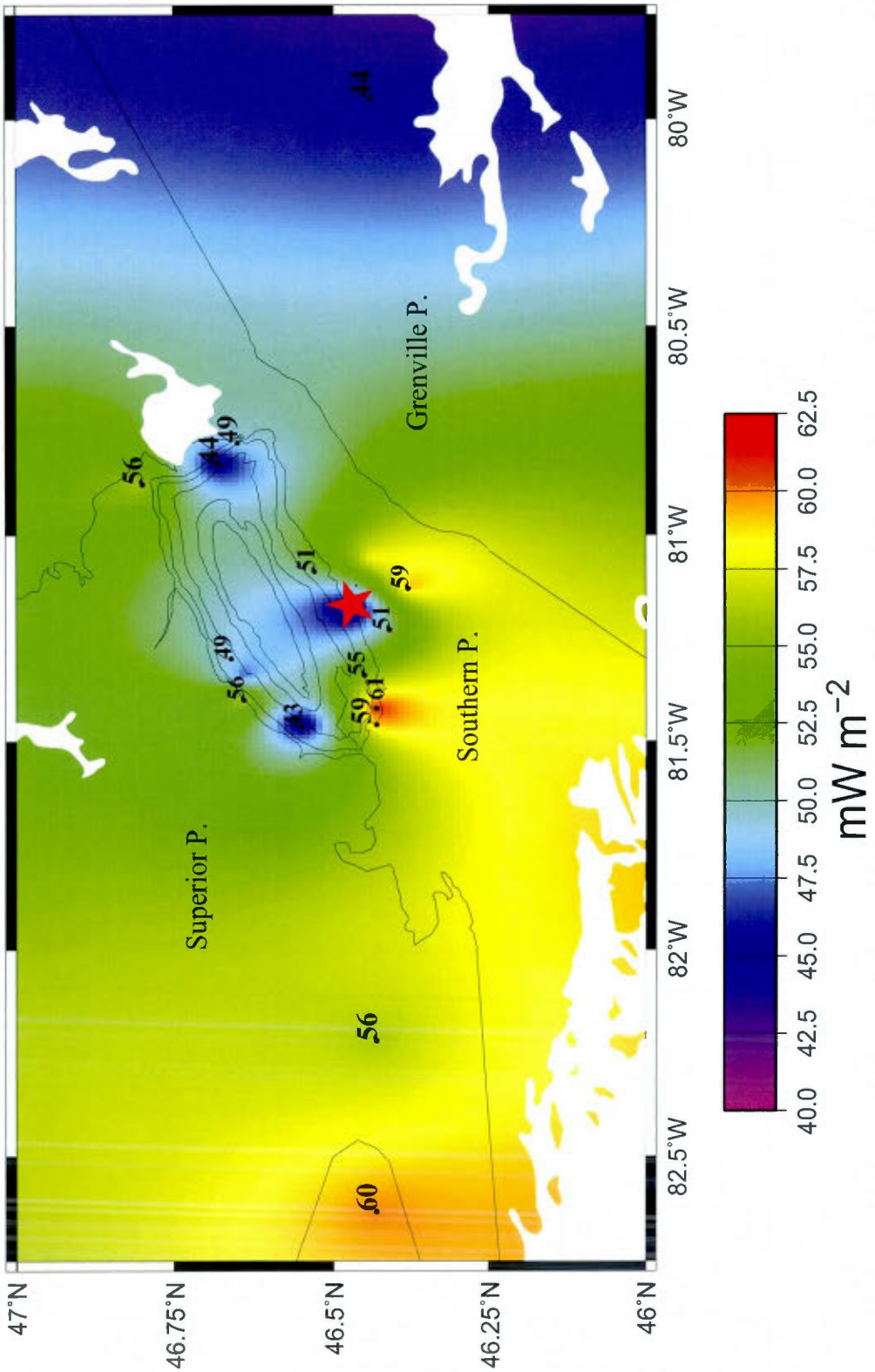
Superior P.
Southern P.
Grenville P.
44
49
56
51
59
51
49
56
55
61
59
43
56
60
47°N
46.75°N
46.5°N
46.25°N
46°N
82.5°W
82°W
81.5°W
81°W
80.5°W
80°W
40.0
42.5
45.0
47.5
50.0
52.5
55.0
57.5
60.0
62.5
mW m^{-2}

Figure 2.13

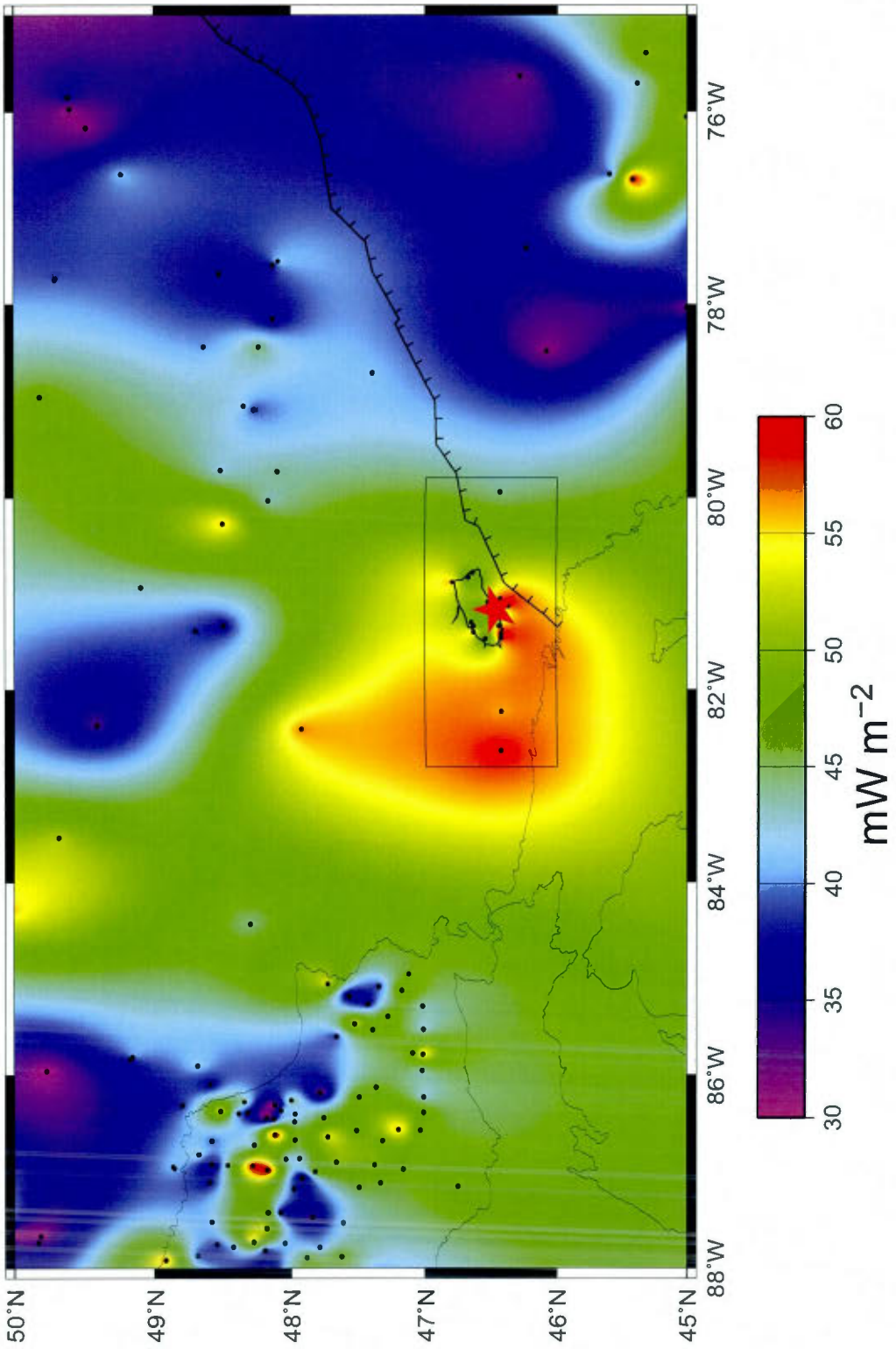
50°N
49°N
48°N
47°N
46°N
45°N
88°W
86°W
84°W
82°W
80°W
78°W
76°W
30
35
40
45
50
55
60
mW m⁻²

Figure 2.14

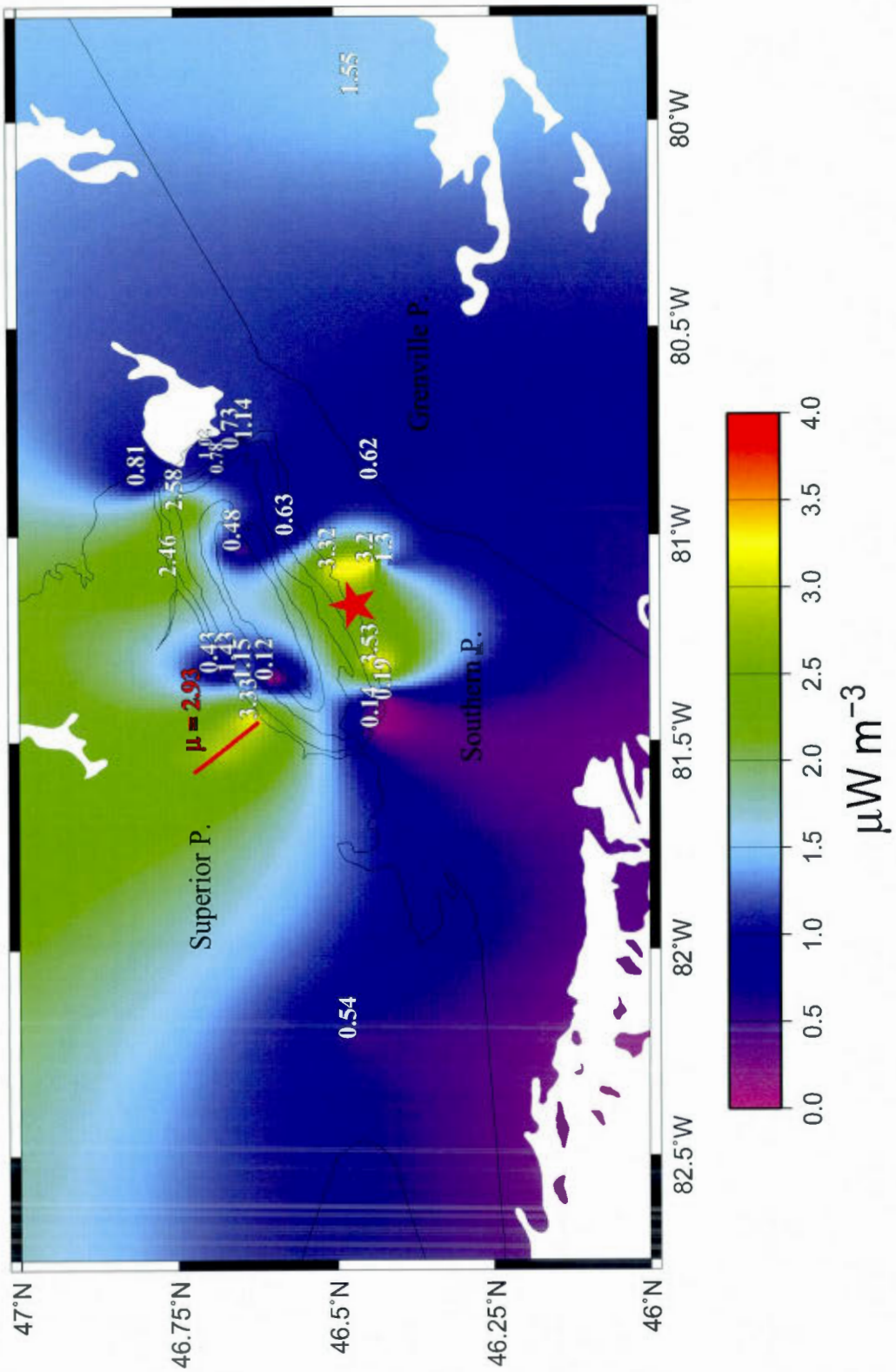
Superior P.
Southern P.
Grenville P.
μ = 2.93
0.81
2.58
0.73
1.14
0.48
0.63
0.62
2.46
3.32
3.2
1.55
0.43
1.15
0.12
3.53
0.19
0.54
47°N
46.75°N
46.5°N
46.25°N
46°N
82.5°W
82°W
81.5°W
81°W
80.5°W
80°W
0.0
0.5
1.0
1.5
2.0
2.5
3.0
3.5
4.0
μW m−3

Figure 2.15

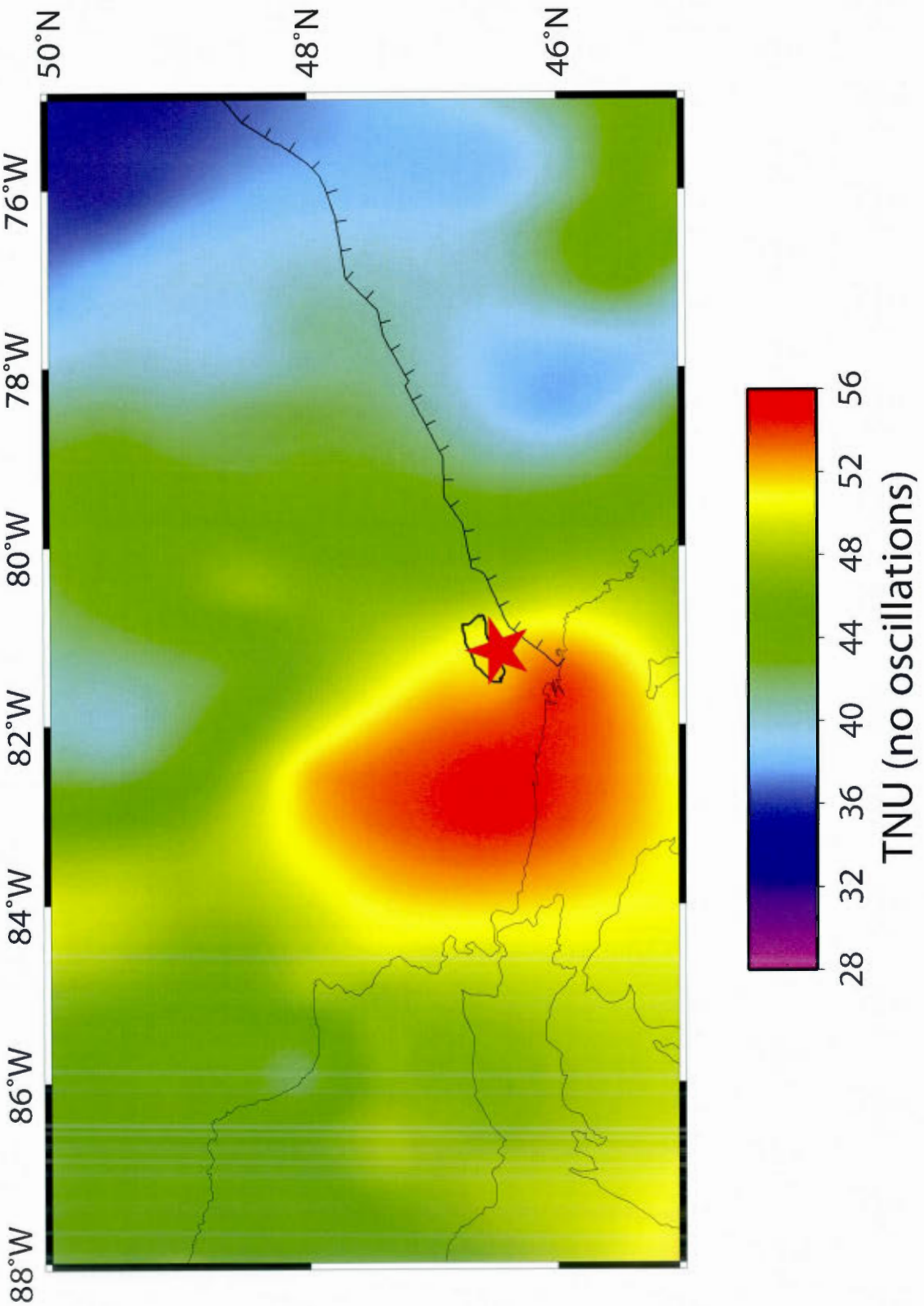
50°N
48°N
46°N
76°W
78°W
80°W
82°W
84°W
86°W
88°W
28
32
36
40
44
48
52
56
TNU (no oscillations)

Figure 2.16

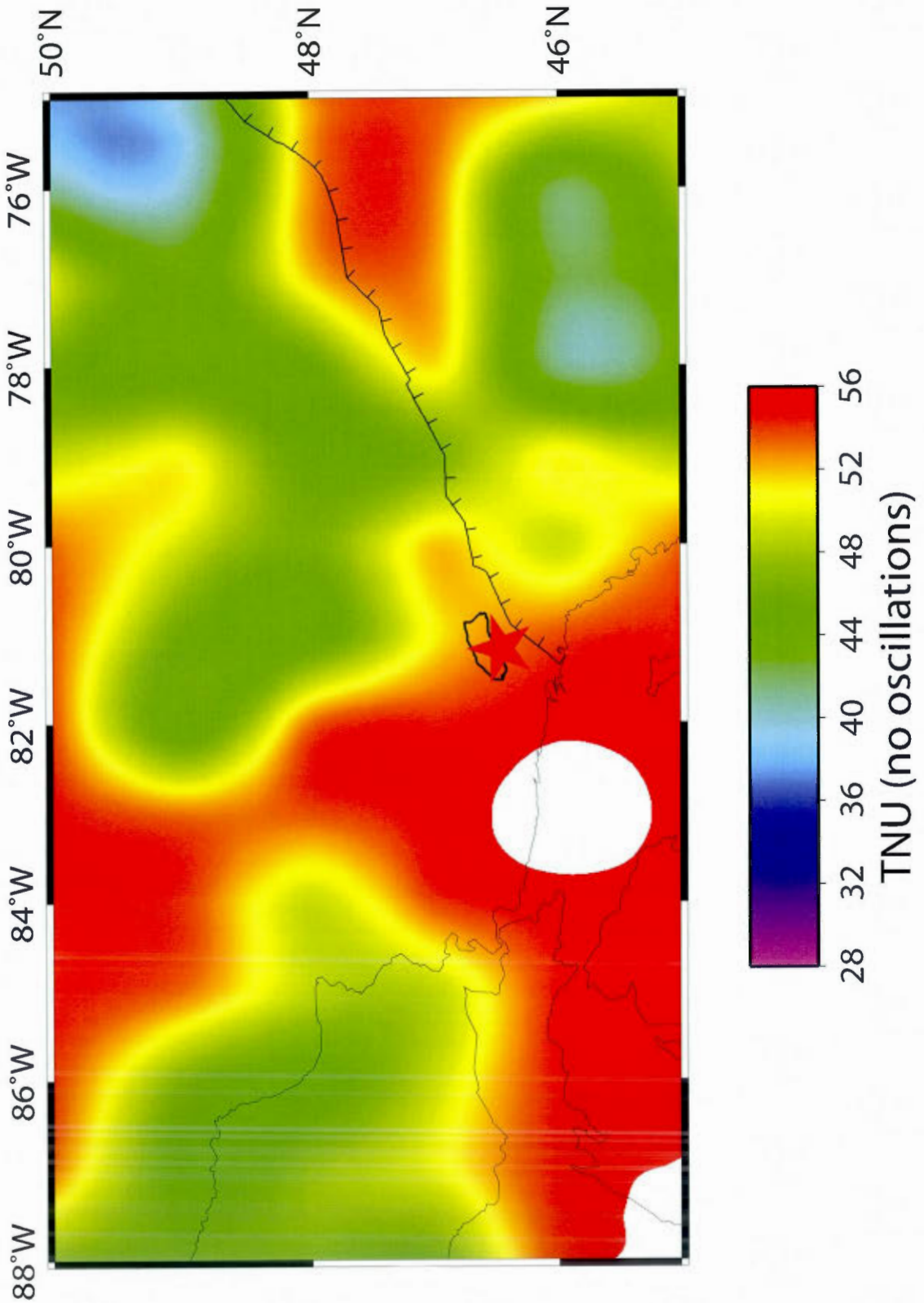
50°N
48°N
46°N
76°W
78°W
80°W
82°W
84°W
86°W
88°W
28
32
36
40
44
48
52
56
TNU (no oscillations)

Figure 2.17

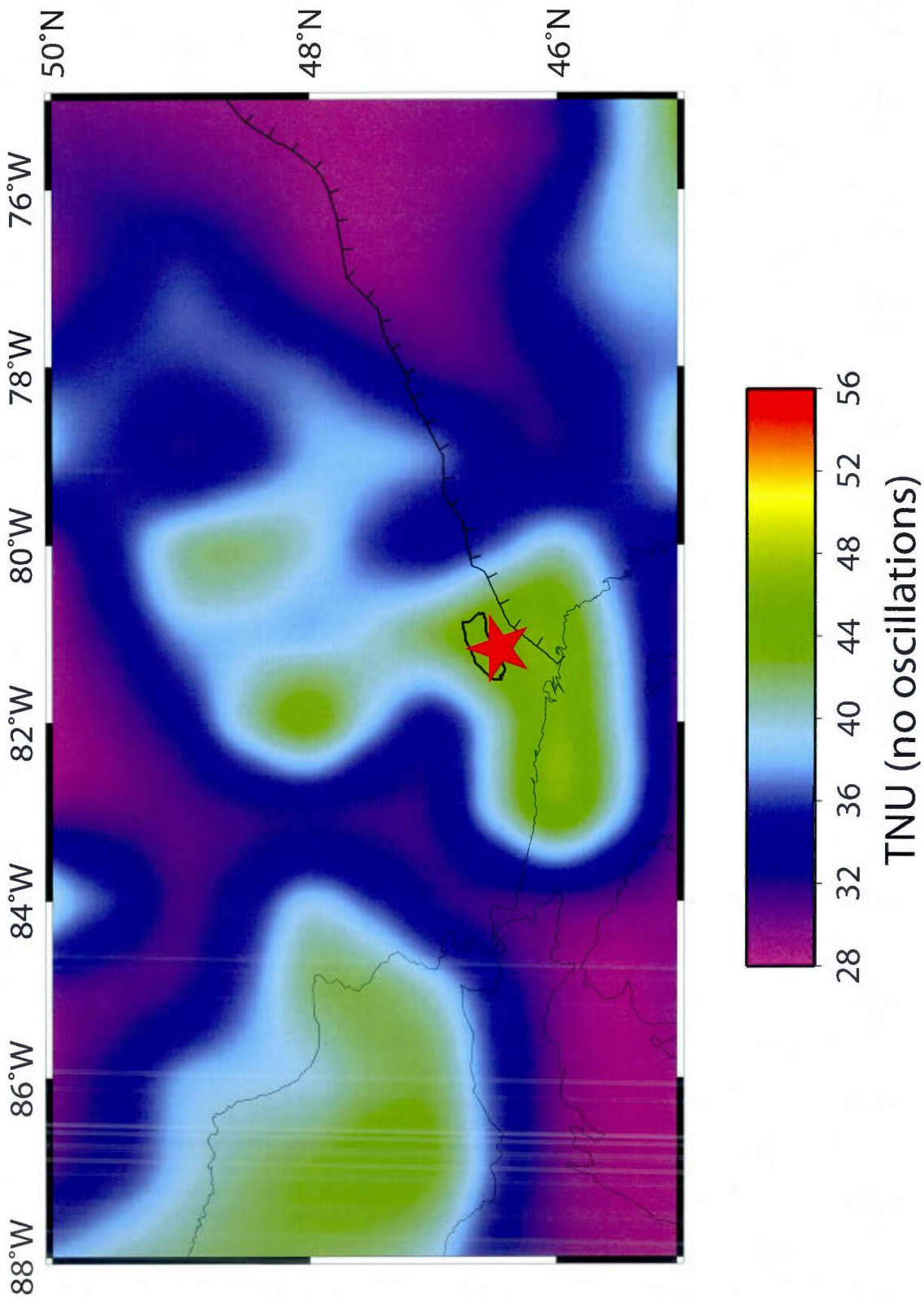
50°N
48°N
46°N
76°W
78°W
80°W
82°W
84°W
86°W
88°W
28
32
36
40
44
48
52
56
TNU (no oscillations)

Figure 2.18

2.A Geo-neutrino detection

Within scintillating liquid, interaction between an electron antineutrino and a proton generates a positron and a neutron :

$$\overline{\nu_e} + p \rightarrow n + e^+ \tag{2.A.1}$$

When captured 210μs later on proton, the wandering neutron releases a 2.2 MeV gamma-ray in concert with the prompt signal from the positron. It is the coincidence of the delayed event that recognizes the antineutrino inverse β decay. The threshold of this reaction is 1.8 MeV. Antineutrinos originating from ^{40}K discharge a maximum energy of 1.31 MeV, which is below the threshold. Only antineutrinos from ^{238}U and ^{232}Th can be detected.

The difficulty in the observation of geo-neutrinos is the very poor number of detectable events because of the very small cross-section of the reaction. The cross section of the reaction, σ, depends on the square of the antineutrino energy as :

$$\sigma_{\overline{\nu}_e p \rightarrow e^+ n} = 9.3 \times E_\nu^2 \times 10^{-44}\text{cm}^2 \tag{2.A.2}$$

where E_ν is the antineutrino energy in MeV.

Averaging the cross-section over the entire energy spectrum gives (Enomoto et al., 2007) :

$< \sigma_{^{238}U} >= 0.404 \times 10^{-48}\text{m}^2$
$< \sigma_{^{232}Th} >= 0.127 \times 10^{-48}\text{m}^2$

Assuming 100% efficiency, the total number of detectable events is proportional to the number of target protons in the detector, Np, times the exposure time, τ, times the total cross-section of the reaction, σ,

$$N_p \times \tau \int \sigma(E_\nu) \frac{d\Phi_i(E_\nu)}{dE_\nu} dE_\nu \tag{2.A.3}$$

where $\Phi_i(E_\nu)$ is the energy spectrum of the antineutrino for isotope i.

Therefore, for a 1.2 kT (10^{32} target protons) detector and 1 year of exposure, the minimum geo-neutrino flux required to observe one event is $10^{32} \times 3.15 \times 10^7 / < \sigma >$; which gives a minimum flux of (Enomoto et al., 2007) :

7.67×10^4 cm^{-2}s^{-1} from ^{238}U antineutrinos
2.48×10^5 cm^{-2}s^{-1} from ^{232}Th antineutrinos

When geo-neutrinos propagate in matter they oscillate from one flavor to another (Gonzalez-Garcia and Nir, 2003). The probability for detecting a geo-neutrino's original flavor changes with distance of propagation L_r, which is the distance traveled from the source to the detector as :

$$P_{\overline{\nu}_e \to \overline{\nu}_e} \approx 1 - \sin^2(2\theta_{12}) \sin^2(1.27 \Delta m^2_{21} L_r / E_{\overline{\nu}_e}) \tag{2.A.4}$$

where θ_{12} and Δm^2_{21} are the oscillation parameters, L_r is the distance in meters and $E_{\overline{\nu_e}}$ is the antineutrino energy in MeV.

The averaged survival probability of an antineutrino within the energy range of 1.8 MeV and 3.2 MeV is 0.56 $\pm$ 0.02 (Enomoto et al., 2007).

The number of antineutrino produced in the Earth is given by the antineutrino luminosity, A, which is given in unit time and per unit mass of isotope :

A for ^{238}U = 7.64 x 10^7 $kg^{-1}s^{-1}$
A for ^{238}U = 1.62 x 10^7 $kg^{-1}s^{-1}$

The flux of geo-neutrino at any point is obtained by integrating over the volume of the Earth :

$$\Phi_i(\vec{r}) = \frac{1}{4\pi} \int_V \frac{A_i(\vec{r'}) \rho(\vec{r'})}{|\vec{r'} - \vec{r}|^2} dV' \tag{2.A.5}$$

where A_i is the luminosity per unit mass for isotopes ^{238}U and ^{232}Th, ρ is the local density. $\vec{r'}$ and $\vec{r}$ are the source and the detector position, respectively. For each isotope, the event

rate at the detector is the product of the flux, Φ_i, by its cross section, σ_i.

Additionally, nearby reactors also release antineutrinos from the β decay of the fission products. Because the number of disintegration is related to the thermal power produced by the reactor, the signal from nearby reactors can be precisely calculated as well as its contribution to the observed geo-neutrino flux.

2.B Measurements

2.B.1 Heat flux

Surface heat flux is the amount of thermal energy that passes through the Earth's surface, per unit of time and per unit area. Conductive heat transport follows Fourier's law, which states that the density of the conductive heat flux is proportional to the temperature gradient where the constant of proportionality is the thermal conductivity of the medium (Fourier, 1822) :

$$Q = -\lambda \frac{\partial T}{\partial z} \tag{2.B.1}$$

Where the thermal conductivity λ is given in $W\ m^{-1}K^{-1}$, the temperature T in Kelvin and the depth z in meter. The heat flux, Q, is normally given in $mW\ m^{-2}$.

Thus, heat flux is determined from measurements of a temperature gradient and the thermal conductivity of the rock. To obtain a temperature gradient, the temperature is measured (at intervals of 10 meters) inside drill holes deep enough ($>$ 300 m) to intercept a steady temperature gradient (that is not disturbed by recent climate changes and surface effects). The temperature is measured using a thermistor calibrated to an accuracy of 0.002 K connected to the end of a long electrical cable. Samples from these holes are collected to calculate the thermal conductivity of the medium. Details on conductivity measurement are given below.

Heat flux measurements are then corrected for ground surface temperature variations following the retreat of the Laurentide ice sheet, 10 kyr ago, following the glacial history model of Jessop (1971). This model has been superseded, but it is still used for consistency

with previous published measurements. The differences in the correction would be very small anyway.

2.B.2 Thermal conductivity

The thermal conductivity is a physical property which measures the ability of a body to transfer thermal energy by conduction. More precisely, the thermal conductivity is the amount of heat transferred per unit area and per unit of time under a temperature gradient of 1 per meter-Kelvin ($W\ m^{-1}K^{-1}$). For heat flux measurements, thermal conductivity is measured on samples from all representative lithologies encountered along the borehole. If possible, core samples (20 cm long) are collected at an interval of about 100 meters, depending on the availability, quality and lithologic changes. Samples with cracks and veins were avoided as they weaken and caused samples to break during their preparation. If core samples are not available, unidentified segments of the core left near boreholes can be used. In this case, lithology throughout the borehole needs to be very homogenous.

Before thermal conductivity can be measured, samples have to be prepared following several long and painstaking steps. First, in each sample, a core is drilled in the direction corresponding to the vertical to obtain cylindrical samples whose ends are parallel to the Earth's surface (perpendicular to the temperature gradient). Each cylindrical sample are then cut into disks of 2, 4, 6, 8, and 10 millimeters thick. The end surfaces of these disks are polished to be perfectly parallel, with an accuracy of 10 to 15 microns, and coated with silver paint. Malleable and highly conductive, silver ensures perfect contact between the sample and the press without changing the conductivity.

The thermal conductivity is measured following the divided bar method developed by Misener and Beck (1960). Prepared disks are put under pressure between two brass columns (material whose thermal conductivity is well-known), one hot and one cold. Then the temperature difference (ΔT) is measured at the ends of each disk of known thickness. The thermal conductivity of a disk is obtained by comparing ΔT of the disk with ΔT of the brass. The thermal conductivity of a sample equal to the inverse slope of the linear relationship between the temperature difference and thickness of the 5 disks.

In this work, core sample preparation and thermal conductivity measurements were performed at the Laboratory of Dynamics of Geological Fluids, at the Institute of Earth Physics in Paris.

2.B.3 Heat production

Heat production is the amount of energy release per unit mass and per unit of time (W kg^{-1}) from the decay of radioactive elements. It is calculated from the concentration of radioactive elements U, Th and K. In this work, heat production was determined at heat flow sites and samples (about 5 cm long segment of core) were collected along with thermal conductivity samples (at the same depth) or from unidentified segments of the core that had been left near boreholes.

Before the radioactive element's concentration can be measured, samples are reduced to fine powders. First, samples are coarsely crushed, using a hydraulic press. These crushed samples are reduced to fine powders using a grinding mill. To avoid cross-sample contamination the "grind and discard" technique is adopted as follows : after sample A has been reduced to powder and the grinding container is cleaned, half of sample B is reduced to powder and discarded, and the container is cleaned again. Then the other half of sample B is processed without being contaminated with sample A. After this procedure is applied, about two grams of each sample are sealed into individual capsules.

These prepared powders are then analyzed by neutron activation analysis (NAA). This method consists of bombarding samples with neutrons, in a small pool-type nuclear reactor, thus becoming radioactive. After samples are sent into a high-resolution spectrometer where gamma rays released from radioisotopes decay are measured and U, Th and K concentrations determined.

Finally the heat generated from radioactive decay is calculated by summing the total contribution of each radioactive element using the following formula :

$$H = 10^{11}(9.52[U] + 2.56[Th] + 3.48[K]) \qquad (2.B.2)$$

where [U] and [Th] are the uranium and thorium concentration in ppm and [K] is the potassium concentration in %. Heat production is calculated in W kg^{-1}. To calculate heat production per unit volume, A, we multiply by the density. For an average crustal density of 2700 kg m^{-3} we obtaine :

$$A = 0.257[U] + 0.069[Th] + 0.094[K] \tag{2.B.3}$$

where A is the heat production per unit volume in μW m^{-3}.

Mean heat production at heat flux sites is obtained by averaging between several samples from all the representative lithologies.

Samples were prepared at University of Quebec in Montreal and neutron activation analyses were performed at the SLOWPOKE Laboratory of the Institute of Nuclear Engineering (University of Montreal).

CONCLUSION GÉNÉRALE

Les données radiométriques aéroportées nous ont permis d'estimer la production de chaleur dans la région de Sudbury. Les cartes construites à l'aide de ces données corrèlent bien avec la géologie régionale et nous ont permis de repérer les régions riches en éléments radioactifs, comme par exemple le Batholite de Cartier. Par contre, en comparant ces données avec des mesures de production de chaleur sur échantillons nous avons observé qu'elles sous-estiment la production de chaleur. Les données radiométriques aéroportées sont sensibles qu'à la partie superficielle de la croûte. Cette couche est affectée par des processus d'érosion et dans de telles conditions, U et K sont facilement lessivés. Par conséquent, la concentration en radioéléments du mort-terrain est plus faible que dans les roches fraîches.

Pour précisément déterminer le flux de géo-neutrino crustal, la radioactivité de la croûte doit être calculée à partir de mesures de flux de chaleur. Ces dernières sont très précises et intègrent la production de chaleur sur l'épaisseur totale de la croûte terrestre.

Toutes les mesures de flux de chaleur dans la région de Sudbury, y compris les nouvelles données présentées dans le chapitre deux cet ouvrage, nous ont permis de faire un premier calcul du flux de géo-neutrino crustal près de SNOLAB. Il en résulte un flux de géo-neutrino de 44 TNU (limite inférieure) et de 52 TNU (limite supérieure). L'incertitude est encore beaucoup plus élevée que la précision souhaitable de 1 TNU, mais elle pourrait être facilement réduite par l'ajout de nouvelles mesures de flux de chaleur.

La majorité des valeurs de flux de chaleur existantes se trouvent sur le pourtour de la structure d'impact et dans la Province du Sud, mais très peu de mesures ont été obtenues plus loin. La prochaine étape serait de fournir des mesures là où le flux de chaleur est inconnu, soit en dehors de la structure et surtout dans le Batholite de Cartier. Les mesures de production de chaleur réalisées le long du transect, la carte la production de chaleur réalisée à partir de données radiométriques aéroportées (Figure 1.5) suggèrent que le Batholite est anormalement radioactif. La forte radioactivité du Batholite pourrait avoir d'importantes conséquences pour les futures expériences sur les géo-neutrinos à SNOLAB.

BIBLIOGRAPHIE

Abbott, D., Burgess, L., Longhi, J., 1994. An empirical thermal history of the Earth's upper mantle. J. Geophys. Res. 99, 13835–13850.

Ames, D. E., Singhroy, V., Buckle, J., Molch, K., 2006. Geology, Integrated Bedrock Geology-Radarsat-Digital Elevation. Data of Sudbury, Ontario ; Geol. Surv. Can., Open File Report 4571.

Araki, T., and 86 collaborators, 2005. Experimental investigation of geologically produced antineutrinos with KamLAND. Nature 436, 499–503.

Arevalo, R., McDonough, W. F., Luong, M., Feb. 2009. The K/U ratio of the silicate Earth : Insights into mantle composition, structure and thermal evolution. Earth Planet. Sci. Lett. 278, 361–369.

Bellini, G., and 89 collaborators, 2010. Observation of geo-neutrinos. Phys. Lett. B 687, 299–304.

Bodorkos, S., Sandiford, M., Minty, B. R. S., Blewett, R. S., 2004. A high-resolution, calibrated airborne radiometric dataset applied to the estimation of crustal heat production in the Archaean northern Pilbara Craton, Western Australia. Precambrian Res. 128, 57–82.

Bristow, Q., 1983. Airborne gamma-ray spectrometry in uranium exploration. Principles and current practice. Int. J. Appl. Radiat. Isot. 32 (1), 199–229.

Buffett, B. A., Jun. 2002. Estimates of heat flow in the deep mantle based on the power requirements for the geodynamo. 29 (12), 120000–1.

Chen, M. C., 2006. Geo-neutrinos in SNO+. Earth Moon and Planets 99, 221–228.

Chouinard, C., Mareschal, J.-C., Jan. 2009. Ground surface temperature history in southern Canada : Temperatures at the base of the Laurentide ice sheet and during the Holocene. Earth Planet. Sci. Lett. 277, 280–289.

Cowan, C. L., Reines, J. F., Harrison, F. B., Kruse, H. W., McGuire, A. D., 1956. Detection of the Free Neutrino : a Confirmation. Science 124 (3212), 103–104.

Curtis, C. D., 1976. Chemistry of rock weathering : fundamental reactions and controls. In : Derbyshire, E. (Ed.), Geomorphology and Climate. Vol. 48. John Wiley Sons, Ltd, London, pp. 25–57.

Darnley, A. G., Cameron, E. M., Richardson, K. A., 1975. The Provincical-Federal Uranium Reconnaissance Program. In : Uranium exploration 1975. Geol. Surv. Can., Paper 75–26, pp. 49–68.

Davies, J. H., Davies, D. R., Feb. 2010. Earth's surface heat flux. Solid Earth 1, 5–24.

Dietz, R. S., 1964. Sudbury structure as an astrobleme. J. Geol. 72, 412–434.

Drury, M., Taylor, A., 1986. Some new measurements of heat flow in the Superior Province of the Canadian Shield. Can. J. Earth Sci. 24, 1486–1489.

Dye, S. T., Aug. 2010. Geo-neutrinos and silicate Earth enrichment of U and Th. Earth Planet. Sci. Lett. 297, 1–9.

Dye, S. T., Guillian, E., Learned, J. G., Maricic, J., Matsuno, S., Pakvasa, S., Varner, G., Wilcox, M., Dec. 2006. Earth Radioactivity Measurements with a Deep Ocean Anti-neutrino Observatory. Earth Moon and Planets 99, 241–252.

Dye, S. T., Guillian, E. H., Jan 2008. Estimating terrestrial Uranium and Thorium by antineutrino flux measurements. Proc. Nat. Acad. Sci. USA 105, 44–47.

Easton, R. M., 2009. Compilation mapping, Pecors-Whiskey Lake area, Superior and Southern Provinces ; in Summary of Field Work and Other Activities. Ont. Geol. Surv., Open File Report 6240, 10.1–10.21.

Eder G., 1966. Terrestrial Neutrinos. Nucl. Phys. 78, 657–662.

Enomoto, S., 2006. Experimental Study of Geoneutrinos with KamLAND. Earth Moon and Planets 99, 131–146.

Enomoto, S., Ohtani, E., Inoue, K., Suzuki, A., 2007. Neutrino geophysics with KamLAND and future prospects. Earth Planet. Sci. Lett. 258, 147–159.

Fiorentini, G., Lissia, M., Mantovani, F., Vannucci, R., 2005. Geo-neutrinos : a new probe of Earth's interior [rapid communication]. Earth Planet. Sci. Lett. 238, 235–247.

Fiorentini, G., Mantovani, F., Ricci, B., Apr. 2003. Neutrinos and energetics of the Earth. Physics Letters B 557, 139–146.

Fogli, G. L., Lisi, E., Palazzo, A., Rotunno, A. M., 2005. KamLAND neutrino spectra in energy and time : Indications for reactor power variations and constraints on the georeactor. Phys. Lett. B 623, 80–92.

Fourier, 1822. Theorie Analytique de la Chaleur. Paris.

French, B. M., May 1967. Sudbury structure, Ontario : Some petrographic evidence for origin by meteorite impact. Science 156, 1094–1098.

Gando, A. and 65 collaborators, Sep. 2011. Partial radiogenic heat model for Earth revealed by geoneutrino measurements. Nature Geoscience 4, 647–651.

Gonzalez-Garcia, M. C., Nir, Y., Mar. 2003. Neutrino masses and mixing : evidence and implications. Rev. Modern Phys. 75, 345–402.

Grasty, R. L., Kosanke, K, L., Foote, R. S., Aug. 1979. Fields of view of airborne gamma-ray detectors. Geophysics 44 (8), 1447–1457.

Hart, S. R., Zindler, A., 1986. In search of a bulk-Earth composition. Chem. Geol. 57, 247–267.

IAEA, 2003. Guidelines for radioelement mapping using gamma-ray spectrometry data. IAEA-TECDOC-1363, Vienna, Austria. 173 pp.

Jaupart, C., Labrosse, S., Mareschal, J.-C., 2007. Temperatures, heat and energy in the mantle of the Earth. In : Bercovici, D. (Ed.), Treatise on Geophysics, The Mantle. Vol. 7. Elsevier, New York, pp. 253–303.

Jaupart, C., Mareschal, J.-C., 1999. The thermal structure and thickness of continental roots. Lithos 48, 93–114.

Jaupart, C., Mareschal, J.-C., 2003. Constraints on crustal heat production from heat flow data. In : Rudnick, R. L. (Ed.), Treatise on Geochemistry, The Crust. Vol. 3. Permagon, New York, pp. 65–84.

Jessop, A. M., Jan. 1971. The distribution of glacial perturbation of heat flow in Canada. Canadian Journal of Earth Sciences 8, 162–166.

Jessop, A. M., Lewis, T. J., 1978. Heat flow and heat generation in the Superior Province of the Canadian Shield. Tectonophysics 50, 55–57.

Kobayashi, M., Fukao, Y., Apr. 1991. The Earth as an antineutrino star. Geophys. Res. Lett. 18, 633–636.

Krauss, L. M., Glashow, S. L., Schramm, D. N., 1984. Antineutrino astronomy and geophysics. Nature 310, 191–198.

Krogh, T. E., Davis, D. W., Corfu, F., 1984. Precise U-Pb zircon and baddeleyite ages for the Sudbury ares. In : Pye, E. G., Naldrett, A. J., Gilbin, P. E. (Eds.), The Geology and Ore Deposits of the Sudbury Structure. Vol. Special 1. Ont. Geol. Surv., pp. 431–446.

Kukkonen, I. T., 1989. Terrestrial heat flow and radiogenic heat production in Finland, the central Baltic Shield. Tectonophysics 164, 219–230.

Lay, T., Hernlund, J., Buffett, B. A., Jan. 2008. Core-mantle boundary heat flow. Nature Geoscience 1, 25–32.

Lay, T., Hernlund, J., Thorne, M. S., Jan. 2006. A post-perovskite lens and D" heat flux beneath the central Pacific. Science 314, 1272–1276.

Lewis, T. J., Bentkowski, W. H., 1988. Potassium, uranium and thorium concentrations of crustal rocks : a data file. Geol. Surv. Can., Open File Report 1744, 165 pp.

Lowell, R. P., Rona, P. A., von Herzen, R. P., Jan. 1995. Seafloor hydrothermal systems. J. Geophys. Res. (Solid Earth) 100, 327–352.

Mantovani, F., Carmignani, L., Fiorentini, G., Lissia, M., Jan. 2004. Antineutrinos from Earth : A reference model and its uncertainties. Phys. Rev. D 69 (1), 013001.

Mareschal, J.-C., Jaupart, C., Jun. 2004. Variations of surface heat flow and lithospheric thermal structure beneath the North American craton. Earth Planet. Sci. Lett. 223, 65–77.

Mareschal, J.-C., Jaupart, C., Phaneuf, C. Perry, C., 2012. Geoneutrinos and the energy budget of the Earth. Journal of Geodynamics 54, 43–54.

Mareschal, J.-C., Pinet, C., Gariepy, C., Jaupart, C., Bienfait, G., Dalla-Coletta, G., Jolivet, J., Lapointe, R., 1989. New heat flow density and radiogenic heat production data in the Canadian Shield and the Quebec Appalachians. Can. J. Earth Sci. 26, 845–852.

Marx, G., 1969. Geophysics by neutrinos. Czech. J. Phys. B 19, 1471–1479.

McDonough, W. F., Sun, S. S., 1995. The composition of the Earth. Chem. Geol. 120, 223–253.

Meldrum, A., Abdel-Rahman, A.-F. M., Wodicka, N., 1997. Documentation of a 1450 Ma contractional orogeny preserved between the 1850Ma Sudbury impact structure and the 1 Ga Grenville orogenic front, Ontario, Canada. Precambrian Res. 82, 265–285.

Minty, B. R. S., 1997. Fundamentals of airborne gamma-ray spectrometry. AGSO J. Aust. Geol. Geophys. 17, 39–50.

Misener, A., Thompson, L., Uffen, R., 1951. Terrestrial heat flow in Ontario and Quebec. Trans. Am. Geophys. Union 36, 1055–1060.

Misener, A. D., Beck, A. E., 1960. The Measurement of heat flow over land. Methods and Techniques in Geophysics, Volume 1, 10.

Mooney, W. D., Laske, G., Guy Masters, T., Jan. 1998. CRUST 5.1 : A global crustal model at $><$ 5 deg $\times$ 5 deg. J. Geophys. Res. (Solid Earth) 103, 727–748.

Müller, R. D., Roest, W. R., Royer, J.-Y., Gahagan, L. M., Sclater, J. G., 1997. Digital isochrons of the world's ocean floor. J. Geophys. Res. 102, 3211–3214.

Oganov, A. R., Ono, S., Jul. 2004. Theoretical and experimental evidence for a post-perovskite phase of $MgSiO_3$ in Earth's D" layer. Nature 430, 445–448.

Palme, H., O'Neill, H. S. C., 2003. Cosmochemical estimates of mantle composition : Mantle and Core. In : Holland, H., Turekian, K. K. (Eds.), Treatise on Geochemistry. Vol. 2. Elsevier, New York, pp. 1–38.

Pauli, W., 1930. Letter to a physicist's gathering at tubingen. Reprinted in Wolfgang Pauli, Collected Scientific Papers 2, 1313.

Perry, H. K. C., Jaupart, C., Mareschal, J.-C., Bienfait, G., 2006a. Crustal heat production in the Superior Province, Canadian Shield, and in North America inferred from heat flow data. J. Geophys. Res. (Solid Earth) 111, B04401, doi :10.1029/2005JB003893.

Perry, H. K. C., Mareschal, J.-C., Jaupart, C., Oct. 2009. Enhanced crustal geo-neutrino production near the Sudbury Neutrino Observatory, Ontario, Canada. Earth Planet. Sci. Lett. 288, 301–308.

Pinet, C., Jaupart, C., Mareschal, J.-C., Gariepy, C., Bienfait, G., Lapointe, R., Nov. 1991. Heat flow and structure of the lithosphere in the eastern Canadian shield. J. Geophys. Res. 96, 19,941–19,963.

Pollack, H. N., Hurter, S. J., Johnston, J. R., 1993. Heat flow from the Earth's interior : analysis of the global data set. Rev. Geophys. 31, 267–280.

Raghavan, R. S., Schoenert, S., Enomoto, S., Shirai, J., Suekane, F., Suzuki, A., Jan. 1998. Measuring the Global Radioactivity in the Earth by Multidetector Antineutrino Spectroscopy. Phys. Rev. Lett. 80, 635–638.

Rothschild, C. G., Chen, M. C., Calaprice, F. P., Apr. 1998. Antineutrino geophysics with liquid scintillator detectors. Geophys. Res. Lett. 25, 1083–1086.

Royer, J. Y., Müller, R. D., Gahagan, L. M., Lawver, L. A., Mayes, C. L., Nürnberg, D., Sclater, J. G., 1992. A global isochron chart. Tech. Rep. 117, Univ. of Tex. Inst. for Geophys., Austin, Tex.

Rudnick, R. L., Fountain, D. M., 1995. Nature and composition of the continental crust : A lower crustal perspective. Rev. Geophys. 33, 267–310.

Rudnick, R. L., Gao, S., 2003. Composition of the continental crust. In : Rudnick, R. L. (Ed.), Treatise on Geochemistry, The Crust. Vol. 3. Permagon, New York, pp. 1–64.

Sass, J. H., Killeen, P. G., Mustonen, E. D., Dec. 1968. Heat flow and surface radioactivity in the Quirke Lake Syncline near Elliot Lake, Ontario, Canada. Can. J. Earth Sci. 5, 1417–1428.

Schneider, R. V., Roy, R. F., Smith, A. R., 1987. Investigations and interpretations of the vertical distribution of U, TH, and K : South Africa and Canada. Geophys. Res. Lett. 14, 264–267.

Sclater, J. G., Jaupart, C., Galson, D., 1980. The heat flow through oceanic and continental crust and the heat loss of the Earth. Rev. Geophys. Space Phys. 18 (1), 269–311.

Shaw, D., Cramer, J., Higgins, M., Truscott, M., 1986. Composition of the Canadian Precambrian Shield and the continental crust of the Earth. In : Dawson, J. e. a. (Ed.), Nature of the Lower Continental Crust. Geol. Soc. London., pp. 257–282.

Taylor, S. R., McLennan, S. M., 1995. The continental crust : Its composition and evolution. Blackwell.

Thompson, W., 1862. On the secular cooling of the earth. Trans. Royal Soc. Edinburgh (XXIII), 295–311.

Vaittinen, T., 1986. Regional radiogenic heat production in Finland as determined with the help of airborne gamma ray measurements. M. Sc. thesis, Helsinki university of technology, department of mining and metallurgy, 62 pp.

Wedepohl, K. H., 1995. The composition of the continental crust. Geochim Cosmochim. Acta 59, 1217–1239.

Wilford, J. R., 1995. Airborne gamma-ray spectrometry as a tool for assessing relative landscape activity and weathering development of regolith, including soils. AGSO Res. Newslett. 22, 12–14.